NTNU

Norwegian University of
Science and Technology

Modeling of the Intermediate Band Tandem Solar Cell

Using the AM1.5 Spectra

Christer Andreas R Linge

Physics

Submission date: May 2011

Supervisor: Turid Worren Reenaas, IFY

Norwegian University of Science and Technology
Department of Physics

Modeling of the Intermediate Band Tandem Solar Cell

Using the AM1.5 Spectra

Christer Andreas Rosendahl Linge

Master's Thesis

NTNU

May 16, 2011

Preface

This thesis marks the end of the Master of Science study in physics at the faculty of Natural Sciences and Technology at NTNU, Norwegian University of Science and Technology in Trondheim.

I would like to thank my supervisor Turid Worren Reenaas for valuable help in discussing my results and for motivating me, as well as reading through my thesis. I also want to thank Maryam Gholami Mayani for input on Matlab coding and in discussing my results, Lars Martin Sandvik Aas for help with Matlab coding and the plotting of the results, and Hanne Lian for help with the graphics. Thanks to Ruth Helene Kongsbak for all her support and for reading through my thesis.

Abstract

In this thesis the results from simulations of a tandem intermediate band solar cell are presented and discussed. Renewable energy sources have become increasingly important, because of global environmental concerns. To make the solar cell technology more viable as an energy source, the study of how to increase the solar cell efficiency is important. The intermediate band solar cell (IBSC) has been introduced as a cell with potential to enhance the efficiency of the conventional single-junction cell. IBSCs have limiting efficiencies of 63.3%. This limit can be further increased by combining two different IBSCs in a tandem cell or combining an IBSC with a conventional single-junction cell.

The principle of detailed balance is used to find the limiting efficiencies for possible band gap combinations. Similar analysis of the intermediate band tandem cell has been done previously for black-body radiation. In this thesis the reference AM1.5 spectra have been used, and concentration levels of 1, 100 and 1000 suns. During the work, a model of the intermediate band solar cell, single-junction cell and the complete tandem cell have been coded in Matlab.

The tandem intermediate band solar cell will have six different band gaps and is hence comparable with a six single-junction tandem cell. Tandem cells with combinations of a single-junction cell and an intermediate band solar cell, having in total four different band gaps, have also been simulated.

In addition to a higher maximum efficiency, the tandem IBSCs are found to have large ranges of useful band gap energies. Semiconductor materials not considered for the single-junction cell or the single intermediate band cells are viable for making tandem IBSCs.

The main results in this thesis conclude that the four terminal tandem IBSC has a maximum efficiency of 54.93% for 1 sun, 62.74% for 100 suns, and 67.23% for 1000 suns. These maximum efficiencies are about 11% higher than that of a single IBSC under the same conditions. The maximum efficiencies for the other tandem cells are all higher than that of a single IBSC, with an increase from 1.50% to 9.05%. A wide range of main band gap combinations for the four terminal tandem cells give high efficiencies, but the range is strongly reduced for the two terminal tandem cell. For variations in the band gaps away from their optimal values, the efficiency is affected mostly by variation of the sub-band gap of the top IBSC.

Contents

Glossary

2xIBSC	tandem cell consisting of two IBSCs
α	absorption coefficient
$\mathfrak{a}$	absorbtance
α_{CV}	absorption coefficient for the process between the VB and CB
α_{H}	absorption coefficient for the process over the largest sub-band gap
α_{L}	absorption coefficient for the process over the smallest sub-band gap
AM	air mass
AM1.5D	air mass 1.5 direct and circumsolar
AM1.5G	air mass 1.5 global
ASTM G173	standard reference spectra for AM1.5
b	incident photon flux
b_a	incident photon flux from the ambient
b_e	emitted photon flux from radiative recombination process
b_s	incident photon flux from the sun
c	speed of light
CB	conduction band
EU	Europe
E	energy / photon energy
E_F	Fermi energy
E_G	main band gap energy
$E_{G,Bot}$	main band gap energy for the bottom cell
$E_{G,Top}$	main band gap energy for the top cell
E_H , E_{High}	largest sub-band gap energy
E_{IV}	energy over the sub-band gap between the VB to the IB
E_{IC}	energy over the sub-band gap between the IB to the CB

E_L , E_{Low}	smallest sub-band gap energy
$E_{L,Bot}$	smallest sub-band gap energy for the bottom cell
$E_{L,Top}$	smallest sub-band gap energy for the top cell
eV	electron volt
ε	emittance
F	geometric factor
F_a	geometric factor for the incident radiation from the ambient
F_s	geometric factor for the incident radiation from the sun
F_X	geometric factor for concentrated incident radiation
GW	gigawatt
h	Planck's constant
I	current
I_L	photogenerated current
I_0	short circuit current for a diode in the dark
IB	intermediate band
IB+S	tandem cell with a single-junction top cell and an IB bottom cell
IBSC	intermediate band solar cell
IRZI	incomplete Riemann Zeta integral
I-V	current-voltage
J_{gen}	generated current density
J_i	current density for cell i
J_{rad}	current density from the radiative recombination process
J_{tot}	total current density calculated with the principle of detail balance
K	Kelvin
k	Boltzmann's constant
m	meter
μ	chemical potential

μ_{CV}	chemical potential over the main band gap
μ_H	chemical potential over the largest sub-band gap
μ_L	chemical potential over the smallest sub-band gap
N	ideailty factor
nm	nano-meter
η	efficiency
$P_{incident}$	power incident to the solar cell surface
$P_{max,cell}$	maximum power generated by the solar cell
q	electron charge
QD	quantum dot
R	reflectivity
S	solar constant
S+IB	tandem cell with an IB top cell and a single-junction bottom cell
SRH	Shockley Read Hall
T	temperature
T_c	solar cell temperature
TWh	terawatt hour
V	voltage
VB	valence band
V_{OC}	open circuit voltage
W	watt
X	concentration factor

Figure List

1 Introduction

The photovoltaic market is currently in rapid growth, with a cumulative installed capacity of roughly 40 GW worldwide in 2010 [1], compared with the cumulative capacity of about 2 GW in 2002 [2]. In 2010 alone there was an added capacity of 16.6 GW, a large increase from the 7.2 GW installed in 2009. With a production capacity of 30 GW in 2010, Europe is leading the way. About 1.2% of the EU's electricity demand can be covered by the photovoltaic power plants the in 2011, with the possibility of producing 35 TWh electricity in one year [1].

The first functional, intentionally made photovoltaic device was by Fritts in 1883 [2], but it was not before 1954 that a solar cell with an efficiency of 6% was demonstrated. A couple of years later NASA started using solar cells as power sources for satellites. The worldwide oil crisis in the 1970's increased the interest for renewable energy sources, such as photovoltaics for a short period. Global environmental concerns did also soon after increase the interest in solar cell technology, especially after the IPCC reports in 2001 and Al Gore was awarded with the Nobel Peace Price in 2007. In the 1980s, the solar cell industry was starting to establish itself in countries around the world. Compared to the other established energy technologies the solar cells were too expensive to be used, except for applications very unpractical or expensive for other energy sources. As solar cell production increased during the following years, partly due to generous subsidies such as feed-in tariffs, a reduction in cost opened up new markets. In 1997 worldwide photovoltaic production reached 100 MW per year [2].

For photovoltaics to get a stronger foothold in the market, more cost effective solar cells are needed. As a response to this there are two ways to go: a reduction in cost as with the second generation thin-film solar cells, or an increase in efficiency like the third generation high-efficient solar cell. Among the third generation solar cells are the intermediate band solar cell and the tandem cell, increasing the efficiency of the cell by utilizing more of the incoming solar energy.

The source to the electric power created by the solar cells is the radiation emitted by the sun, hence radiation physics is an important aspect of understanding how a solar cell works. Chapter 2 discusses the radiation emitted from the sun, and both the black-body radiation and the AM1.5 spectra used in the calculations. Both the sun and the solar cell emit radiation with a distribution similar to that of a black body, and the equation for the emitted photon flux is essential to the solar cell model.

The physics of the basic solar cell itself and how it operates is treated in chapter 3. In addition the principle of detailed balance is presented as a method for finding the limiting efficiency of a solar cell. Possible ways to increase the efficiency of the cell is discussed. In chapter 4 one of the methods to increase the efficiency by use of an intermediate energy band is presented. Basic principles of how the intermediate band solar cell works and the theoretical limiting efficiency of the cell are presented in this chapter, as well as how this cell can be realised. Another multiple band gap cell, the tandem cell is the focus of chapter 5. In this chapter both the tandem cell consisting of single-junction cells and intermediate band cells are treated.

The model used in for calculating the limiting efficiencies is presented in chapter 6, where the parameters for the simulations and the code itself are discussed. Further improvements to the code are also suggested in this chapter.

In chapter 7 the results from the simulations are given along with discussions, and the conclusions are given in chapter 8.

2 Radiation from the sun

The solar cell converts sunlight into electric power, and thus understanding the radiation from the sun is therefore important for simulating the efficiency of a solar cell. This chapter will describe properties of the radiation from the sun, starting in section 2.1 with the black-body radiation. The electromagnetic radiation from the sun hitting the earth's surface will be treated in section 2.2. The solar cell performance dependence on spectral distribution and intensity will be presented in section 2.3.

2.1 Black-body radiation

This section is based on the book "Third Generation Photovoltaics" by M. Green [3].

A black-body is an object that is a perfect absorber of light and therefore also a perfect emitter. Although the perfect black-body represents a theoretical ideal, physical objects can approach close to black-body properties. Not only does the sun emit radiation close to a black-body at a temperature of about 5800 K [4], but as the ideal solar cell is a good absorber, the cell will also relate to the black-body as an emitter. The physics of black-body radiation is consequently very important in relation to solar cell physics.

The energy flux emitted from a black-body at a temperature T per unit surface area into a hemisphere over the energy range, E_1 to E_2 are given by

$$\dot{E}(E_1,E_2)=\frac{2\pi}{h^3c^2}\int_{E_1}^{E_2}\frac{E^3}{e^{E/kT}-1}dE \tag{2.1.1}$$

where h is Planck's constant, c the speed of light, k Boltzmann's constant, and E the photon energy.

The photon flux emitted is calculated from (2.1.1) by dividing with the photon energy:

$$\dot{N}(E_1,E_2)=\frac{2\pi}{h^3c^2}\int_{E_1}^{E_2}\frac{E^2}{e^{E/kT}-1}dE \tag{2.1.2}$$

2.2 Solar spectra at the surface of the earth

This section is based on the two books "Solar electricity" by T. Markvart [4], and "Solar cells" by M. A. Green [5].

Only a small part of the light emitted from the sun will reach the earth, since the sun emits light in all directions from its surface. The average incident power outside earth's atmosphere

per unit area on a plane perpendicular to the rays is known as the solar constant, and equals on average

$$S = 1367\, W / m^2 . \tag{2.2.1}$$

As the sunlight passes through the earth's atmosphere, some of the energy is lost due to:

- Rayleigh scattering or scattering by molecules in the atmosphere. This mechanism is most effective at short wavelengths.
- Scattering by aerosols and dust particles.
- Absorption by the atmosphere, in particular by the gases: oxygen, ozone, water vapour and carbon dioxide.

Due to absorption and scattering, the distance travelled through the atmosphere affects the intensity and spectral distribution of the solar radiation that hits the earth's surface. The length of the path is described by the air mass (AM), a ratio compared to the minimum length when the sun is directly overhead (AM1). In general terms the air mass is calculated in a following manner

$$Air \text{ mass} = \frac{1}{\cos\theta} \tag{2.2.2}$$

where θ represents the angle of the sun to the surface normal (,the zenith angle).

The solar spectrum just outside the earth's atmosphere is referred to as the air mass zero (AM0) spectrum. The AM0 spectrum differs from the 6000 K black-body radiation as shown in figure 2.1. This is due to varying transmissivity for the different wavelengths in the sun's atmosphere.

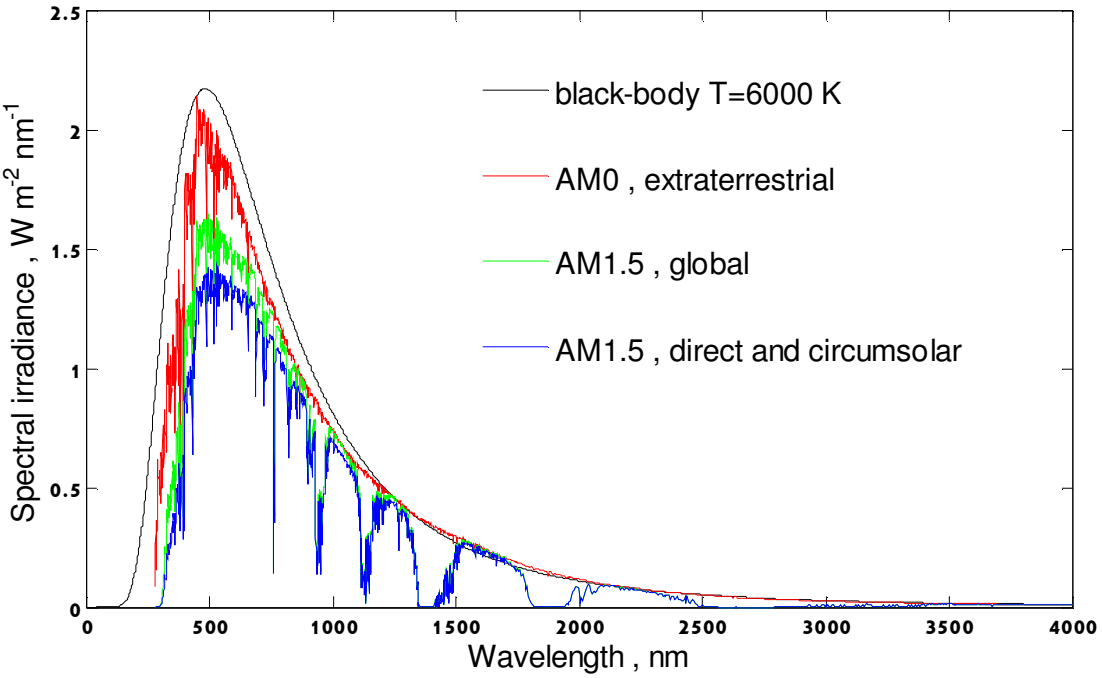

Figure 2.1: Spectral distributions for black-body (6000K) radiation, AM0 radiation, AM1.5 global and direct radiation (from the reference spectra ASTM G173-03 [6]).

The two AM1.5 spectra labelled "global" and "direct and circumsolar" differ because the global spectrum includes the diffuse radiation; radiation scattered in the atmosphere that still reaches the earth's surface. The direct and circumsolar radiation includes only the radiation from the solar disk and circumsolar radiation, as seen from the earth's surface. The circumsolar radiation is the irradiance within a +/- 2.5 degree field of view centered on the 0.5 degree diameter solar disk, but excludes the radiation from the solar disk itself [6]. In the next section the importance of the last spectrum will become clear. Details of how the AM1.5 spectra are used in the simulations is found in section 6.2.

2.3 Spectral dependence of solar cell efficiencies

The current produced by a photovoltaic cell is directly dependent on the photon flux. As the absorption rate for the photons varies with photon energy, both the intensity of the radiation and its distribution over different photon energies affect the efficiency of the cell. The physical processes in the cell will be explained in greater detail in the next chapter.

To increase the irradiance on the cell, concentration devices can be used [5]. Concentrators focus light onto the cell, but the higher the concentration ratio the smaller range of angles for the light rays will be focused on the cell. At a concentration ratio higher than 10, the concentrator will only accept the direct radiation. To include concentrated systems in the simulations, spectral distribution for the direct and circumsolar radiation is needed. These systems will be discussed in more detail in section 3.4.

3 Solar cell basics

This chapter is based on the book "The Physics of Solar Cells" by J. Nelson ,[7]. The basic principles of how a solar cell device works are presented in section 3.1. Section 3.2 covers the topics of generation and recombination in the cell. The principle of detailed balance is explained in section 3.3. Concentrator systems are discussed in section 3.4 and other methods to increase the efficiency in section 3.5.

3.1 Principle of operation

The solar cell converts electromagnetic energy to electric energy and is, in most cases, essentially a pn-junction under illumination. The absorbed photons excite electrons from the valence band to the conduction band, where the electrons are free to move and thus conduct a current. The empty state that is left in the valence band is referred to as a "hole", so that absorption of one photon leads to the creation of an electron-hole pair. The electron and the hole can then be separated by an electric field or by a gradient in the charge space density. If the electron and the hole are separated before they recombine, they can reach the outer contacts of the cell and be fed to an external circuit. The higher potential of the electrons on one side compared to the holes' potential on the other side of the cell generates a potential difference, the electromotive force that drives the current through a load in the external circuit.

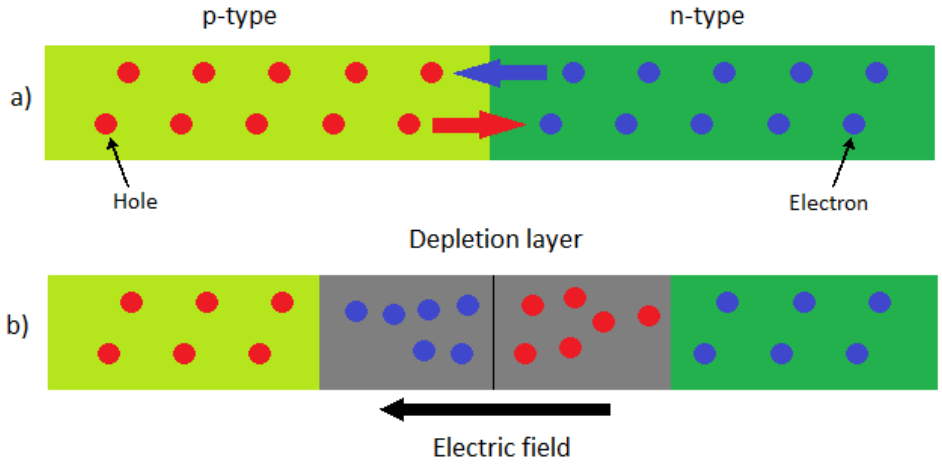

Figure 3.1: a) Electrons diffuse from the n-type material to the p-type material. b) An electric field is created in the depletion layer opposing the diffusion of electrons.

A pn-junction is created by n-doping one part and p-doping another part of the same semiconductor, see figure 3.1. An n-type doped semiconductor has impurities added, which have more valence electrons than the bulk material. The additional electron is not used in the strong directional covalent bonding and is therefore only loosely bound in a Coulombic bond with its atom. Similarly a p-type doped semiconductor has impurities added. These impurities

have one less valence electron than the bulk material. The impurity atoms become ionised by removing a valence electron from another bond to complete the bonding with the four neighbouring atoms, thus releasing a hole into the valence band. N-type semiconductors have an increased Fermi level while p-type semiconductors will have a decreased Fermi level.

The loosely bound electrons in the n-type doped material will diffuse to the ionised impurities in the p-type material (figure 3.1 a), and be used in the bonding of the impurity atoms. This space charge sets up an electric field opposing the diffusion, (figure 3.1 b). The energy bands are sketched in figure 3.2 below.

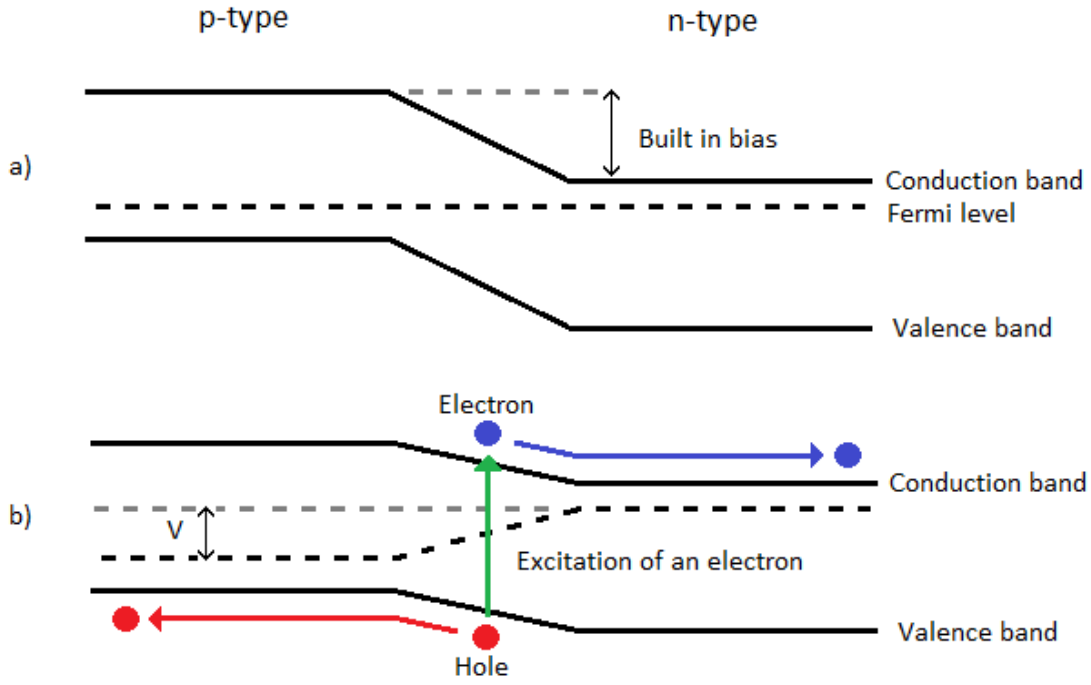

Figure 3.2: a) Band gap diagram of a pn-junction in equilibrium. b) Band gap diagram of a pn-junction under illumination. V is the potential difference between the two outer contacts and is the voltage output of the cell.

As seen in figure 3.2 the illuminated cell will have a raised potential, creating a split in the Fermi level over the junction. This split in the Fermi level provides a difference in the potential between the two contacts of the device. The electron is excited and separated from the hole, as seen in figure 3.2 b), by the electric field and can be fed to the outer circuits.

The current in a solar cell can be expressed as

$$I(V) = I_L - I_0(e^{qV/NkT_c} - 1) \qquad (3.1.1)$$

where I_L is the current generated by the absorbed light, and the second term is called the dark current or diode current, which depends on the voltage V over the cell. N is an ideality factor and has a value typically between 1 and 2. I_0 is a constant of usually much lower value than I_L, q the charge on the electron, and T_C is the cell temperature [3].

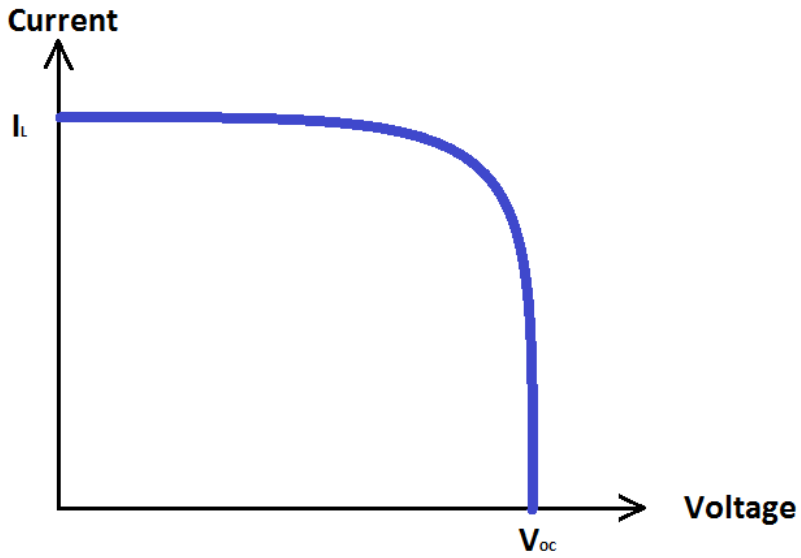

Figure 3.3: A sketch of an I-V plot for an ideal solar cell

Figure 3.3 shows the current voltage relationship of an ideal solar cell. V_{OC} is a notation for the open circuit voltage; the voltage over the contacts when the contacts are not connected through an external circuit. As can be seen from figure 3.3, the current will decrease fast to zero as the voltage gets close to the open circuit voltage. The power a cell can produce is found by multiplying the cell voltage with the current:

$$P(V) = I(V) \cdot V \tag{3.1.2}$$

To find the highest efficiency for a cell, the power output of the cell needs to be optimized for the voltage and divided by the total incident power from the sunlight:

$$\eta = \frac{\left(I(V) \cdot V \right)_{\max}}{P_{incident}} = \frac{P_{\max,cell}}{P_{incident}} \tag{3.1.3}$$

3.2 Generation and recombination

Generation is an excitation event which increases the number of free carriers available to carry charge. The opposing event reducing free carriers by relaxation is called recombination. Energy conservation requires these events to occur by particle interaction with incident photons, phonons or other particles in the material. Semiconductor material has an energy band gap between the conduction band and the valence band. Electrons have no possible energy states to occupy in this gap, with an exception of traps or localised states in the gap. These traps are an effect of impurities or defects in the material. Transitions over this band gap therefore have an energy threshold equal to the energy of the band gap.

3.2.1 Generation

Generation of free carriers requires energy, since the electrons are excited to a higher energy state. The energy can be provided by phonons (lattice vibrations), photons (photogeneration) or already excited electrons in the material, see figure 3.4. Excited electrons in the conduction band and holes created in the valence band will quickly relax to the edges of their band. This process is called thermalisation, as the energy dissipates by creating phonons and thereby increasing the material temperature.

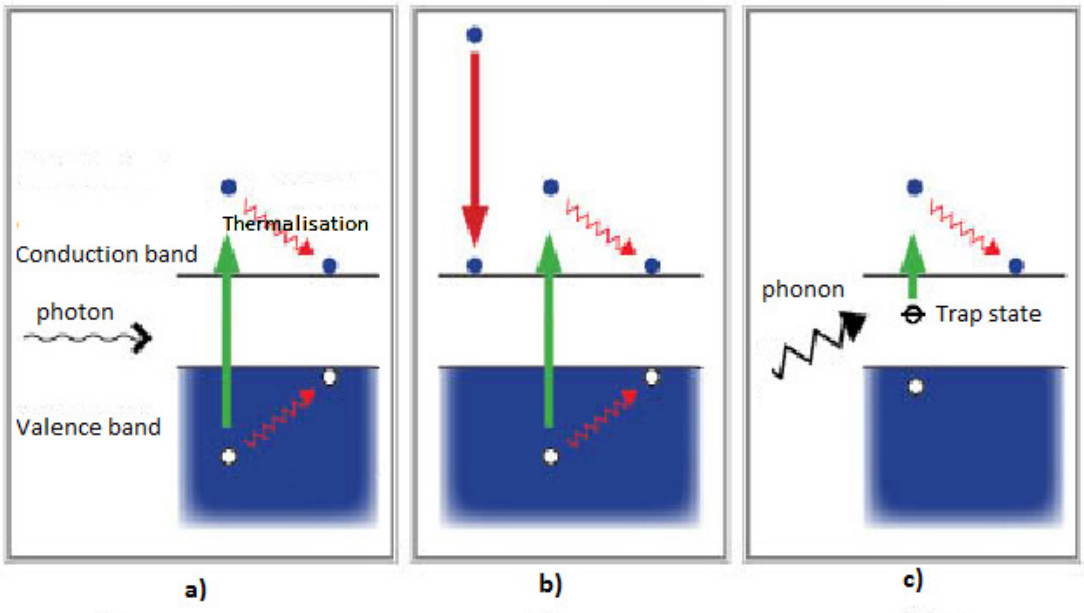

Figure 3.4: Generation of free carriers. The carriers are relaxed to the band edge by thermalisation. a) Photogeneration, b) generation by kinetic energy transfer between particles (Auger generation), and c) electron excited from trap state by phonons.

Generation by energy transfer between particles will be described in section 3.5. Photogeneration is the most important process in solar cells as it normally provides far more mobile carriers than the other methods of generation. Assuming that all photons are absorbed to generate free carriers, the rate of carrier generation from photogeneration, per unit area, at a depth x in the material is given by

$$g(E,x) = \left(1 - R(E)\right)\alpha(E)b(E)e^{-\int_0^x \alpha(E,x')dx'} \tag{3.2.1}$$

where b(E) is the incident photon flux at a given energy, α(E) is the absorption coefficient and R(E) is the reflectivity of the surface of normally incident light. The exponential term is added as a fraction of the light already will be absorbed in the material at the depth x.

Integrating over all the photon energies will give the total generation rate at x:

$$G(x) = \int g(E,x)dE \tag{3.2.2}$$

Auger generation will be treated in section 3.5.1. Electrons excited from trap states to the conduction band contribute little to the generation rate of free carriers. The probability for an electron to be excited from the valence band to the conduction band through trap states is very small. These electrons are most likely relaxed into the trap state from the conduction band. Although excitation of electrons through several steps by localised states, from the valence band to the conduction band is possible, it is very unlikely to contribute much to the generation rate. If these contributions are neglected the lower integration limit of (3.2.2) can be set to that of the band gap.

3.2.2 Recombination

Recombination describes the transition of an electron to a lower energy state, where it recombines with a hole. The process releases energy by photon emission (radiative recombination), phonon emission (non-radiative recombination) or transferring kinetic energy from the electron or hole to another free carrier (Auger recombination), see figure 3.5.

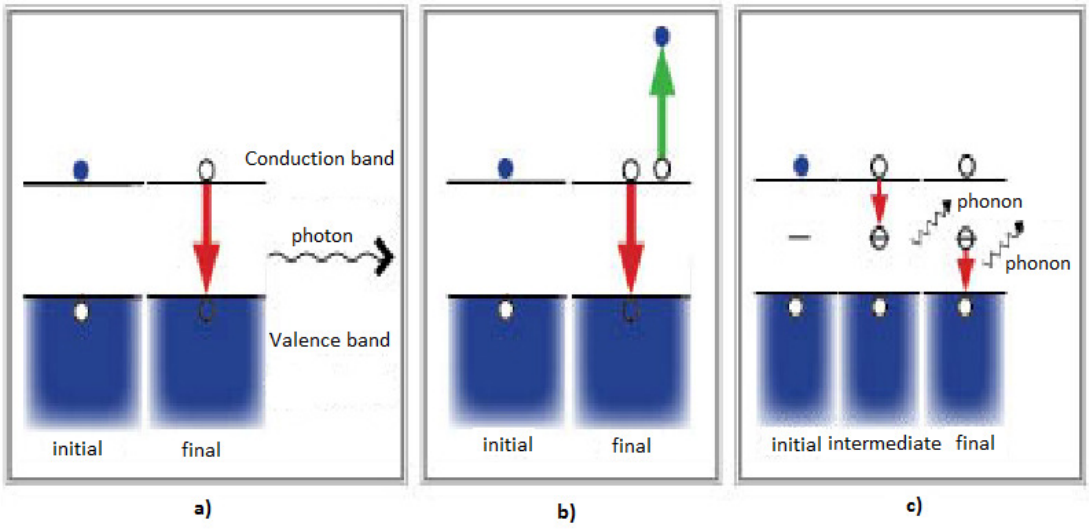

Figure 3.5: Recombination of "electron-hole pairs". a) Radiative recombination, b) Auger recombination , and c) recombination through a trap state by phonon emission.

Both radiative recombination and Auger recombination are unavoidable processes in a semiconductor material. Relaxation by emission of phonons through trap states, also known as Shockley Read Hall recombination (SRH), is avoidable as it is a result of localized states in the band gap of the material. The localised states are a result of impurities and defects in the semiconductor material and can potentially be avoided or removed during fabrication. Usually, the Shockley Read Hall recombination is dominant for real solar cells, but the Auger recombination rate can be higher for situations with a high density of mobile carriers.

3.3 Detailed balance

The principle of detailed balance is one of the fundamental physical limitations on the performance of the photovoltaic cell. As the cell absorbs photons, it will also emit photons by thermal radiation. By looking at the device from the outside, the photon flux entering the cell and leaving the cell surface can be calculated. Assuming a perfect mirror on the back of the cell both simplifies the calculations and increases the efficiency of the cell by leaving only one surface for the cell to emit radiation. Under the assumption that each photon absorbed adds one charge carrier to the current, the generated current density by absorption is given by

$$J_{gen}(E) = q\big(1-R(E)\big)a(E)b(E) \tag{3.3.1}$$

where a(E) is the absorptance, the probability of absorption of a photon of energy E, R(E) is the reflectivity at the surface and b(E) the incoming photon flux. For incident black-body radiation b(E) is given as

$$b(E) = b_s(E) + (1-\frac{F_s}{F_a})b_a(E) \tag{3.3.2}$$

where $b_S(E)$ is the incident photon flux from the sun

$$b_s(E) = F_s \frac{2}{h^3c^2}\frac{E^2}{e^{E/kT_s}-1} \tag{3.3.3}$$

and $b_a(E)$ from the ambient

$$b_a(E) = F_a \frac{2}{h^3c^2}\frac{E^2}{e^{E/kT_a}-1} \tag{3.3.4}$$

F_a and F_S are geometrical factors, and are a result of the distance from the source. At the surface of the source the factor equals π, but at a given distance from the source the factor reduces to

$$F = \pi \sin^2\theta \tag{3.3.5}$$

where θ is half the angle subtended by the radiating source to the point where the flux is measured. For the sun as seen from earth this angle is θ=0.26° and as a result $F_s = 2.16\cdot 10^{-5}\pi$.

The emitted radiation from the cell is restricted only to be a result of the radiative recombination. The cell is assumed to radiate like a black-body, but under illumination a part of the electron population will have a raised electrochemical potential. The spectral photon flux per unit surface area from a body of temperature T_C and with a chemical potential μ, with a surrounding medium with refractive index n_o, can be expressed as

$$b_e(E,\mu) = n_0^{\,2}\frac{2\pi}{h^3c^2}\frac{E^2}{e^{E-\mu/kT_c}-1} \tag{3.3.6}$$

The refractive index for air is very close to one, simplifying $b_e(E, \mu)$ to

$$b_e(E,\mu) = \frac{2\pi}{h^3 c^2} \frac{E^2}{e^{E-\mu/kT_c} - 1} \tag{3.3.7}$$

The current density lost in radiative recombination is given by

$$J_{rad}(E,\mu) = q\left(1 - R(E)\right)\varepsilon(E) b_e(E,\mu) \tag{3.3.8}$$

where R(E) is the reflectivity of the cell surface and ε(E) is the probability of photon emission called emittance. The emittance will equal the absorptance, because the probability of an electron to be excited by a photon is equal to the probability of an electron spontaneously recombining and emitting a photon.

$$\varepsilon(E) = a(E) \tag{3.3.9}$$

The net current density is simply given from retracting (3.3.1) from (3.3.8):

$$J_{tot}(E,\mu) = J_{gen}(E) - J_{rad}(E,\mu) \tag{3.3.10}$$

Assuming μ is constant everywhere in the cell and assuming no voltage loss in the contacts, the chemical potential μ is equal to q multiplied with the voltage over the cell contacts. The total current density is then given by integrating over all energies:

$$J_{tot}(V) = \int q\left(1 - R(E)\right) a(E)\left(F(E) - b_e(E, qV)\right)\, dE \tag{3.3.11}$$

The maximum efficiency for the cell is found for zero reflectivity and an absorptance equal to one, for energies higher than the band gap:

$$\begin{aligned} R(E) &= 0 \quad \forall\ \mathrm{E} \\ a(E) &= 0 \quad \mathrm{E} < \mathrm{E}_G \\ a(E) &= 1 \quad \mathrm{E} > \mathrm{E}_G \end{aligned} \tag{3.3.12}$$

The total current density is then given by

$$J_{tot,\mathrm{limit}}(V) = q \int_{E_G}^{\infty} F(E) - b_e(E, qV)\ \mathrm{dE} \tag{3.3.13}$$

The maximum efficiency will be given by optimizing (3.3.13) multiplied with the voltage and divide by the incident power density:

$$\eta_{\mathrm{limit}} = \frac{\left(J_{tot,\mathrm{limit}}(V) \cdot V\right)_{\max}}{P_{density,incident}} \tag{3.3.14}$$

This limit is the highest theoretical efficiency of a pn-junction solar cell and is called the "Schokley-Queisser limit", after the first to calculate the limit for a solar cell. For radiation from a black-body at a temperature of 6000 K, the efficiencies are 31% and 40.8% for a cell

with no concentration and maximum concentration respectably. The estimated efficiencies for direct normal irradiance from the ASTM Standard (E891-87) reference radiation are 32.5% and 44.6%, for no concentration and maximum concentration respectably [8] .

These efficiencies are the highest limit for a single pn-junction solar cell. Because of other recombination processes and resistance in the solar cell, the highest practical efficiency reached is 27.6% for a single-junction cell measured under the global AM1.5 spectrum (ASTM G-173-03) [9]. When calculated from laws of thermodynamics, the maximum efficiency possible for solar cells is 86,8% [3], with an ambient temperature at 300K and the temperature of the sun at 6000K. This is far higher than the "Shokley-Queisser limit". Section 3.5 will discuss methods to increase the efficiency, narrowing the difference between the "Shokley-Queisser limit" and the thermodynamic limit.

3.4 Concentrator systems

Concentration of the sunlight has already been introduced and as seen in the previous section increased the original "Shokley-Queisser limit" of 31% to 40.8% [8]. The concentrators collect light over a large area and then focus it on the surface of the solar cell. Photon flux incident on the cell is increased by multiplying with a factor X, which is basically dependent on the ratio between the area of the collection area and the cell surface. As mentioned earlier, only the normal incident radiation will be focused on the cell.

Concentrating the light is equivalent to expanding the angular range subtended by the sun and consequently increase the geometrical factor:

$$F_X = \pi \sin^2 \theta_X = X \sin^2 \theta_{sun} \tag{3.4.1}$$

As the angle θ_X can only be expanded to 90°, the maximum concentration X_{max} is 46050.

The increase in photon flux will increase the open circuit voltage of the cell and hence increase the efficiency of the cell. By an adjustment of equation (3.1.1) where the current is set to 0, the open circuit voltage for a cell under concentrated light is found to be

$$V_{oc}(X) = \frac{NkT}{q} \ln\left(\frac{X \cdot I_L}{I_0} + 1\right) \approx V_{oc}(1) + \frac{NkT}{q} \ln X \tag{3.4.2}$$

Assuming that the ratio between the maximum voltage and open circuit voltage are unchanged, and likewise for the maximum current and short circuit current, the increase in efficiency is found by dividing (3.4.2) with the open circuit voltage under no concentration, $V_{OC}(1)$. The efficiency will consequently be increased by a factor

$$1 + \frac{NkT}{qV_{oc}(1)} \ln X \tag{3.4.3}$$

In real concentrated systems the dark current is also affected. Increasing the cell temperature and large carrier densities leads to high injection conditions which will lower the effect on the

open circuit voltage in (3.4.2). High injection conditions effects the radiative and Auger recombination, as they will no longer be nonlinear with the high carrier density.

3.5 Over the S-Q limit

As seen in the earlier section, concentrator systems increase the solar cell efficiency by increasing the intensity of the light incident on the cell. In this section other methods of increasing the solar cell efficiency will be presented. These methods will increase the efficiency of the cell by reducing the thermalisation losses and making the cell absorb a larger part of the incident radiation.

3.5.1 "Hot" carrier solar cells and impact ionisation

"Hot" carrier solar cells are designed to be able to collect the excited carriers while they are still "hot", which means before they relax by thermalisation to the band edges. The "excess" kinetic energy will then contribute to the output power rather than heating up the cell. Collection of the carriers must happen quickly, and the phonon-carrier interactions must be severely slowed down. A similar approach is to use the "excess" kinetic energy of the carriers to generate more mobile carriers, called impact ionisation or Auger generation. The phonon-carrier interactions need to be reduced so that radiative and Auger processes are dominant. Auger generation is the reverse of the Auger recombination. A collision between an excited electron in the conduction band and an electron in the valence band excites the latter to the conduction band. Thus several mobile carriers can be generated by one photon and increase the efficiency of the cell.

3.5.2 Multiple band gap solar cells

Another method to use the energy of the photons more efficiently, is to increase the number of band gaps. With the use of multiple band gaps, more of the irradiance spectrum can be used without a huge loss to thermalisation processes. Tandem cells use multiple junctions with different band gaps to increase the cells efficiency, but intermediate band solar cells have extra band gaps in a single junction. The principle and effect of these methods are explained in the following chapters.

4 Intermediate band solar cells

This chapter is based on papers by A. Luque and A. Martí [10, 11]. The intermediate band solar cell is a device that has theoretical efficiency limits surpassing that of the single-junction cell, by absorbing more of the incident radiation without loss in voltage. In the first section, the working principle of the intermediate band solar cell is introduced. Section 4.2 covers two possibilities for implementing an intermediate band to a semiconductor. The detailed balance principle for an intermediate band solar cell is discussed in section 4.3.

4.1 The working principle of the intermediate band solar cell

Intermediate band solar cells are designed with an additional energy band in the band gap between the conduction band and the valence band. The main band gap (E_G) between the conduction band and the valence band is then split into two sub-band gaps, the smallest E_L and largest E_H. Electrons can be excited to the conduction band directly from the valence band or through the intermediate band, as shown in Figure 4.1.

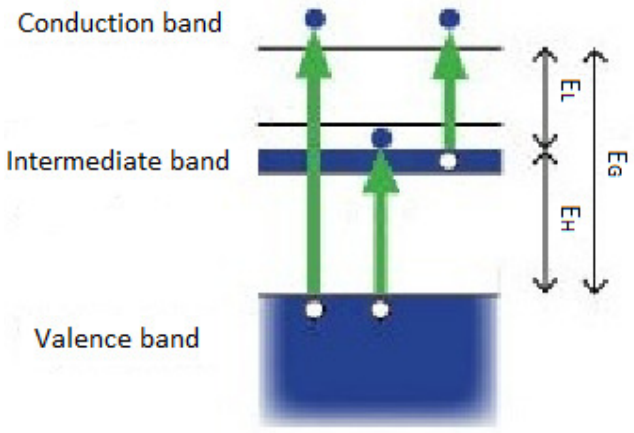

Figure 4.1: Simplified band diagram showing the possible photogeneration processes. E_L is the smallest sub-band gap and E_H the largest, E_G denotes the main band gap.

The increase in efficiency by the intermediate band is from the use of photons with energy lower than the main band gap. As these photons can excite electrons to and from the intermediate band, they can be absorbed and contribute to increased current. For the device to work optimally, a photon needs to excite electrons over the largest band gap possible for its energy. Under ideal circumstances the absorption coefficients should be:

$$\alpha_{CV} = \begin{cases} 1 & \text{for } \mathrm{E}_{photon} > E_G \\ 0 & \text{for } \mathrm{E}_{photon} < E_G \end{cases}$$
$$\alpha_{H} = \begin{cases} 1 & \text{for } \mathrm{E}_{photon} > E_H \\ 0 & \text{for } E_G < \mathrm{E}_{photon} < E_H \end{cases} \qquad (4.1.1)$$
$$\alpha_{L} = \begin{cases} 1 & \text{for } \mathrm{E}_{photon} > E_L \\ 0 & \text{for } E_H < \mathrm{E}_{photon} < E_L \end{cases}$$

In practical devices this will not be achievable. Figure 4.2 shows the difference between the ideal case (a) and a more realistic case (a).

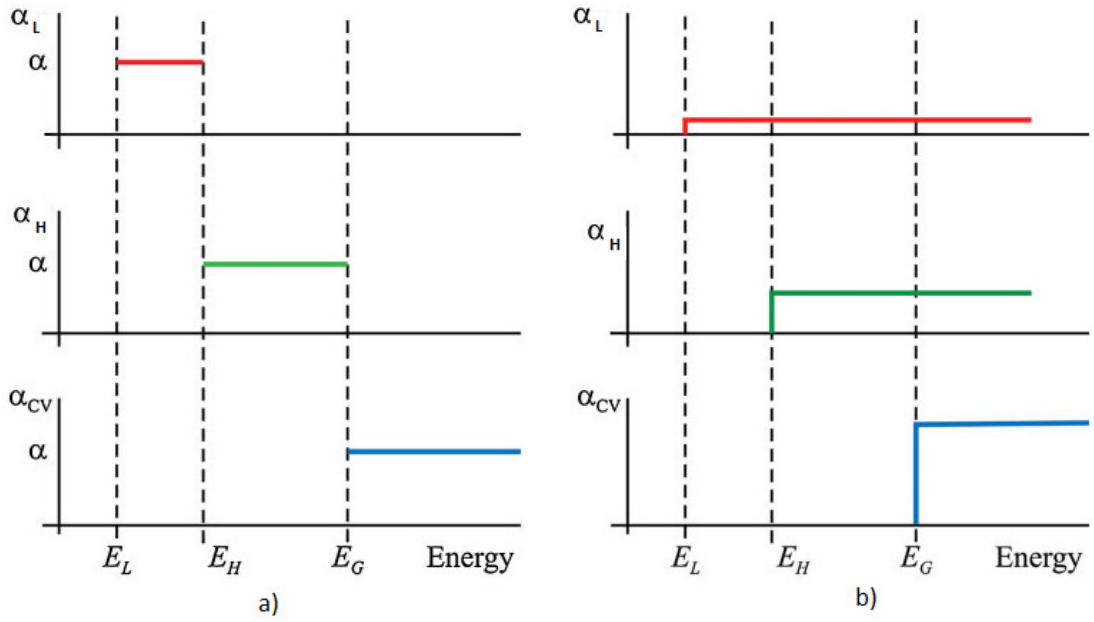

Figure 4.2: Showing two different plots of the absorption coefficients. a) The ideal case and b) a more realistic case. Figure from [10] with altered symbols to match this thesis.

The ideal case in figure 4.2 a) follows the ideal case represented in (4.1.1). In the more realistic case for a practical device in figure 4.2 b), all absorption coefficients are non-zero for the higher energies. It is then preferable that the absorption coefficient is highest for the largest band gaps, and decrease in the order of smaller gaps.

Electrons need to be collected only from the conduction band and holes only from the valence band, for the intermediate band solar cell to operate as intended. The electrons in the different energy bands then need to be associated with three distinct chemical potentials, or quasi-Fermi levels. The intermediate band also needs to be isolated from the metal contacts to the outer circuit. To achieve distinct quasi-Fermi levels, the gaps between the energy bands need

to be larger than the maximum phonon energy. The bands will then be thermally isolated. If the bands are not thermally isolated the cell will operate as a single-junction cell.

The intermediate energy band needs to have delocalized electron-states, as in the conduction band and the valence band, to maximize the device efficiency. Electrons in delocalized states will have a distinct momentum, explained in quantum mechanics as the Heisenberg's uncertainty principle [12]. This aids the transport of electrons and suppresses phonon scattering. The momentum is conserved at phonon-electron interactions, and if the electron has a distinct momentum state the probability of interactions between the particles decreases. At localised states in the main band gap electrons will have a wide range of momentum states, and therefore have a higher probability for relaxing through phonon interactions. Even as the gap between the energy bands is larger than the maximum phonon energy, multiple phonon scattering can still be allowed and the electron can relax to lower energy states by emission of several phonons.

In steady state conditions such as in a solar cell under illumination, there can be no conservation of charge in the intermediate band. The number of electrons excited from the valence band to the intermediate band needs to equal that from the intermediate band to the conduction band. To maximize the effective absorption the intermediate band should be half-filled, leaving unoccupied states to receive electrons from the valence band and occupied states to promote electrons to the conduction band.

4.2 Quantum dot and bulk intermediate band

Two concepts of implementing an intermediate band in the semiconductor band gap is described in this section, based on [10]. The first concept is based on quantum dots, which are nano-crystals of a material immersed in a semiconductor material, or the barrier material. The intermediate band would in this case typically arise from the confined states of the electrons in the conduction band tridimensional potential wells, originated by the conduction band offset between the dot and barrier material [10]. In the previous section it is discussed why the intermediate band needs to be partially filled, and this is achieved by n-type doping in the barrier. The quantum dots need to be close enough in proximity to each other to create an energy band, with delocalized states as to prevent SRH recombination.

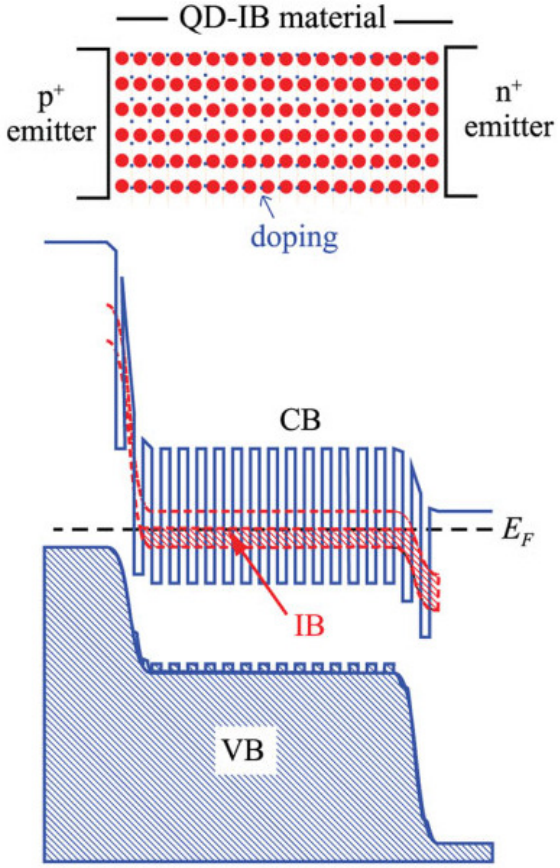

Figure 4.3: Simplified band gap diagram of a quantum dot intermediate band solar cell. Quantum dots are placed in a "near" intrinsic layer between a p-type and n-type doped semiconductor material [10].

The quantum dots are placed in a layer of close to intrinsic material, between a p-type and a n-type doped material, see figure 4.3. As also seen in figure 4.3, the energy bands should be flat in the intrinsic layer, to acquire partial filling of the intermediate band [13]. The highest current efficiencies published for a quantum dot intermediate band solar cell is 18.3%, which is lower than for the comparing reference cell with an efficiency of 23.77% [10].

Bulk intermediate band material is the second concept. Here the actual material has an intermediate energy band structure. A high concentration of impurities producing deep levels in the semiconductor may produce intermediate band materials with reduced non-radiative recombination. As these materials can support higher densities of intermediate band states, they can lead to stronger absorption of sub-band gap photons. The low absorption of these photons is one of the reasons for the low efficiency of the quantum dot intermediate band solar cells.

4.3 Detailed balance of the intermediate band solar cell

The principle of detailed balance for the intermediate band solar cell was first described by A. Luque and A. Martí [11], and is presented in this section. Conditions similar to the case of a single-junction cell as in section 3.3 is assumed: non-radiative transitions between the bands are forbidden, a mirror at the back restricts emission out the front surface of the cell, the reflectivity at the cell surface is set to zero, and the carrier mobility is infinite. This means that only radiative recombination and photogeneration are the allowed transitions between the energy bands. The three quasi-Fermi levels are also constant through the device as a consequence of infinite carrier mobility. The absorption coefficients have optimum values as in (4.1.1), and the intermediate band width is assumed negligible. Every absorbed photon contributes to excite one electron, and all electrons excited to the conduction band contribute to the output current of the cell.

The total current density extracted from the conduction band is given by:

$$J_{tot} = J(E_G, \infty, \mu_{CV}) + J(E_H, E_G, \mu_H) \tag{4.2.1}$$

where the functions J(·) are

$$J(E_{\min}, E_{\max}, \mu) = q \int_{E_{\min}}^{E_{\max}} F(E) - b_e(E, \mu) \, \mathrm{dE} \tag{4.2.2}$$

The factors in (4.2.2) are the same as in (3.3.13), and the chemical potentials are over the relevant band gaps. The first term in (4.2.1) is the total current density gained from the absorption and emission processes over the main band gap. The second term is the total current density from the same processes between the intermediate band and the conduction band. There can be no charge accumulation in the intermediate band, as explained in the previous section, and consequently the number of electrons in the band is constant. This gives one constraint to the value of the internal chemical potentials:

$$J(E_L, E_H, \mu_L) = J(E_H, E_G, \mu_H) \tag{4.2.3}$$

Equation (4.2.3) also reveals why it is irrelevant if the smallest band gap is between the intermediate band and the conduction band or the intermediate band and the valence band, as equation (4.2.1) is the same regardless. The chemical potentials also have the following second constraint:

$$\mu_L + \mu_H = \mu_{CV} = qV \tag{4.2.4}$$

where V is the voltage over the cell contacts. By solving these two equations the chemical potential (μ_H) in (4.2.1) can be found. The efficiency of the intermediate band solar cell can then be found as for the single-junction cell in (3.3.14).

In the paper by A. Luque and A. Martí [11] the highest efficiency is found to be 63.1% for maximum concentrated illumination from a black-body source at 6000K, and with a cell temperature of 300K. Another multiple band gap cell, the tandem cell, capable of numerous band gaps in one cell is treated in the next chapter.

5 Tandem cells

This chapter is based on [7] and [3]. Tandem cells are similar to intermediate band solar cells with multiple band gaps, but the band gaps in the tandem cells are distributed over an equal amount of junctions. The fundamental principle of increased efficiency is absorption of a larger part of the spectrum by use of several single-junction cells in one device. Spectral-distribution over the different junctions is described in the first section. The difference between two terminal cells and four terminal cells are treated in section 5.2. In section 5.3 intermediate band solar cells in tandem are discussed.

5.1 Spectrum splitting and stacking

The increase in efficiency of the tandem cell depends on the optimal use of the photon energy, as for the intermediate band cell, photons should preferably excite electrons over the largest band gap possible. Thermal losses by relaxing to the band edge are then minimal. One way is to split the spectrum in to various energy ranges, and direct the different ranges to the cell with the appropriate band gap. This could be done by use of spectrally sensitive mirrors illustrated in figure 5.1 (a).

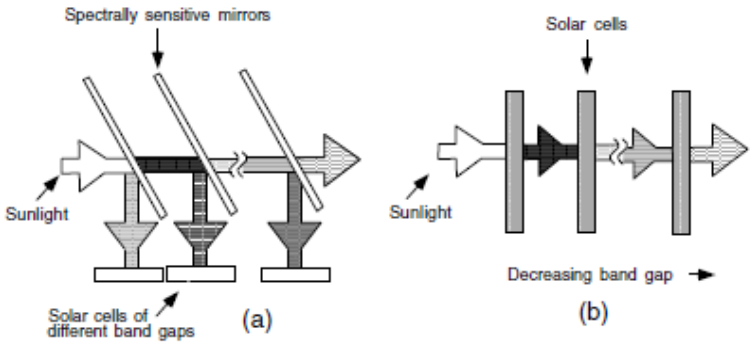

Figure 5.1: Tandem cell concepts: (a) Spectrum splitting and (b) cell stacking. The figure is from [3].

Figure 5.1 also shows the concept of cell stacking (b), another and more practical way to split the spectrum. In this concept the tandem cell is constructed by stacking cells with decreasing band gap energies. In principle, high energy photons are absorbed by the top cell with the largest band gap. Photons with lower energies than the band gap of the top cell are not absorbed and travel through to the next cell.

Cell stacking allows for interaction between the cells. The cells emit radiative radiation both out the front surface and to the adjacent cells as illustrated in figure 5.2. This radiation can be absorbed by other cells and contribute to the generated current. The efficiency of the tandem cell can be slightly increased by isolating the cells with a wavelength filter. The filter transmits only photons of a lower energy than assigned to it, and will reflect higher energy photons emitted back to the cell, illustrated in Figure 5.2 (b).

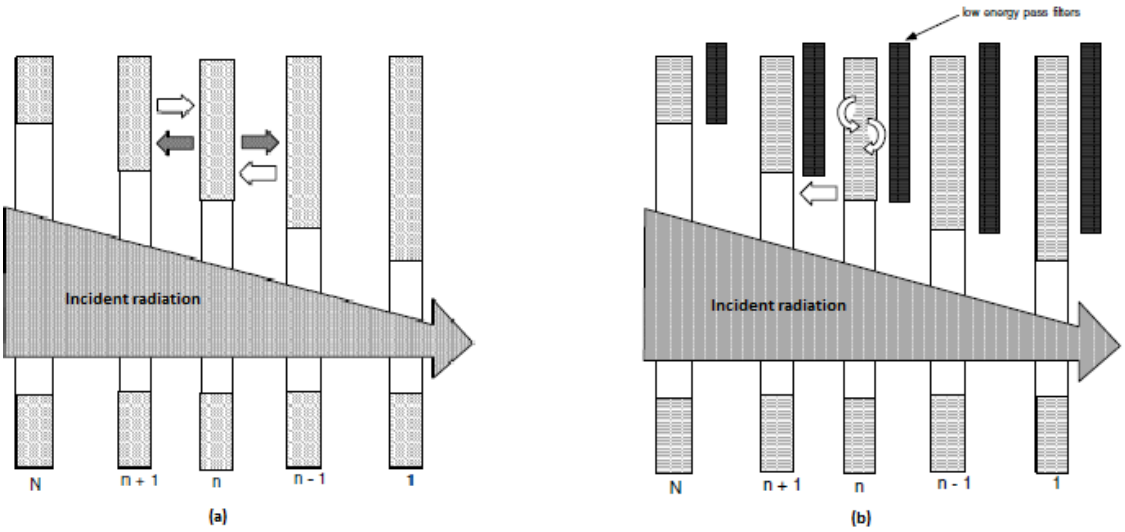

Figure 5.2: Radiative connections between the N cells in tandem: (a) Tandem cell with no wavelenght filters, "free" thermal radiation emition and absorption between the cells and (b) tandem cell with filters between each cell, reflecting part of the radiative radiation back to the emitting cell [3].

In the following sections of this chapter wavelength filters between each cell will be assumed as this assures highest efficiency, and simplifies the calculations by removing the thermal interactions between the cells.

5.2 Two or more terminals

Tandem cells can have two or more terminals (contacts) to the external circuit. The concept is illustrated for a tandem cell with two band gaps (or two single-junction cells) in figure 5.3.

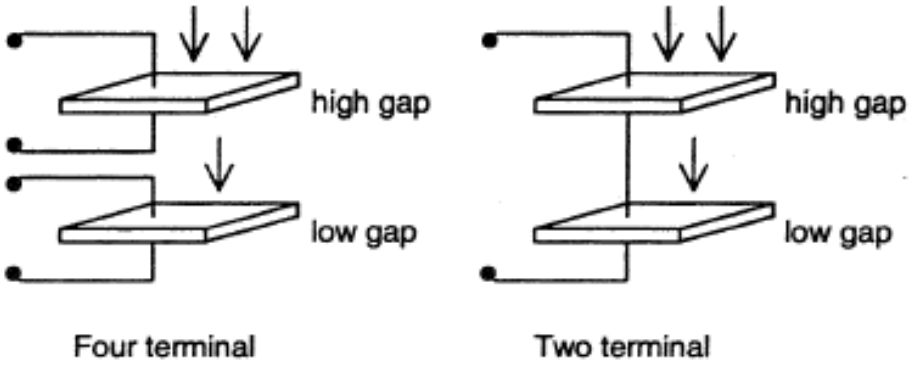

Figure 5.3: Tandem cell in two terminal (series connected) and four terminal (separately connected) configurations [7].

As seen on the left in figure 5.3, the four terminal cell contains two separately connected single-junction cells. Tandem cells with separate connections for each cell can be treated as

several single-junction cells illuminated by different parts of the spectrum. All the individual cells can then operate at the voltage giving maximum efficiency for that cell. The two terminal tandem cell to the right in figure 5.3 has two single-junction cells connected in series. This concept is more appealing as it has the possibility of integrating different junctions in one multilayered device. To connect the different p-n junctions, tunnelling junctions are used. The tunnelling junction is a heavily doped n-p junction connected to the p terminal of one cell and the n terminal of the next.

The efficiency of the tandem cell with more than two terminals is calculated by adding the power output of each separate cell and dividing the sum by the power of the total spectrum. With the use of equation (4.2.2) the highest efficiency using detailed balance is found to be

$$\eta_{\text{unconnected Tandem}} = \frac{\left(J_1(E_{G1}, E_{G2}, qV_1)\cdot V_1\right)_{\max} + \left(J_2(E_{G2}, E_{G3}, qV_2)\cdot V_2\right)_{\max} + ... + \left(J_N(E_{GN}, \infty, qV_N)\cdot V_N\right)_{\max}}{P_{density,incident}} \quad (5.2.1)$$

In the two terminal tandem cell, all the separate cells are series connected. This means that all the cells must have the same current density:

$$J = J_1 = J_2 = ... = J_N \quad (5.2.2)$$

To find the highest efficiency, the total voltage of all the separate cells multiplied with the current needs to be maximized:

$$\eta_{\text{connected Tandem}} = \frac{\left(J_1(E_{G1}, E_{G2}, qV_1)\cdot (V_1 + V_2 + ... + V_N)\right)_{\max}}{P_{density,incident}} \quad (5.2.3)$$

The constraint on the two terminal tandem cell will decrease its efficiency compared to the tandem cell with separate terminals for each single-junction cell, as seen in figure 5.3.

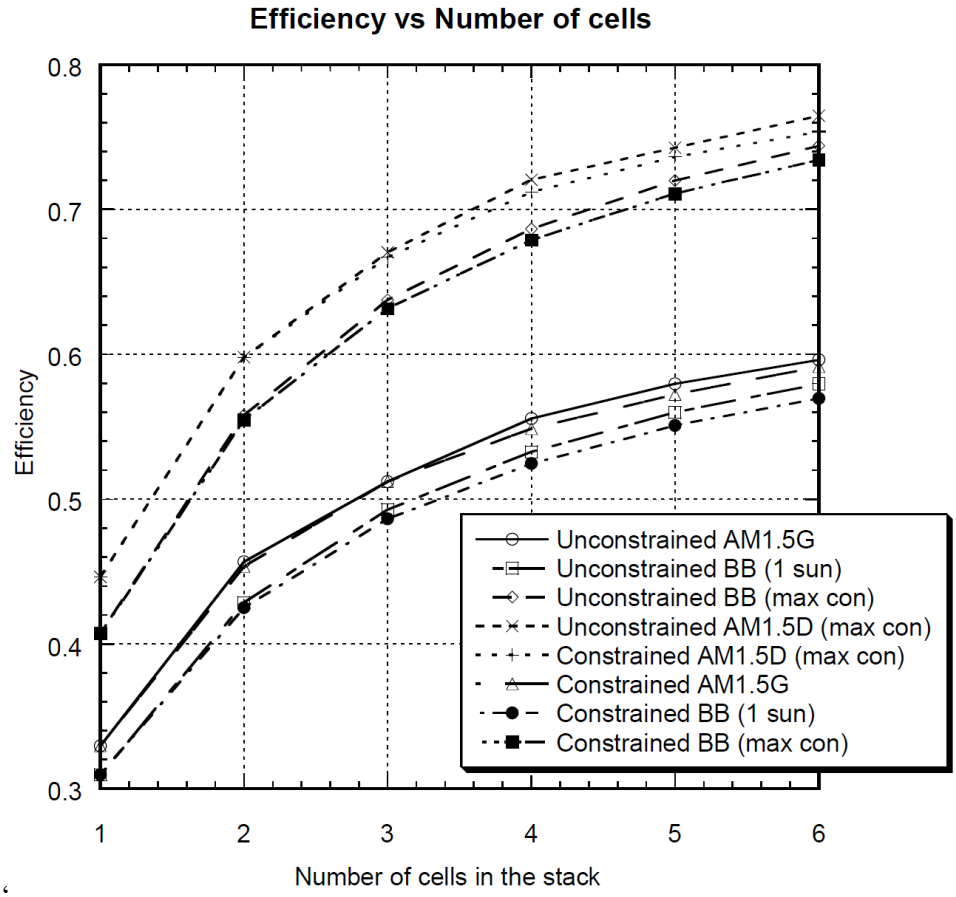

Figure 5.4: Unconstrained and two terminal limiting efficiencies for various radiation sources [14].

Figure 5.4 shows that the decrease in efficiency for the tandem cell with two terminals is small compared to the efficiency. For the AM1.5 global radiation, the largest decrease in efficiency is from 55.6% to 54.9% for the tandem cell consisting of four single-junction cells [14], a 1.26% difference in efficiency .

5.3 Intermediate band solar cells in tandem

Intermediate band solar cells can also be arranged in tandem cells, both series connected and separately connected, leading to a tandem cell with a reduced number of junctions and still several different band gaps. Each of the intermediate band solar cells has three different band gaps. In a tandem cell the intermediate band solar cells are be stacked similar as for the single-junction cells; the cell with the highest band gaps is on top and the rest of the cells will be stacked by decreasing band gap widths, see figure 5.5.

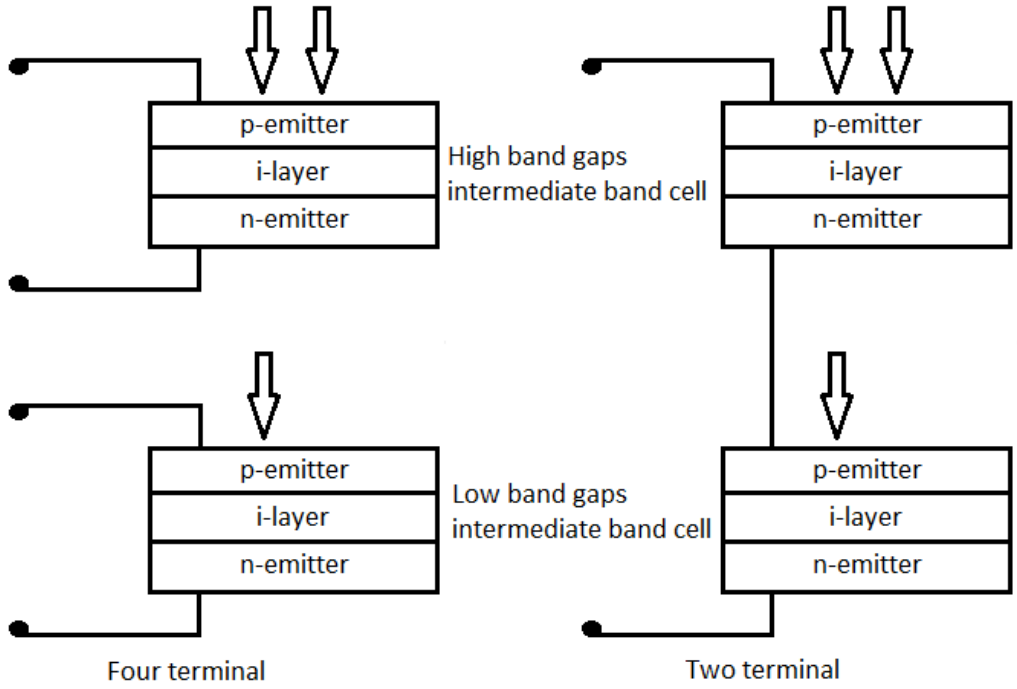

Figure 5.5: Two terminal and four terminal tandem intermediate band solar cells.

Calculations for each separate intermediate band can be handled as in chapter 4, and then used in the equations in the previous section as for single-junction cells. The voltage over each separate cell is consistent with the voltage over the main band gap of the intermediate band solar cell. If the absorption coefficients are ideal as in equations (4.1.1), only the photons with lesser energy than the lowest sub-band gap of the intermediate cell is transmitted through to the next cell in the stack.

6 Modeling of solar cell efficiencies

In this chapter both Matlab as a modeling tool and the code for the simulations will be discussed. The first section presents the use of Matlab for solar cell simulations. In section 6.2 the spectra used and changes made to the tabulation is discussed. The code itself and methods used in the calculation is treated in section 6.3. Section 6.4 is devoted to discuss problems with the simulation code and possible further improvements. Most of the Matlab code used in the simulations for this master thesis is found in Appendix A.

6.1 Matlab as a modeling tool

Matlab is a program usually used for numerical analysis and matrix operations. The data from the calculations are stored in huge matrixes, which can easily be accessed in Matlab. Matlab allows use of functions and as some operations are run several times, this is advantageous. NTNU provides Matlab as a computational tool and it is used in other master and PhD projects at the department of physics. This is partly the reason why Matlab has been chosen as a modeling tool for this thesis. The scripts in Matlab need to be compiled each run, which makes it slower than scripts written in other programs. It is possible to compile the Matlab-code before running the code to reduce the run-time, but as an inherent function in Matlab is used in the calculations in this master project, the compilation does not reduce the run-time significantly. Running the simulation in Matlab has proven to be very time consuming and this affects energy resolution in the simulations.

6.2 The solar spectra

The ASTM G173 spectra are reference spectra for air mass 1.5 and modelled by using SMARTS (version 2.9.2). The modelled spectra are available from the National Renewable Energy Laboratory (NREL) website [6]. The global AM1.5 spectrum (AM1.5G) includes both the diffuse and the direct light, and is modelled for a 37° tilted surface facing the sun (that is, the surface normal points to the sun, at an elevation of 41.81° above the horizon). It has a total irradiance of 1000.37 W/m² (calculated in Matlab). The direct and circumsolar AM1.5 spectrum (AM1.5D) is the direct radiation on a surface normal to the direction of the sun, and has a total irradiance of 900.14 W/m² (calculated in Matlab). Figure 2.1 shows all of the ASTM G173 spectra, including the extraterrestrial AM0 spectrum.

The calculated ASTM G173 spectra on NREL's website range from 0.31 eV to 4.428 eV in photon energies. The photon flux at photon energy 4.428 eV is less than 1 $m^{-2}nm^{-1}$, so photon flux values at higher energies are not needed. For photon energies lower than 0.31 eV there is still a considerable photon flux even if the intensity of the light is small, because of the low photon energy. As there are no values for the photon flux at these values for the available ASTM G173 spectra, the band gaps with lower energy than 0.31 eV will receive a smaller photon flux in the simulations than what they should for a more complete spectrum.

The radiation distributions from ASTM G173 are tabulated for varying wavelength steps, but have in this thesis work been interpolated using Matlab to steps of 1 nm. This is done to simplify the calculations of the photon flux as all steps now have the same length. The photon flux from the ASTM G173 spectra is calculated by summing the photon flux from one wavelength to another. (As the band gap energies are in eV, the photonenergy for each wavelength has been calculated and used to find the intervals needed in each case.) Since the flux data used in this project have a 1 nm step, the photon flux in a given wavelength interval will have some deviation from the values in the ASTM G173 tables. The interpolated AM1.5 spectra used in this simulation have a total irradiance of 1000.37 W/m² for the global AM1.5 spectrum and 900.14 W/m² for the direct AM1.5 spectrum. These values for the total irradiance are equal to the rounded values to two decimals for the ASTM G173 spectra found on NREL's website, and close to the normally used total irradiance of 1000 W/m² for the global radiation and 900 W/m² for the direct radiation.

6.3 The solar cell simulations

The aim for the simulations is to calculate the limiting efficiencies, using the principle of detailed balance, for tandem cells with either two IBSCs or a combination of an IBSC and a single-junction cell. The theoretical model for detailed balance is explained in section 3.3 for the single-junction cell, in section 4.3 for the IBSC, and section 5.2 and 5.3 for the tandem cell. Assumptions made in these sections are used in the simulations. A perfect wavelength filter, as presented in section 5.1, between the two cells in the tandem cell is used in the simulations. The connection between the two separate cells in the two terminal case is assumed to be an ohmic contact with no loss. Efficiency and optimum IB gaps are found for ranges of main band gaps (E_G) for both solar cells.

The steps for the band gap energies are set to 0.05 eV. Higher resolution for the bottom cell is not feasible, because the simulation code is time consuming to run. In the simulations the bottom cell main band gap is also set to be smaller than the lowest band gap of the top cell, reducing the run time for the bottom cell simulations. The models include both tandem cells of two intermediate band solar cells and tandem cells with one single-junction cell and one intermediate band cell. Voltage and current characteristics of each cell have been calculated for the top and bottom cell separately. The common variable for the top and bottom cell is the photon energy that splits the spectrum between them. This photon energy is the lowest photon energy that can be absorbed by the top cell, and therefore also the upper limit to the photon energy absorbed by the bottom cell.

The voltage and current characteristics for the conventional single-junction cell is found by calculating equation (3.3.13) for 500 different voltages. The voltage range is in each case from the voltage where the current has a change from the short circuit current value, to the open circuit voltage. For a single cell the highest efficiency is found from this dataset by use of equation (3.3.14).

Similar calculations are done for the intermediate band solar cell, with the use of equation (4.2.1). Additional calculations are needed to include the constraint in equation (4.2.3). If the constraint in equation (4.2.3) is not met, the lower of the two current densities is used in equation (4.2.1) to calculate the total current density. The smallest electron flow is selected

because the electrons need to be excited over both sub-band gaps to contribute to the current. If the flow of electrons from the valence band to the intermediate band is larger than the flow from the intermediate band to the conduction band, the intermediate band will start to fill up with electrons. With less empty states in the intermediate band there will be fewer states for electrons to be excited to, and the flow of electrons to the intermediate band from the valence band will decrease, as the probability of excitation is proportionally dependent on the number of empty states in the intermediate band. More occupied states will increase the probability of exciting an electron from the intermediate band to the conduction band. Similarly, if the flow of electrons from the intermediate band is larger than the flow into the intermediate band, there will be an increase in empty electron states. This will increase the flow of electrons to the intermediate band and decrease the flow from the band, again because the excitation of electrons is dependent on the number of empty and occupied states in the intermediate band.

The data from the top and bottom cell have then been used to calculate both the separately connected (four terminal) and the series connected (two terminal) tandem cell. To find the total maximum efficiency for the separately connected tandem cell, the maximum efficiencies for the top and bottom cell are simply added. For the series connected tandem cell the calculation is a bit more tedious, as the two cells need to have an equal current. The current-voltage characteristics of the two cells have therefore been evaluated together by use of interpolation to find the maximum efficiency. Band gap combinations that provide the highest efficiency for the complete tandem cell are used.

Since the AM1.5 spectra only have data for photon energies larger than 0.31 eV, the lowest band gap used in the simulations is set to 0.30 eV. Photon flux values for the AM1.5 spectra between 0.30 eV and 0.31 eV are not added in the simulations, and consequently the absorbed photon flux in cells with a band gap set to 0.30 eV will be lower than it should for more complete spectra. Lower band gaps are also more affected by the Auger recombination process through phonon interaction, so very low band gaps are realistically less viable for solar cell devices.

The maximum band gap energy for the top cell is set to 4.80 eV. The AM1.5 spectra have essentially no photons of energies larger than 4.42 eV. Ohmic contacts on semiconductors with extremely high band gaps are difficult to produce [15] and therefore a cell with band gap larger than 4.80 eV is unlikely to be used in real devices. The highest main band gap used for the single-junction cell used on top of an IBSC is only 2.8 eV, since a higher value would require a significantly increase in run time for the model of the bottom IBSC. The complete ranges are presented in table 6.1 below.

Table 6.1: Band gap ranges for the tandem cells

Cell	Lowest sub-band gap (eV)	Main band gap (eV)
Top , IBSC	**0.7 - 2.35**	**1.1 - 4.8**
Bottom , IBSC	**0.3 - 1.35**	**0.65 - 0.275**
Top , single-junction		**0.7 - 2.8**
Bottom , single-junction		**0.3 - 2.3**

6.4 Discussion of the code

In retrospect, it can be argued that the runtime of the code could be improved, and more band gaps could have been evaluated. The calculation of the emitted radiation from the radiative recombination is the (single) operation that consumes most of the runtime. To reduce the runtime, the calculations could be done by a linear combination of incomplete Riemann zeta integrals, as described in a paper by M. Levy and C. Honsberg [16], instead of the canonical Bose-Einstein integral used in this thesis.

The photon flux data for photon energies between 0.30 eV and 0.31 eV could have been extrapolated from the AM1.5 spectra to correct for the missing photon flux data in this energy range. This would especially improve the results for the efficiency of the cell where all band gaps are at their lowest. The lowest band gap in the calculations could also have been set to 0.31 eV. The method for calculating the incident photon flux from the AM1.5 specta could also have been improved to be more accurate.

7 Results and discussion

This chapter contains the results and discussion of efficiencies as a function of band gap sizes for the two and four terminal tandem cells, with single-junction and intermediate band solar cells (IBSCs) in various configurations. The efficiencies have been calculated for the AM1.5 spectra under a concentration of 1 sun, 100 suns, and 1000 suns. For concentrated radiation, the AM1.5 direct spectrum is used, as concentrator systems do not use the diffuse radiation.

The efficiencies of the solar cells are calculated using the principle of detailed balance, described in sections 3.3 and 4.2. In chapter 6 the model used in the simulations was described in detail.

In section 7.1 results from the simulations used in this thesis will be validated by comparing results from this work and other publications, using the same parameters.

Results from tandem cells with two IBSCs are presented and discussed in section 7.2. The tandem cells with a combination of IBSC and single-junction cells are treated in section 7.3. In these two sections the maximum efficiencies for the main band gaps of the two connected cells are presented and discussed, as well as the optimum sub-band gaps at the maximum efficiencies. Differences in the two and four terminal tandem cell are also covered.

The calculations are made with band gap energy steps of 0.05 eV. Band gap combinations between the selected numerical values can possibly yield higher efficiencies than found in this thesis. The figures showing plots of the various results are also affected by the large energy steps, and have a slightly low resolution. The consequences of the large energy steps are discussed in section 7.4.

Fabrication of IBSC with very specific band gap combinations can be difficult to achieve. In section 7.5 the band gaps giving the tandem cells high efficiencies are more closely examined.

7.1 Validation of the Matlab code

To validate the Matlab code, the model is used to calculate results that can be compared with other work. First the tandem IBSC is calculated for black body radiation and compared with the PhD thesis by Elisa Anotlin Fernández [15]. In this thesis work the performance of the tandem IBSCs are simulated using the AM1.5 spectra. The inclusion of the AM1.5 spectra in the Matlab code is tested by comparing the model for a single IBSC with results in a paper by S.P. Bremner [17], where the AM1.5 spectra is used.

7.1.1 Tandem IBSC under black body illumination

In the PhD thesis by Elisa Anotlin Fernández [15] the efficiencies of tandem cells have been calculated using the principle of detailed balance. The efficiencies for the same band gap combinations as found in the PhD thesis are calculated. The results are listed in table 7.1,

together with the results from the PhD Thesis. The incident radiation is taken to be that of a black body at 6000K under maximum concentration and the cell temperature is set to 300 K.

Table 7.1: Efficiencies of the tandem cell under maximum concentration of black body radiation (6000K), and cell temperature at 300 K. Results from this project (6th column) and Ref. [15] (5th column) for the given band gap energies.

$E_{G,Top}$	$E_{G,Bot}$	$E_{L,Top}$	$E_{L,Bot}$	Phd Thesis Efficiency (%)	This Work Efficiency(%)
2 IBSC, four terminal					
3.62	1.13	1.53	0.37	73.2	73.11
2 IBSC, two terminal					
2.98	0.93	1.21	0.29	72.7	72.70
Single-junction top cell and IBSC bottom cell, four terminal					
2.39	1.59		0.55	68.6	68.6
Single-junction top cell and IBSC bottom cell, two terminal					
1.65	1.39		0.47	64.6	64.59
IBSC top cell and single-junction bottom cell, four terminal					
2.48	0.49	0.96		68.5	68.43
IBSC top cell and single-junction bottom cell, two terminal					
2.83	0.52	1.13		67.9	67.85

As we can see from table 7.1, the results from this project and the PhD thesis have equal results when rounded off to one decimal, except for the four terminal IB tandem cell and the tandem cell with an IB top cell and a single-junction bottom cell. The IBSC tandem cell has the highest difference of about 0.12%, even lower when considering rounding off the efficiency to one decimal.

Discussion

The differences in efficiency values in table 7.1 are difficult to explain without comparing the codes in detail. The same spectrum is used, and hence it can not be responsible for the anomalies. As the current densities for the processes over both sub-band gaps are near equal in the simulations used in this master project, the efficiencies are not affected by which of the two current densities in equation (4.2.3) is used in equation (4.2.1). Difference in the method used to calculate the emitted photon flux can result in a small difference in the efficiency, but it is more likely that there is some variance in the code when finding the optimum voltage for the cells. As the code for the two terminal tandem cell is more extensive and complicated it would be expected that the largest difference would be found here, but table 7.1 shows the opposite. An increase in the number of voltage points in this thesis work to get a better accuracy, did not affect the efficiencies noticeably.

Even if there is a difference in the efficiencies compared with the results in [15], the dissimilarities are relatively small. The tandem model is therefore assumed to be well suited for an analysis of the intermediate band tandem solar cell.

7.1.2 Intermediate band solar cell with AM1.5 spectra

In a paper by S. Bremner, M. Levy and C Honsberg [17], the intermediate band solar cell has been modelled for the AM1.5 spectra. The same band gap values and concentration levels as in that paper have been used to reproduce results in this work. Band gap energies have been set at a range between 1.00 eV and 1.55 eV for the largest gap (0.99 eV and 1.60 eV in [17]) and 0.50 eV to 1.00 eV for the smallest gap (0.50 eV to 0.99 eV in [17]), with a step of 0.01 eV. The AM1.5 spectra from ASTM G-173 is used in this thesis and it is assumed that this is also used in [17], as the paper is published in 2008 and the G-173 spectra has been used as the standard AM1.5 spectra since 2003.

The maximum efficiencies and band gap energies from the referred paper are shown together with the efficiencies at the same band gap energies from this thesis work in table 7.2. We see from the table that the efficiencies in [17] are slightly larger than in this work, for the selected band gap values. Therefore the band gaps was varied slightly to find the maximum efficiencies for the simulations in this work, see table 7.2. In figure 7.1 the efficiencies calculated in ref [17] (left column) and this work (right column) are plotted as a function of the band gaps.

Table 7.2: Comparing band gap energies at the highest efficiencies from this thesis and the Ref. [17].

Source	Eg (eV)	E_{High} (E_{IV} in [17]) (eV)	E_{low} (E_{IC} in [17]) (eV)	Suns	Efficiency (%)
[17], peak D	2.4	1.48	0.92	1	49.4
This thesis	2.4	1.48	0.92	1	49.30
This thesis, max	2.42	1.49	0.93	1	49.41
[17], peak C	2.06	1.33	0.73	100	56.8
This thesis	2.06	1.33	0.73	100	56.21
This thesis, max	1.93	1.23	0.7	100	56.37
[17], peak B	1.94	1.24	0.7	1000	60.9
This thesis	1.94	1.24	0.7	1000	60.65
This thesis, max	1.91	1.22	0.69	1000	60.80

The band gap energies of the peak efficiency values are in fairly good agreement, see table 7.2. At the band gap combinations with the maximum efficiencies in [17], the largest deviation in efficiency is less than 1.04%. The largest deviation of both efficiency and band gap energies for maximum efficiency is found for the concentration value of 100 suns. In

figure 7.1 (b) the peak B is seen to also have a high efficiency at 100 suns, and at band gap energies very close to the highest efficiency from the results in this project.

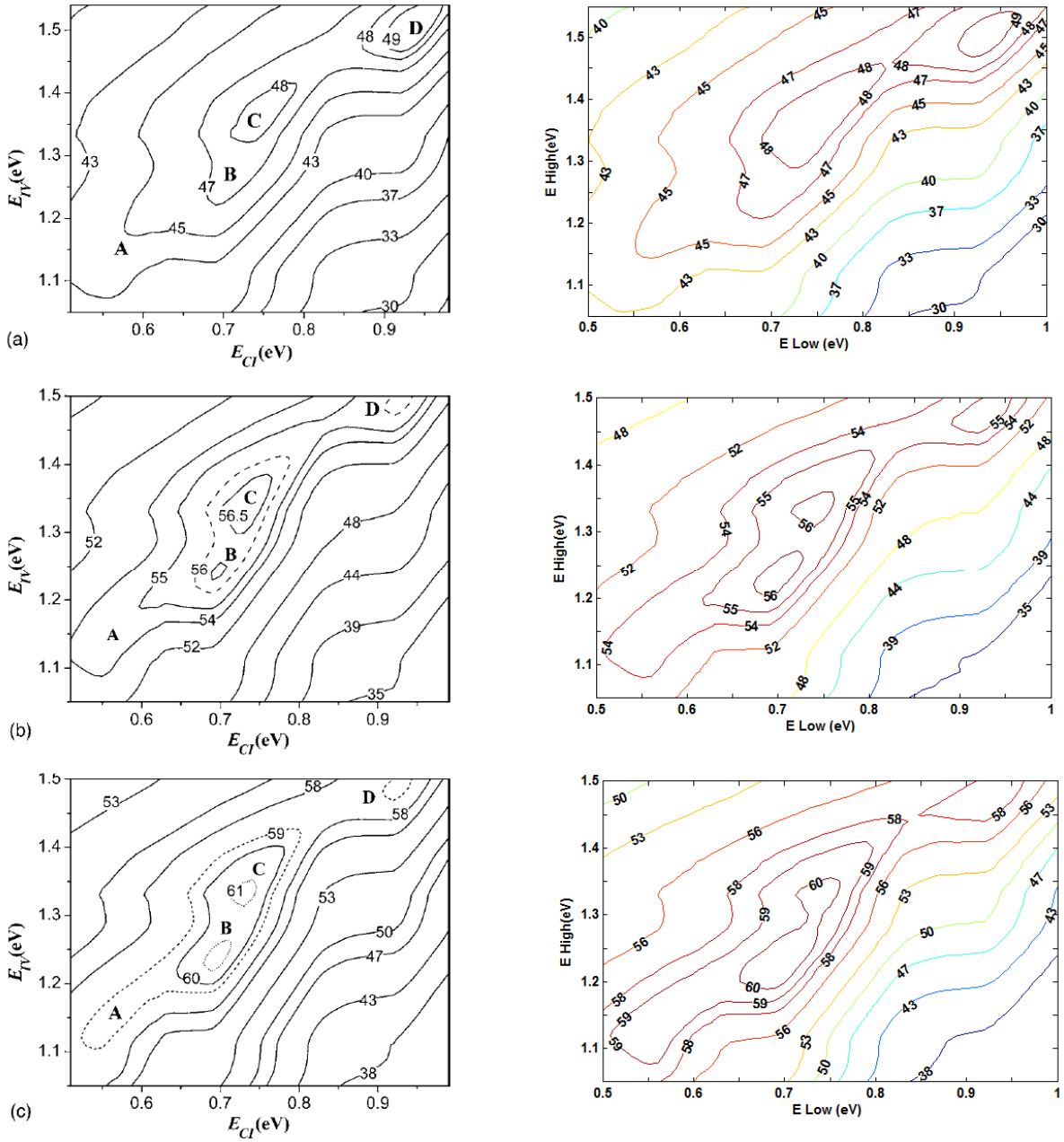

Figure 7.1: Efficiency contour plots under concentration (a) 1 (AM1.5 G), (b) 100 (AM1.5 D), and (c) 1000 (AM1.5 D). Plots on the right are results from this thesis work, while the plots on the left are Ref. [17]. Efficiency is given in percentage. Note that there are some small differences in the length of the axes.

Figure 7.1 shows that the efficiency contours follow a similar pattern for all concentration levels. The results from this master's project show higher efficiency for most band gap combinations under the global radiation, with no concentration of the light, see figure 7.1 a). This is very noticeable by the wider range of band gap combinations providing the cell with

efficiency over 48%. Efficiencies for 1000 suns concentration (figure 7.1 c) are also higher close to the lowest energy values for both band gaps.

For most band gap combinations with E_{High} values above 1.15 eV, the efficiencies for concentration level of 100 (b) and 1000 (c) are higher in [17]. This is for example clearly seen at band gap values near E_{High} = 1.43 eV and E_{Low} = 0.84 eV, also close to E_{High} = 1.10 eV and E_{Low} = 0.90 eV, and E_{High} = 1.40 eV and E_{Low} = 0.53 eV.

Discussion

The dissimilarities in efficiency are not easily explained as the scripting code cannot be compared in detail, but as the difference in efficiency is about 10 times larger than for the tandem cell with black body radiation discussed in 7.1.1, it is more likely the error is in the handling of the spectra. Differences in the photon flux absorbed because of the interpolation of the spectra, as well as the method used to find the highest and lowest photon energies limiting the summation of the flux, will result in some deviation in efficiency. This is coherent with the similarity in the deviations found for the results using the same direct spectrum for both 100 and 1000 suns concentration.

In [17] the radiative recombination has been calculated using a rapid flux calculation technique based on incomplete Riemann Zeta integrals (IRZIs). As this method has not been used in this thesis, there will possibly be deviations in the calculated photon flux emitted from the cell. In many cases the smallest of the current densities will not be completely equal, as equation (4.2.3) states they should be. In this thesis the smaller of the two current densities will then be added to the total current as the last current density in equation (4.2.1). If the comparing paper has a higher accuracy in solving equation (4.2.3) or only uses the current density gained from the transitions between the intermediate band and the conduction band, it would explain some of the lower efficiencies in the results from this master's project.

The similar traits for the contours in figure 7.1 and an error of only 1.04% in the maximum efficiencies makes the model viable for simulating the intermediate band solar cell with the use of the AM1.5 spectra.

7.2 Tandem IBSC under AM1.5 illumination

In this section the tandem cell composed of two IBSCs will be treated. The cell has been simulated for the concentration levels 1, 100 and 1000 suns. Results for both the two and four terminal cell are presented, starting with the four terminal tandem cell. High efficiency is a term assigned to efficiencies above 90% of the maximum efficiency for the cell under the same conditions. In the efficiency plots the 90% efficiency is shown indicated by a black line.

As there are six different band gaps in the tandem cells consisting of IBSCs, some notations are introduced to make the text more readable. $E_{G,Top}$ and $E_{G,Bot}$ refers to the main band gap energies of the top and bottom cell respectively. The notations $E_{L,Top}$ and $E_{L,Bot}$ will refer to the lowest sub-band gap of the top and bottom IBSCs.

7.2.1 Four terminal IBSC

The four terminal tandem cell has the highest efficiency, as both the top cell and the bottom cell operate at their optimum voltage.

Efficiencies at 1 sun

The efficiency for the cell simulated for 1 sun concentration is presented in figure 7.2.

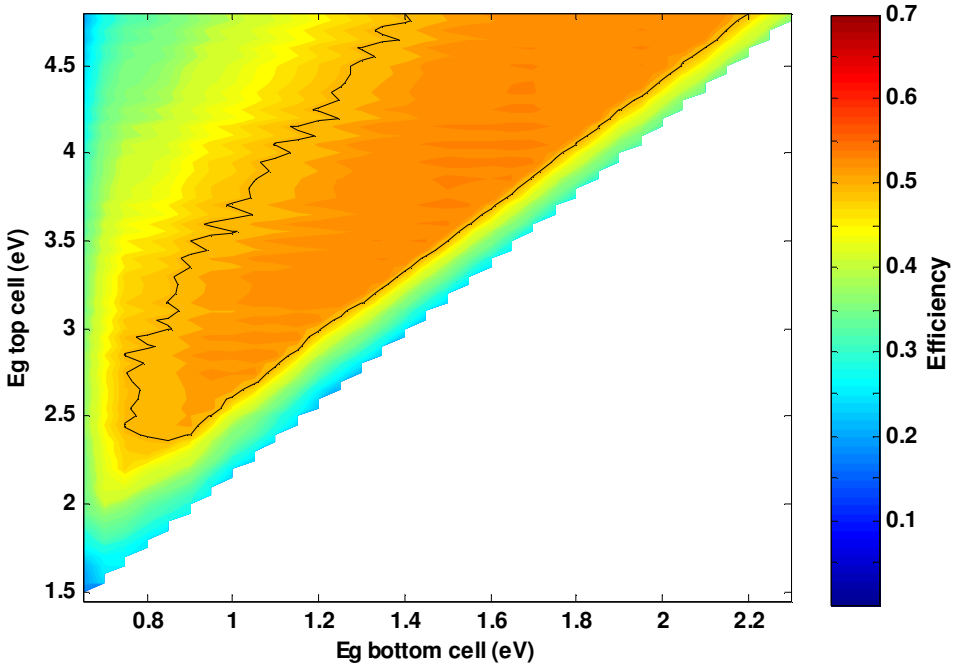

Figure 7.2: Efficiency of the tandem cell under 1 sun, area function of the main band gap energies of the top and bottom cell.

The maximum efficiency is 54.93%, for a top and bottom cell main band gap energy of 4.05 eV and 1.65 eV respectively, and lowest band gap energy of 1.80 eV and 0.55 eV respectively. For band gap combinations with $E_{G,Top}$ in the range of 2.40 eV to 4.80 eV and $E_{G,Bot}$ in the range of 0.75 eV to 2.15 eV, efficiency over 49.44% (90% of 54.93%) is achieved, represented by the black line in figure 7.2. The band gap range giving high efficiencies for $E_{G,Top}$ is limited by the simulation, as values above 4.80 eV for $E_{G,Top}$ are not included. Larger band gap ranges for both $E_{G,Top}$ and $E_{G,Bot}$ giving high efficiencies are thus expected.

As it would be interesting to see how much and at what band gap energies the top and bottom cell contribute to the cell total power, the separate contributions to the total efficiency from the bottom and top cell are displayed in figure 7.3 and 7.4.

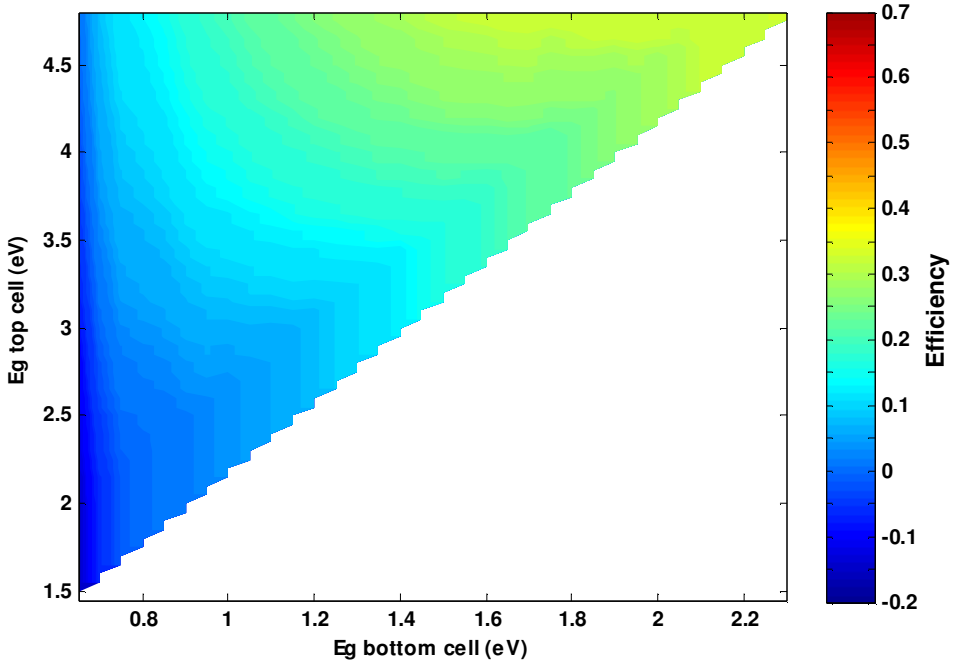

Figure 7.3: Efficiency at different band gap energy values for the bottom cell under 1 sun concentration.

The bottom cell reduces the efficiency of the complete tandem cell for some combinations with bottom main band gap energies in the range 0.65 eV to 0.75 eV, see figure 7.3. The efficiencies for the bottom cell increase with an increase of $E_{G,Bot}$ and consequently also $E_{G,Top}$.

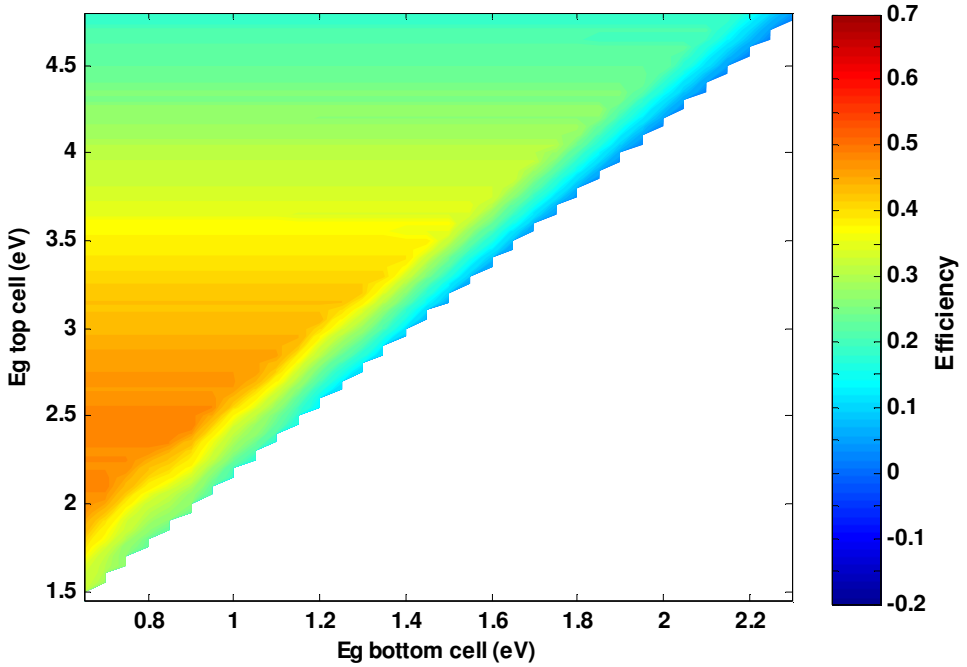

Figure 7.4: Efficiency for different main band gap combinations for the top cell under 1 sun concentration.

The top cell has the highest efficiency within the $E_{G,Top}$ range from 1.75 eV to 3.40 eV, but the efficiency then decreases as $E_{G,Top}$ increases. For each value of $E_{G,Top}$, the efficiency drops when $E_{G,Bot}$ is increased close to its maximum for that specific value of $E_{G,Top}$. At these band gap combinations the efficiency for the bottom cell is also increasing rapidly, see figure 7.3.

Discussion

The tandem cell consisting of two IBSCs has an increase in the limiting maximum efficiency of 11% compared to the single IBSC in section 7.1.1 (, from 49.41% to 54.93%). Series connected cells are expected to have an even lower increase in efficiency. Similar to the single IBSC, the tandem cell has high efficiency for a wide range of main band gap energies. The band gap combinations for the top and bottom cell that provide the highest efficiency for the tandem cell, are mostly at band gap energies that are above or below the optimum values for the single IBSC. $E_{G,Top}$ values are above the optimum band gap values for the single IBSC, but the highest $E_{G,Bot}$ values are also optimum for the single IBSC. Figure 7.5 shows the maximum efficiency for a single IBSC at the different main band gap values. Semiconductor materials that cannot be used for single IBSC, can then be considered for high efficiency tandem cells.

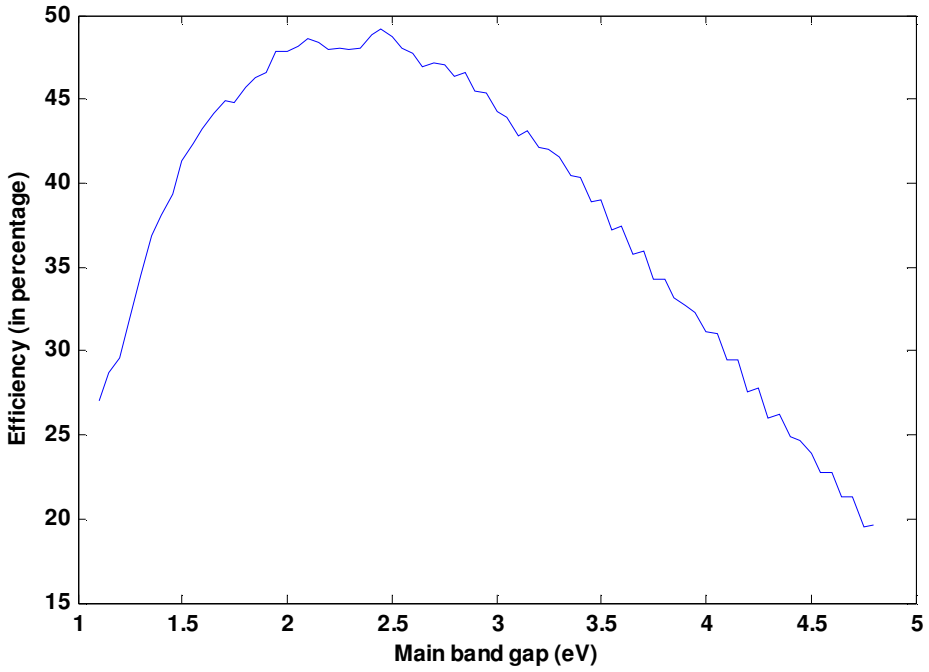

Figure 7.5: The maximum efficiencies for the single IBSC at various main band gap values.

With main band gap energies for the top cell from 3.15 eV to 4.80 eV (the highest band gap used) and for the bottom cell from 1.05 eV to 2.15 eV, there are combinations that give efficiencies over 52% for the tandem cell. At most of these band gap energies, the single IBSCs have lower efficiencies, see figure 7.5, but an increase in efficiency close to 20% is feasible with such IBSCs in a tandem cell.

As can be expected, the top cell contributes more to the power output for low band gap energies, and the power decreases as the band gap increases. At larger band gaps more of the

radiation is transmitted through the top cell and absorbed by the bottom cell, hence increasing the power output of the bottom cell and reducing the power output of the top cell. For a given value of $E_{G,Top}$ there is a decrease in efficiency of the top cell and increase in the bottom cell efficiency as $E_{G,Bot}$ is getting increasingly closer to its highest value, for that specific value of $E_{G,Top}$. This is a result of an increase in $E_{L,Top}$ at these band gap regions, as seen in figure 7.10 later in this section. The increase in $E_{L,Top}$ is due to a restriction in the model, mentioned in section 6.3, where $E_{G,Bot}$ needs to be smaller than $E_{L,Top}$. This causes the values for $E_{L,Top}$ to increase in these regions to compensate for higher values of $E_{G,Bot}$, and as these values of $E_{L,Top}$ are not the optimum for the top cell the efficiency is reduced. The effect of this is also seen in the efficiency of the complete tandem cell.

The bottom cell has a negative current at low band gap energies and consequently a negative efficiency in the simulations. Figure 7.6 shows the photon fluxes absorbed and emitted for the bottom IBSC using the AM1.5G spectrum under 1 sun concentration, where the band gaps are set at $E_{L,Top}$ = 1.15 eV, $E_{G,Bot}$ = 0.30 eV and a varying $E_{G,Bot}$ from 0.65 eV to 0.85 eV. In figure 7.7 the same case has been simulated using the black-body radiation (6000K). The photon fluxes are the total flux from the bottom IBSC; the sum of flux absorbed (or emitted) for the main band gap and one of the sub-band gaps. Only the flux from the processes over one of the sub-band gap is used. The sub-band gap process that has the lowest emitted flux compared to the absorbed flux is chosen, similar to the other simulations in this thesis. This causes the flux to fluctuate in value for the different main band gap energies. As the flux has been calculated for a varying $E_{G,Bot}$ value of 0.01 eV in each step, the graphs only show the photon flux roughly, and do not show the exact flux value for the continuous energy spectrum of $E_{G,Bot}$.

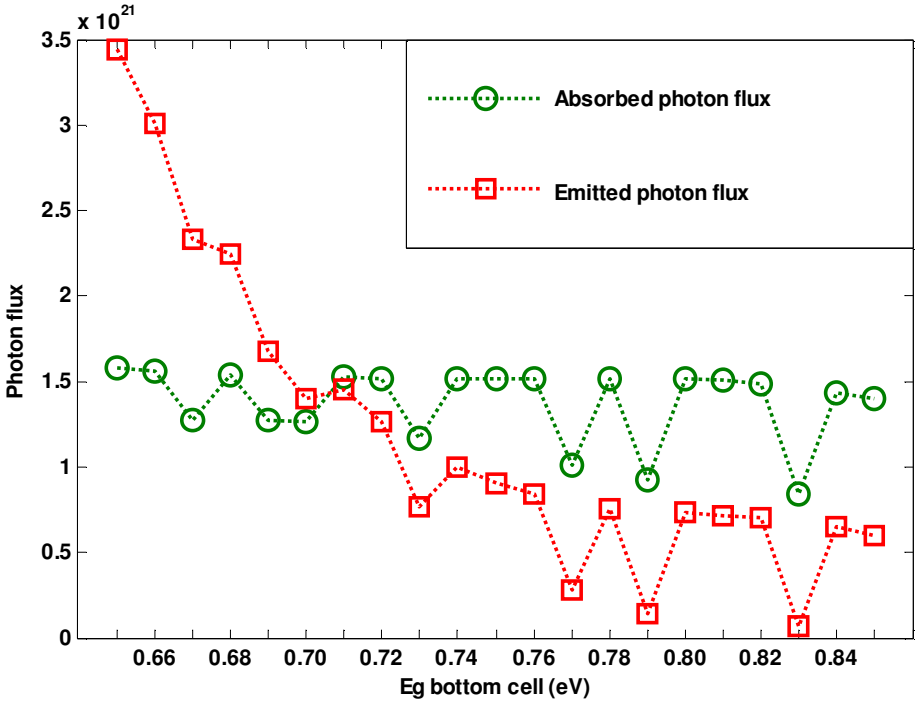

Figure 7.6: Photon flux emitted (red) and absorbed (green) by the bottom IBSC, using the AM1.5G radiation with 1 sun concentration. Only the points at 0.01 eV steps are results from the calculation.

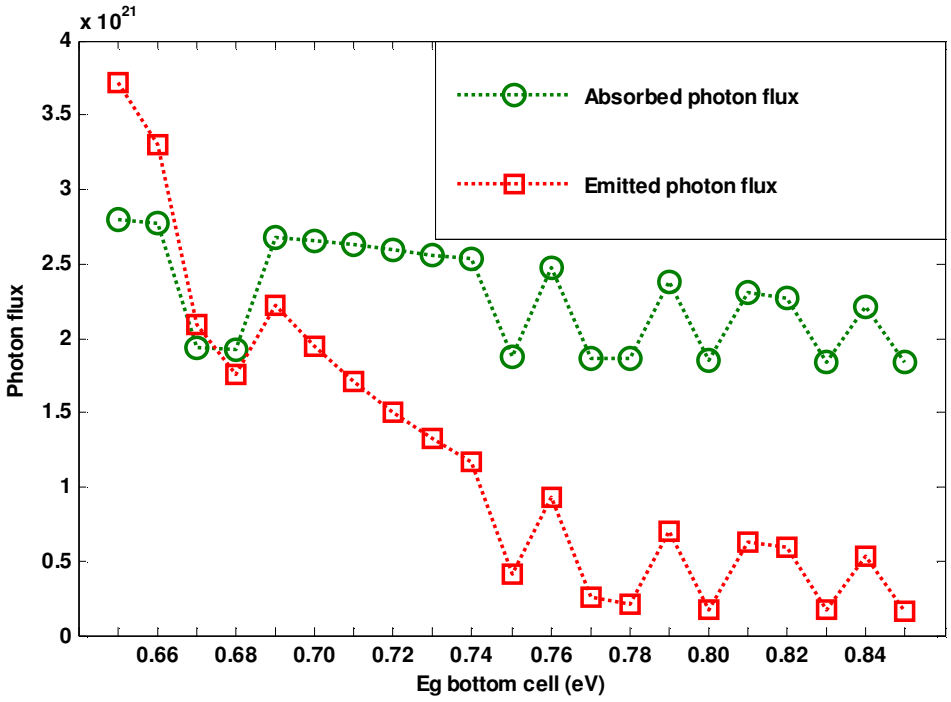

Figure 7.7: Photon flux emitted (red) and absorbed (green) by the bottom IBSC, using the black-body radiation (6000K) with 1 sun concentration. Only the points at 0.01 eV steps are results from the calculation.

Figures 7.6 and 7.7 both show a higher emitted photon flux than absorbed for the lowest main band gaps of the bottom cell. The photon flux from the black-body spectrum is higher than the flux from the AM1.5 spectrum. This is probably an effect of the AM1.5 spectra missing data for the photon flux at photon energy lower than 0.31 eV. The negative current contribution by the bottom cell is clearly an effect of the high emitted photon flux, and not an effect of the missing data for the AM1.5 spectra, as the simulations using the black-body radiation has a similar result.

Efficiencies at 100 and 1000 suns

The efficiencies for the tandem IBSC with concentrated sunlight are shown in figure 7.8 for 100 suns and figure 7.9 for 1000 suns. For concentrated sunlight the bottom cell does not have a negative efficiency, as was the case with no concentration.

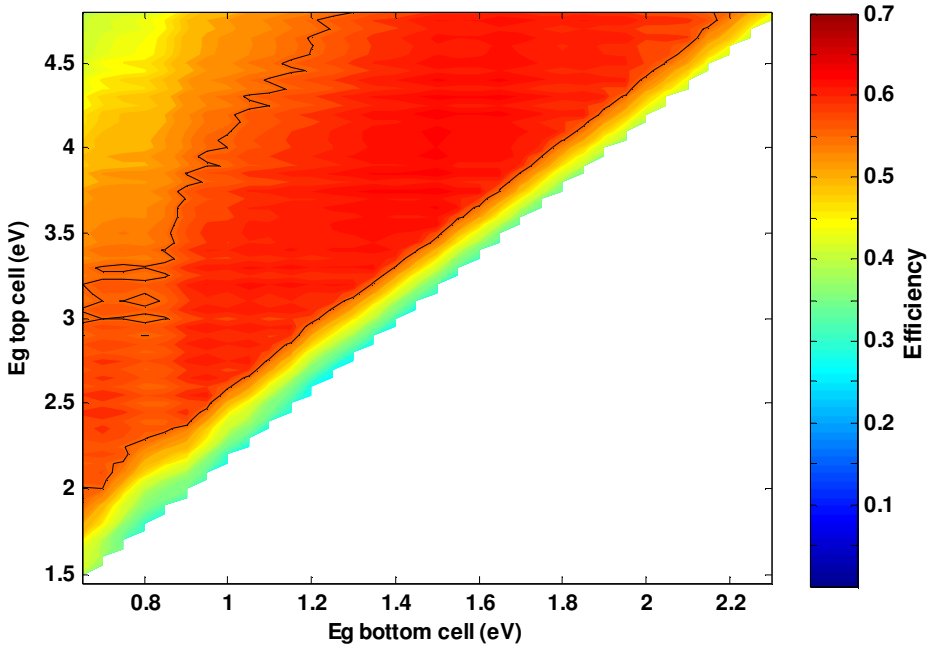

Figure 7.8: Efficiency of the tandem cell under 100 suns, area function of the main band gap energies of the top and bottom cell.

The maximum efficiency for 100 suns concentration is 62.74%. It is found at the main band gap energies 3.75 eV and 1.50 eV, and at the lowest sub-band gap energies 1.65 eV and 0.50 eV for the top and bottom cell respectively. The tandem cell has a high efficiency over 56.47%, with band gap combinations found at the $E_{G,Top}$ range from 1.95 eV (, even if the plot seems to show 2.00 eV,) to 4.80 eV and the $E_{G,Bot}$ range from 0.65 eV to 2.15 eV.

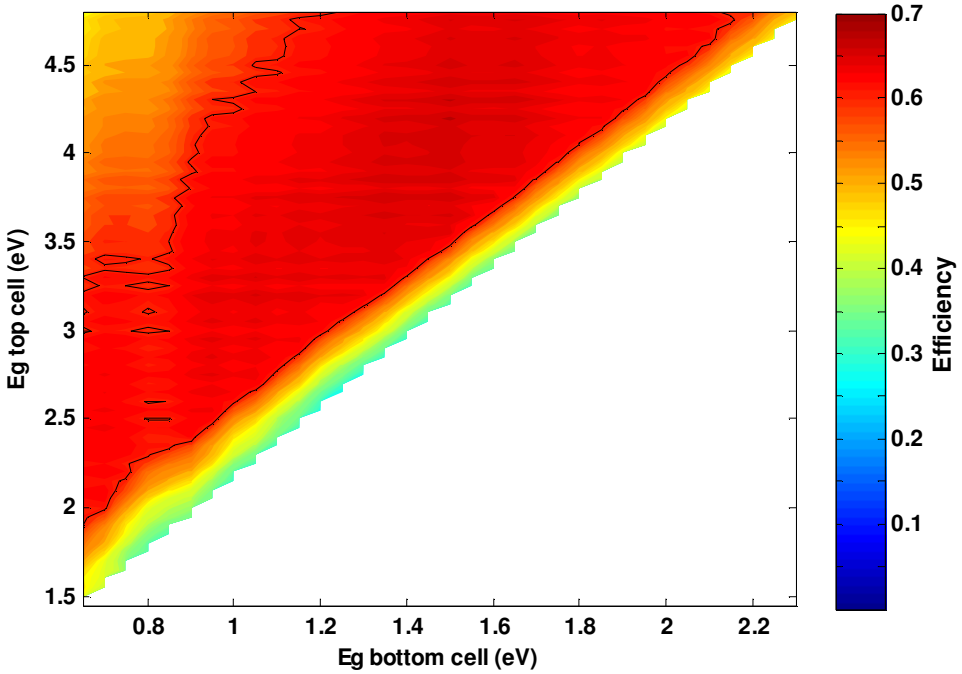

Figure 7.9: Efficiency of the tandem cell under 1000 suns, area function of the main band gap energies of the top and bottom cell.

The maximum efficiency for 1000 suns concentration is 67.23%, with the main band gap energies 4.30 eV and 1.50 eV, and lowest sub-band gap energies 1.95 eV and 0.50 eV for the top and bottom cell respectively. Band gap combinations that give efficiencies over 60.51% are found at the range for $E_{G,Top}$ from 1.90 eV to 4.80 eV and for $E_{G,Bot}$ from 0.65 eV to 2.15 eV. Both of the efficiency plots for tandem cells under concentrated sunlight show a high efficiency for wide ranges of band gap combinations, similar to the plot in figure 7.2 for the cell under no concentration.

Discussion

Compared to the single cell IBSCs under concentrated radiation, the maximum efficiency has an increase close to 11% for the tandem cells, which is similar to the case with no concentration. Since the efficiency is only calculated for band gap energies with a 0.05 eV step, there will probably be band gaps between the steps that provide higher efficiencies. The band gap energies at the maximum efficiencies vary a lot for the different concentration values, but there are local efficiency peaks at similar band gap combinations for all the various levels of concentration. The range of band gaps that provide the tandem cell with high efficiency increases with concentration level. It is most noticeable for the top cell ranges from the concentration level of 1 sun to 100 suns, while there is only a slight increase from 100 suns to 1000 suns. The increase in the band gap range is possibly a consequence from the difference in the light distribution, as the diffuse radiation is not used by the cell under concentrated light. The diffuse radiation increases the photon flux at high photon energies and could then have the discussed effect on the band gap ranges.

Sub-band gap energies

The sub-band gaps in the IBSC are the gaps between the valence band and the intermediate band and between the intermediate band and conduction band. The efficiency of an IBSC is very dependent on the position of the intermediate band in the main band gap, and consequently also on the sub-band gap energies. How the optimum sub-band gap energies change for the variation in the main band gaps is hence also presented for each of the tandem cells in this chapter.

The optimum band gap energies for the lower sub-band gaps in the top ($E_{L,Top}$) and bottom ($E_{L,Bot}$) IBSC are displayed in figures 7.10 to 7.15. These are the band gap combinations for the highest tandem cell efficiencies, and the figures show the optimum lowest sub-band gaps for the specific main band gaps.

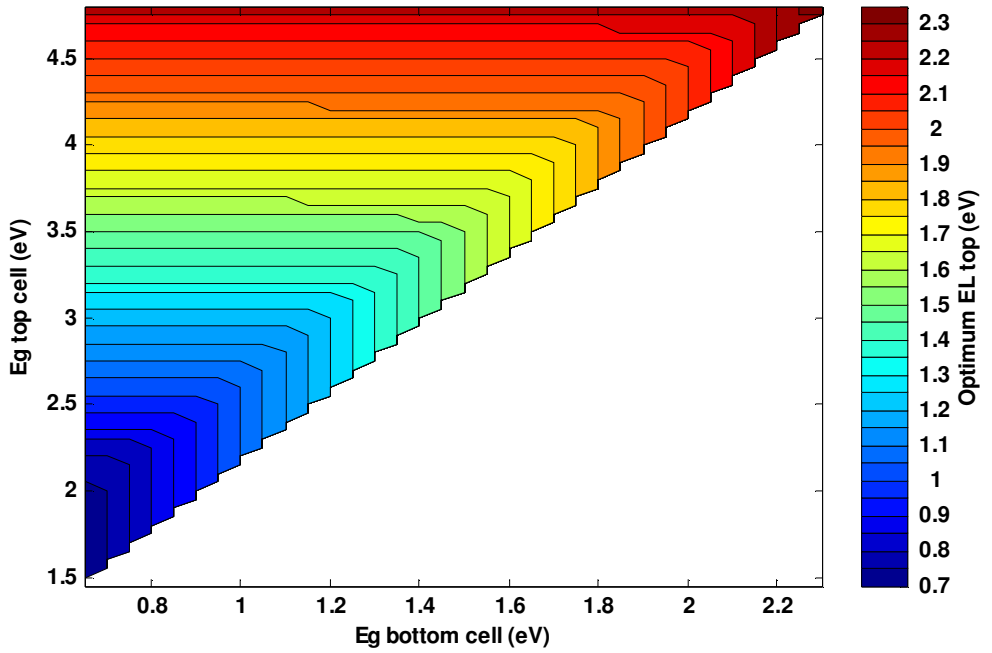

Figure 7.10: The optimum lowest sub-band gap energies for the top cell ($E_{L,Top}$). Concentration level is 1 sun.

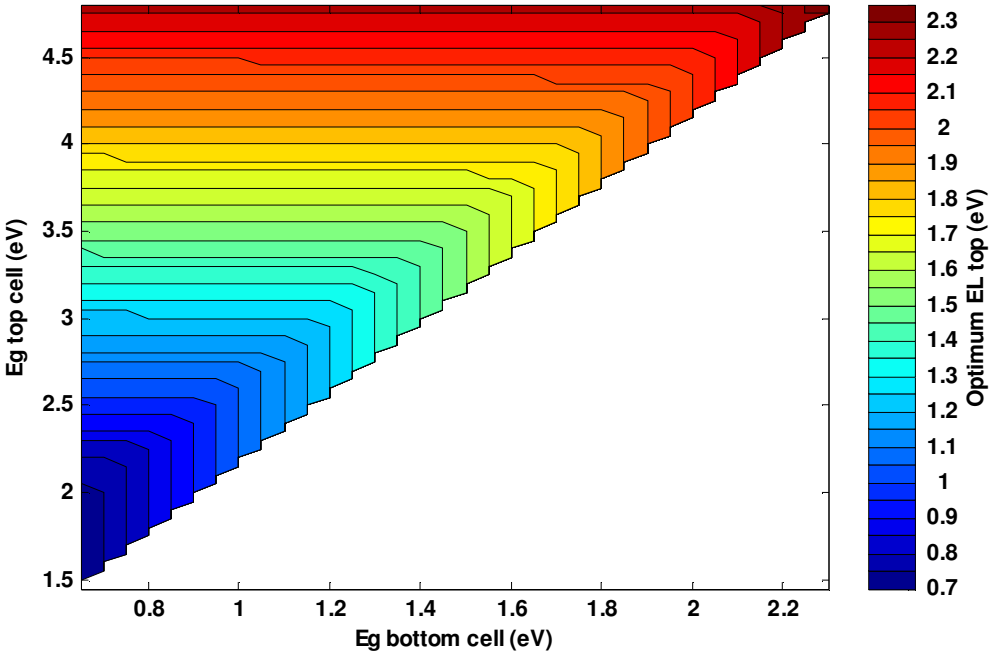

Figure 7.11: The optimum lowest sub-band gap energies for the top cell ($E_{L,Top}$). Concentration level is 100 suns.

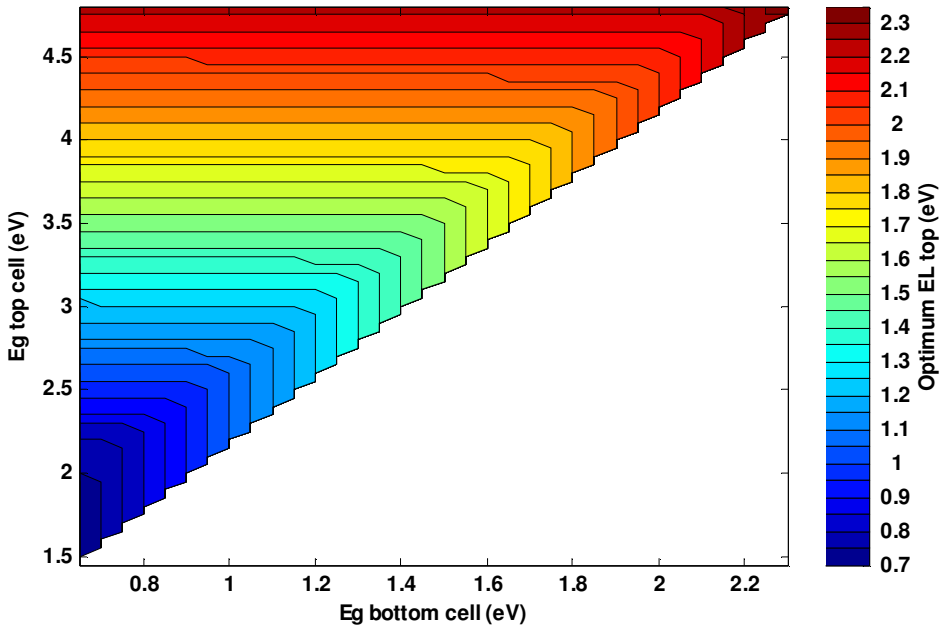

Figure 7.12: The optimum lowest sub-band gap energies for the top cell ($E_{L,Top}$). Concentration level is 1000 suns.

Figure 7.10, 7.11 and 7.12 all show that $E_{L,Top}$ increases as the top main band gap increases. The optimum lowest sub-band gap is almost constant for each of the main band gap energies of the top cell, but increases sharply as the bottom main band gap increases closer to its maximum value. The concentration level seems to have a small effect on the optimum $E_{L,Top}$ values.

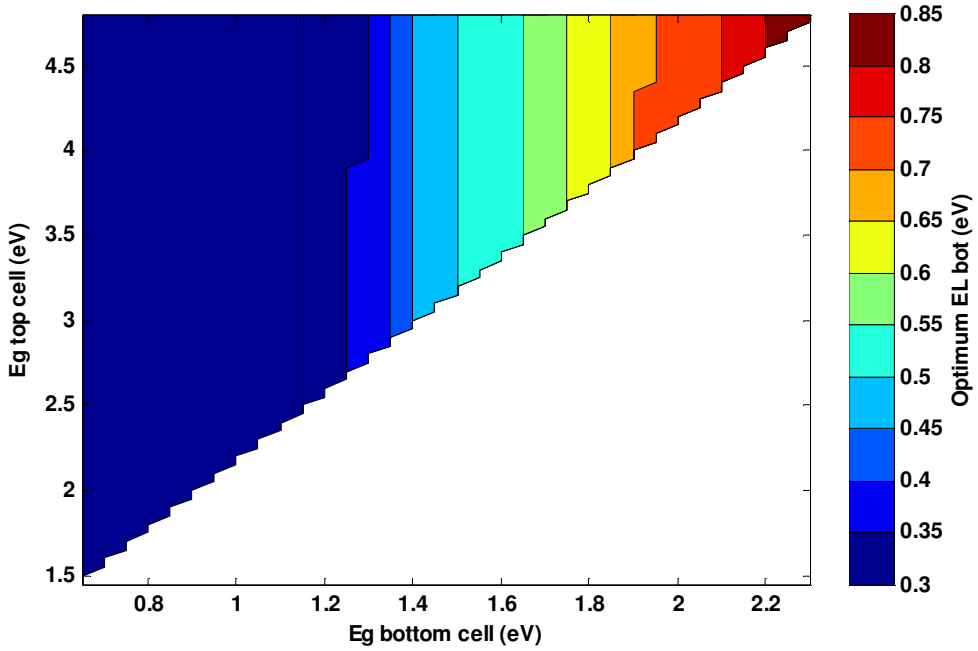

Figure 7.13: The optimum lowest sub-band gap energies for the bottom cell ($E_{L,Bot}$). Concentration level is 1 sun.

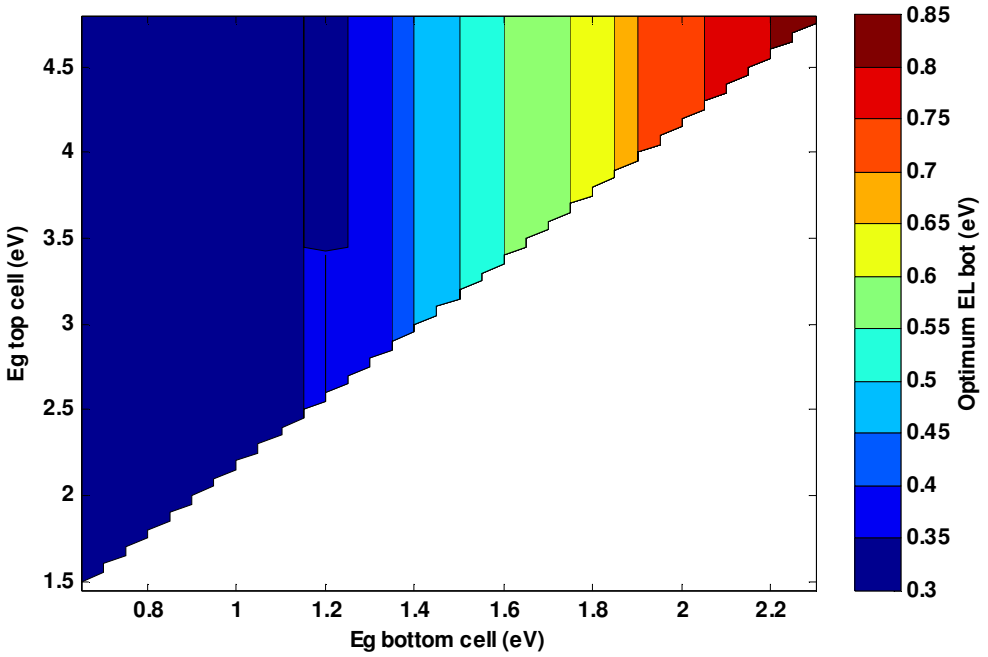

Figure 7.14: The optimum lowest sub-band gap energies for the bottom cell ($E_{L,Bot}$). Concentration level is 100 suns.

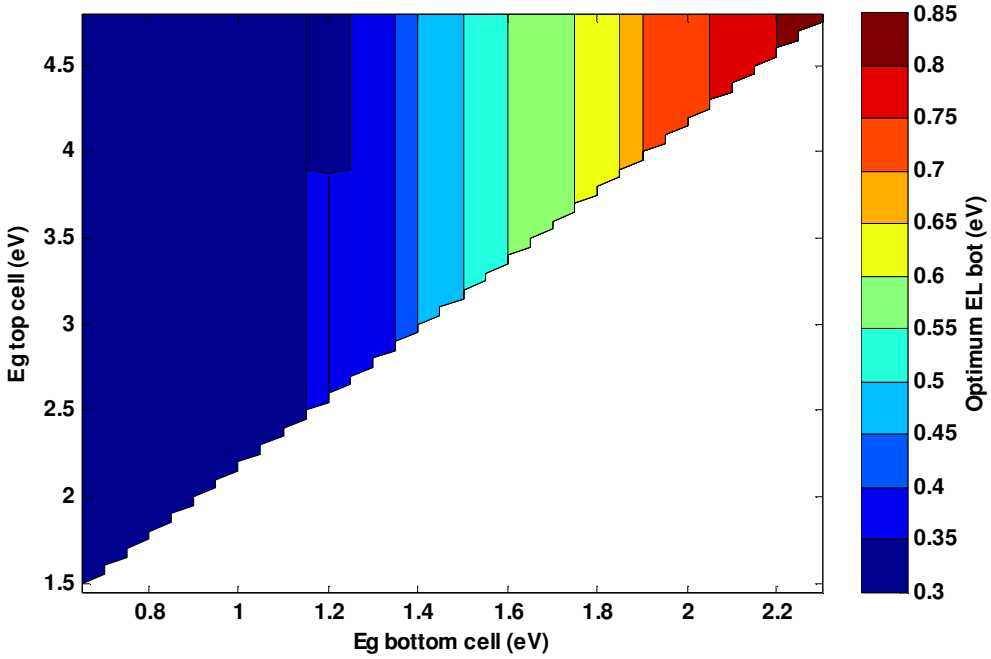

Figure 7.15: The optimum lowest sub-band gap energies for the bottom cell ($E_{L,Bot}$). Concentration level is 1000 suns.

The optimum lowest band gap values are similar for all concentration levels. $E_{L,Bot}$ is at its minimum (0.30 eV) for all $E_{G,Bot}$ values up to 1.10 eV. The optimum lowest sub-band gap then increases with higher values of $E_{G,Bot}$, with some small irregularities at the value of $E_{G,Bot}$ close to 1.20 eV and also at 1.90 eV for the 1 sun concentration. Figure 7.14 and 7.15 show that for $E_{G,Bot}$=1.20 eV, $E_{L,Bot}$ drops in value when $E_{G,Top}$ is over 3.85 eV.

Discussion

The optimum lowest sub-band gap for both the top and the bottom cell increases as the respective main band gap increases. As a result, a similar ratio between the two sub-band gaps will remain for the various main band gap energies. The electrons need to be excited over both sub-band gaps to be collected by the cell contacts. High efficiencies will then be found when the absorbed photon flux is divided similarly for the processes over the two sub-band gaps.

As discussed previously in this chapter, the increase in $E_{L,Top}$ in figure 7.10, 7.11 and 7.12 for high values of the bottom main band gap is a consequence of constrictions in the model ($E_{L,Top} > E_{G,Bot}$).

The optimum $E_{L,Bot}$ values have some irregular behaviour when $E_{G,Bot}$ is about 1.2 eV. It is clearly seen for the case with 100 and 1000 suns concentration in figure 7.14 and 7.15 at $E_{G,Bot}$ = 1.20 eV. For high values of $E_{G,Top}$ (3.90 eV for 1000 suns), the optimum value for $E_{L,Bot}$ drops to 0.30 eV. This is an effect of an increase in the current in the bottom cell, as the photon flux absorbed by the bottom cell increases as the value of $E_{L,Top}$ is raised. For a more detailed study of this behaviour, the I-V characteristics for the $E_{L,Bot}$ values 0.30 eV (red curve), 0.35 eV (blue curve) and 0.40 eV (black curve) for an IB bottom cell at 1000 suns are plotted in figures 7.16, 7.17 and 7.18. The characteristics for two different values of $E_{L,Top}$ (1.80 eV and 1.45 eV) are displayed, each for a corresponding $E_{G,Top}$ value above and below 3.90 eV. In figure 7.16 the I-V characteristics where $E_{G,Bot}$ has the value 1.20 eV are plotted.

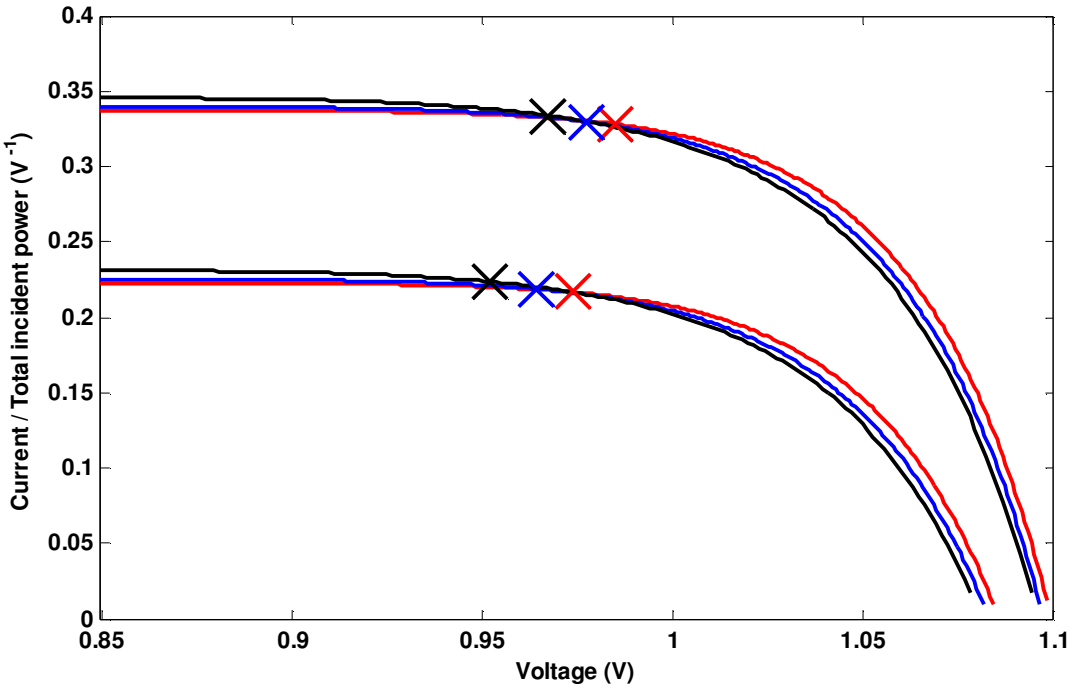

Figure 7.16: I-V plots for the bottom IBSC in a tandem cell (1000 suns concentration) with $E_{G,Bot}$ = 1.20 eV, for 3 different values of $E_{L,Bot}$ and two different values for $E_{L,Top}$. The three highest current values are from the results where $E_{L,Top}$= 1.80 eV, and three lowest currents have $E_{L,Top}$=1.45 eV. The values for $E_{L,Bot}$ are: 0.30 eV (red) , 0.35 eV (blue) and 0.40 eV (black). The crosses show the point of highest power.

Figure 7.16 shows that the I-V characteristics of the different $E_{L,Bot}$ values are very close for these main band gap values. It is clear that when $E_{L,Top}$ is raised from 1.45 eV to 1.80 eV the current is significantly increased in the bottom cell. Thus a small increase in voltage has a larger effect on the efficiency. As can be seen from Figure 7.16, the curves for the lowest values of $E_{L,Bot}$ have a higher voltage at the same current. The efficiencies from the bottom cell used in figure 7.16 vary from 32.21% to 32.31% and from 21.09% to 21.28%.

$E_{G,Bot}$ has the value 1.00 eV in figure 7.17 and 1.35 eV in figure 7.18.

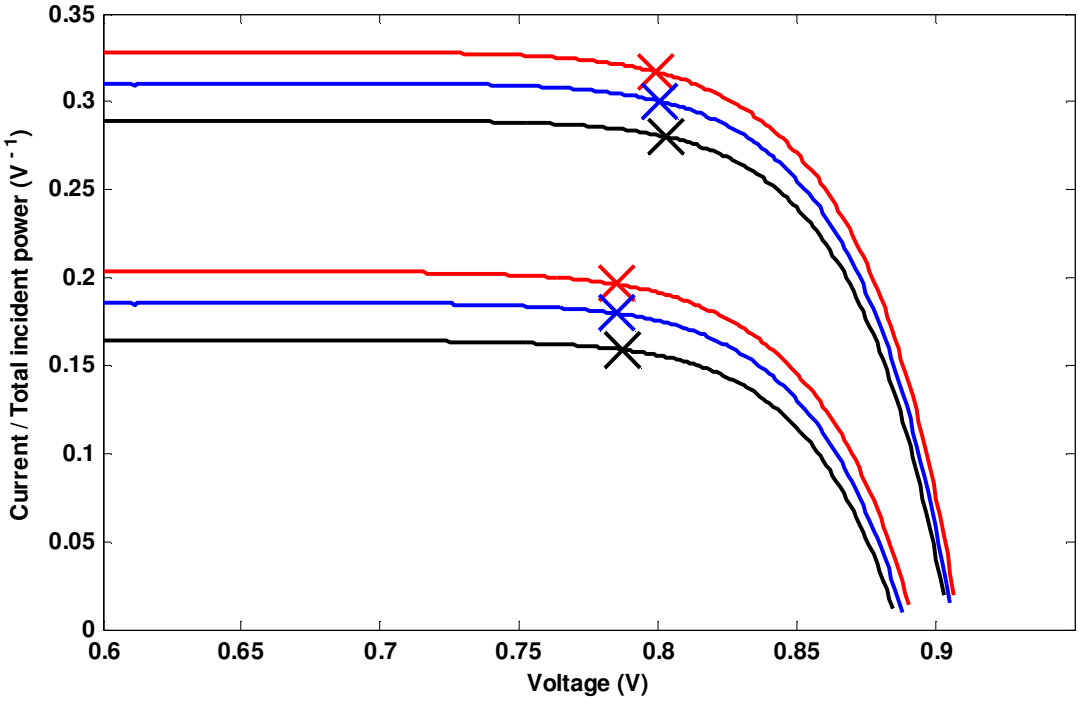

Figure 7.17: I-V plots for the bottom IBSC in a tandem cell (1000 suns concentration) with $E_{G,Bot}$ = 1.00 eV, for 3 different values of $E_{L,Bot}$ and two different values for $E_{L,Top}$. The three highest current values are from the results where $E_{L,Top}$= 1.80 eV, and three lowest currents have $E_{L,Top}$=1.45 eV. The values for $E_{L,Bot}$ are: 0.30 eV (red) , 0.35 eV (blue) and 0.40 eV (black). The crosses show the point of highest power.

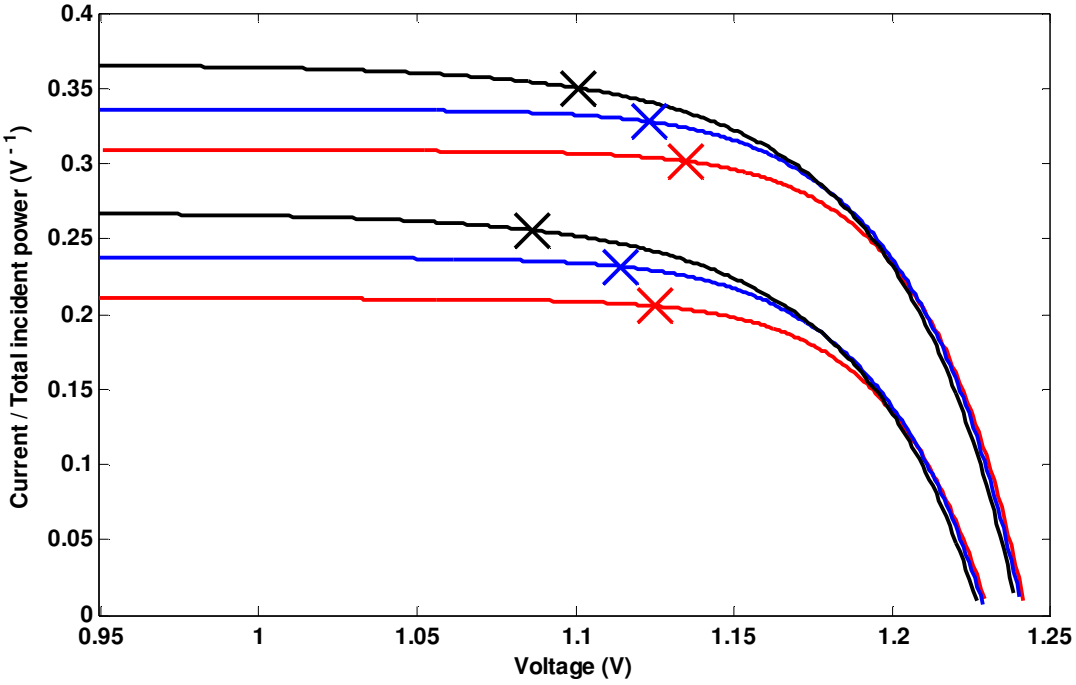

Figure 7.18: I-V plots for the bottom IBSC in a tandem cell (1000 suns concentration) with $E_{G,Bot}$ = 1.35 eV, for 3 different values of $E_{L,Bot}$ and two different values for $E_{L,Top}$. The three highest current values are from the results where $E_{L,Top}$= 1.80 eV, and three lowest currents have $E_{L,Top}$=1.45 eV. The values for $E_{L,Bot}$ are: 0.30 eV (red) , 0.35 eV (blue) and 0.40 eV (black). The crosses show the point of highest power.

The reason that there are irregularities only for a few of the $E_{G,Bot}$ values, is because at these values the current-voltage characteristics for the three different $E_{L,Bot}$ values are very similar to each other. For other values of $E_{G,Bot}$, the I-V plots have larger differences in current densities, as can be seen from the figures 7.17 and 7.18.

A rule of thumb used in positioning the IB in the main band gap is to have the smallest sub-band gap size set to about a third of the main band gap. As the IBSCs in the tandem cell show a higher ratio for the top cell for all $E_{G,Top}$ and for some values of $E_{G,Bot}$ for the bottom cell, the ratios have been compared with the single IBSC used in section 7.1.2. Figure 7.19 shows the ratios for all three IBSCs under the AM1.5G spectrum and with a concentration level of 1 sun. The optimum lowest sub-band gaps for the top IBSC used to calculate the ratios are the $E_{L,Top}$ values found for the $E_{G,Bot}$ value of 0.65 eV. The ratios for the bottom cell are calculated using the $E_{L,Bot}$ values for the $E_{G,Top}$ value of 4.80 eV.

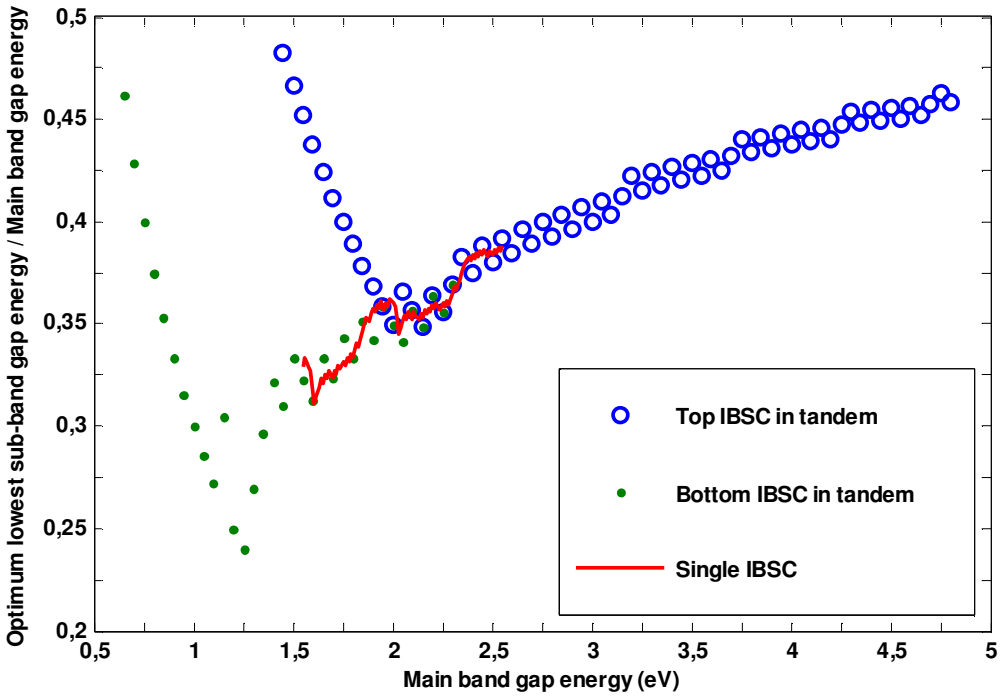

Figure 7.19: The ratios between the optimum lowest sub-band gap and the main band gap of the IBSCs. The ratio for a single IBSC (red), the top IBSC in a tandem cell (blue) and the bottom cell in a tandem cell (green) are all shown in the plot. Concentration level set to 1 sun.

In figure 7.19 there are some high ratios for the smallest main band gaps for both of the IBSCs in the tandem cell. This is most likely a consequence of constricting the smallest sub-band gap to 0.70 eV for the top IBSC and 0.30 eV for the bottom IBSC. The ratio values below the main band gap energy of 1.95 eV for the top IBSC and below the main band gap value of 1.2 eV for the bottom cell, are thus ignored.

The band gap ratios for the three IBSC seem to follow a similar increase in the optimum value for the smallest sub-band gap, as the main band gap increases. It is seen in figure 7.19 that the ratio for a single IBSC for main band gap energies above 2 eV is also higher than one third. The largest deviation in ratio for the tandem IBSCs from the ratio for a single IBSC is below 5%, and it is concluded that connecting an IBSC in a four terminal tandem cell has a small effect on the ratio between the smallest sub-band gap and the main band gap. An exception to this is for some main band gaps of the bottom IBSC, for example when $E_{G,Bot}$ is close to 1.20 eV, as discussed earlier in this section.

7.2.2 Two terminal IBSC

The following results are for the series connected tandem cell with two IBSCs. The two IBSCs are constrained by having an equal current, as described in section 5.2.

Efficiencies for 1, 100 and 1000 suns

The following three figures show the efficiency for the two terminal tandem IBSC with the concentration levels 1, 100, and 1000.

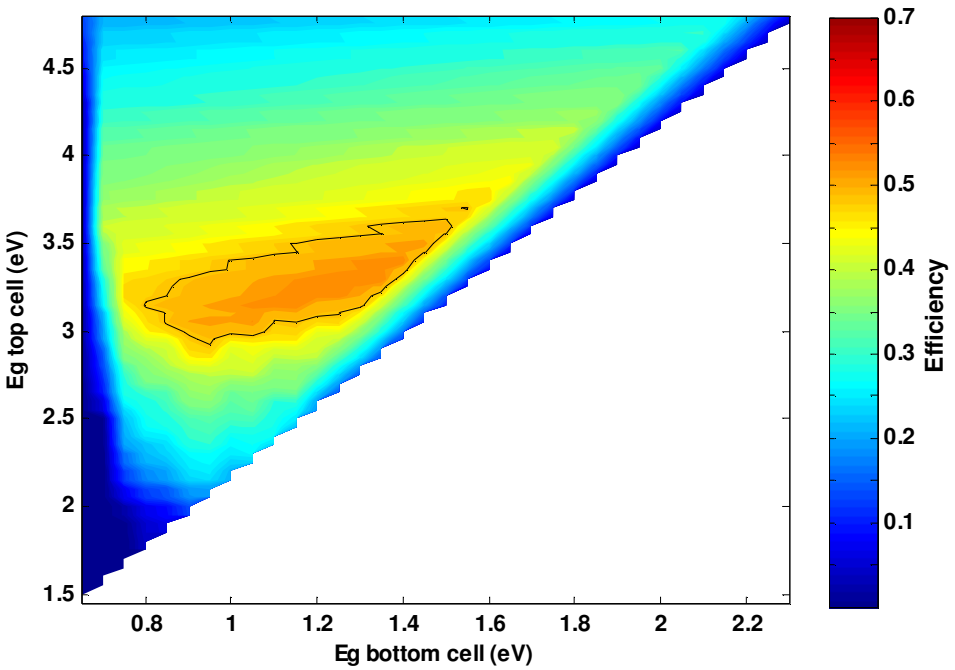

Figure 7.20: Efficiency of the series connected tandem cell under 1 sun, area function of the main band gap energies of the top and bottom cell.

For the lowest concentration level the maximum efficiency is 53.88% with the following band gap values: $E_{G,Top}$ at 3.30 eV , $E_{G,Bot}$ at 1.35 eV, $E_{L,Top}$ at 1.40 eV and $E_{L,Bot}$ at 0.40 eV. The efficiency is over 48.49% for band gap combinations in the range of $E_{G,Top}$ from 2.95 eV to 3.70 eV and $E_{G,Bot}$ from 0.80 eV to 1.55 eV. Comparing figure 7.20 with figure 7.2 shows that the range of band gap combinations providing the cell with high efficiency is much lower than for the four terminal cell.

The efficiency has not been calculated for the band gaps of the bottom cell where the current is negative, because this would result in a negative efficiency for the complete tandem cell. In figure 7.20 this band gap area has instead an efficiency set to zero. The negative efficiency in the bottom IBSC has already been discussed in section 7.2.1.

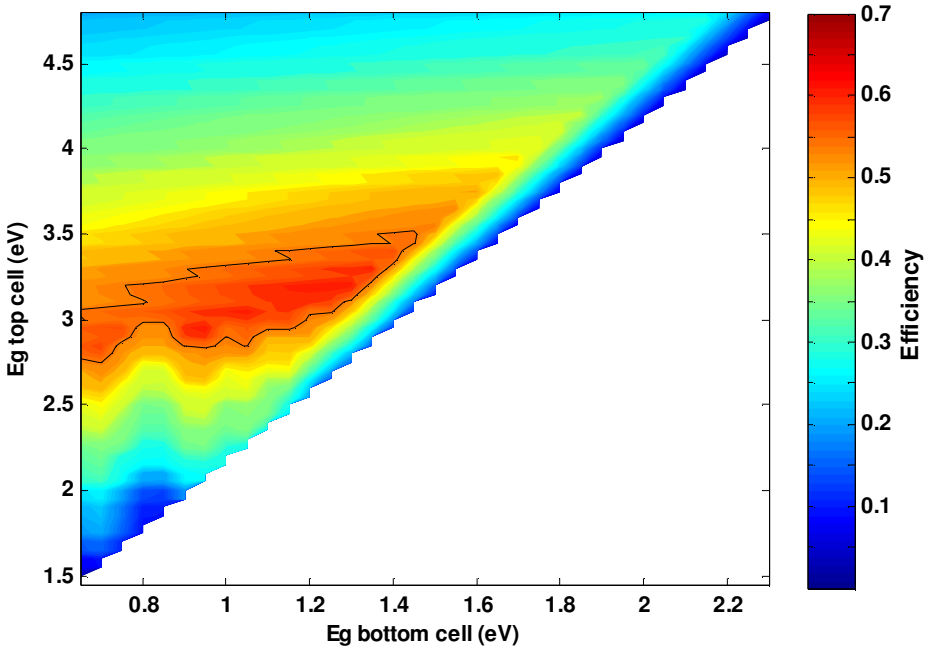

Figure 7.21: Efficiency of the series connected tandem cell under 100 suns, area function of the main band gap energies of the top and bottom cell.

For the cell under 100 suns the maximum efficiency is increased to 61.01%, with the band gap values: $E_{G,Top}$ = 3.20 eV , $E_{G,Bot}$ = 1.25 eV , $E_{L,Top}$ = 1.35 eV and $E_{L,Bot}$ = 0.35 eV. Band gap combinations in the $E_{G,Top}$ range from 2.75 eV to 3.50 eV and the $E_{G,Bot}$ range from 0.65 eV to 1.45 eV give efficiencies over 54.91%.

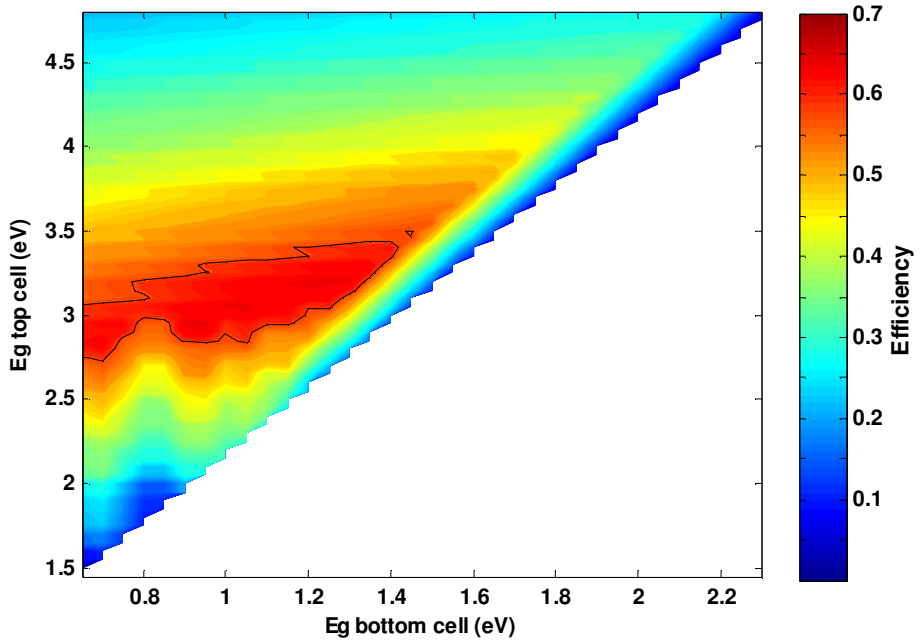

Figure 7.22: Efficiency of the series connected tandem cell under 1000 suns, area function of the main band gap energies of the top and bottom cell.

The maximum efficiency for a cell under radiation with concentration level 1000 is 65.34% with band gap energy values: $E_{G,Top}$ = 2,95 eV, $E_{G,Bot}$ = 0.95 eV , $E_{L,Top}$ = 1.20 eV and $E_{L,Bot}$ = 0.30 eV. For band gap combinations in the $E_{G,Top}$ range from 2.75 eV to 3.50 eV and the $E_{G,Bot}$ range from 0.65 eV to 1.45 eV, efficiency over 58.81% is achieved.

Discussion

The maximum efficiencies for the series connected tandem cell are concentrated at a smaller range of band gaps than for the separately connected cell. This is more noticeable than the decrease of the maximum efficiency, which is a decrease of 2.8% points at most. Compared to the four terminal tandem cell, the range of different semiconductor material that will provide a two terminal cell with high efficiency is much smaller.

Low efficiency at high values of $E_{G,Top}$ when compared to the four terminal cell, is mainly a consequence of a low photon flux absorption in the top cell, thus causing a low current in the top IBSC. As the two cells are series connected, the bottom cell, which has high photon flux absorption at this band gap combination, will not provide the complete cell with a high current as for the four terminal case.

The main band gap ranges with high efficiency for the concentration levels 100 and 1000 are the same, indicating that these main band gap energies would provide good efficiency for two terminal tandem cells under concentrated radiation. The high efficiency main band gap ranges for the cell under 1 sun are at higher energies than the cells under 100 and 1000 suns. This is similar to the results for the four terminal cell, and probably an effect of the difference in the radiation distributions AM1.5G and AM1.5D.

Sub-band gap energies, top cell

The following three figures show the optimum lowest band gaps of the top cell ($E_{L,Top}$) of the series connected tandem IBSC for 1, 100 and 1000 suns.

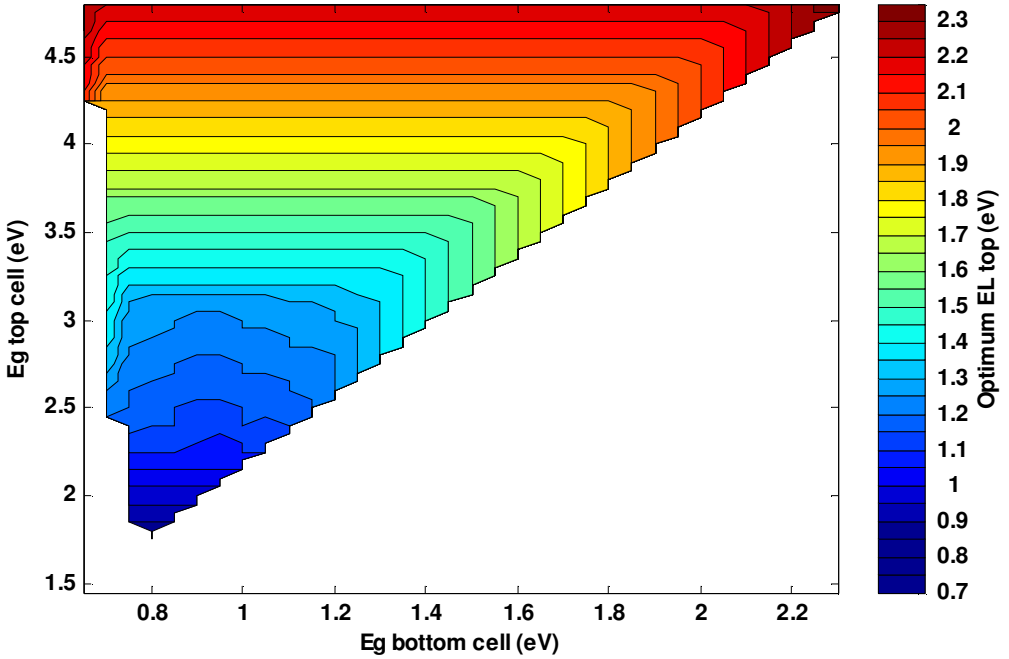

Figure 7.23: The optimum lowest sub-band gap energies for the top cell ($E_{L,Top}$). Concentration level is 1 sun.

The optimum top cell sub-band gaps are very similar to that of the four terminal tandem cell; the smallest sub-band gap increases with the main band gap of the top cell. The difference from the four terminal tandem cell is most significant at the $E_{L,Top}$ range 1.45 eV to 3 eV. In the four terminal case in figure 7.10, $E_{L,Top}$ is more stable for each main band gap energy of the top cell.

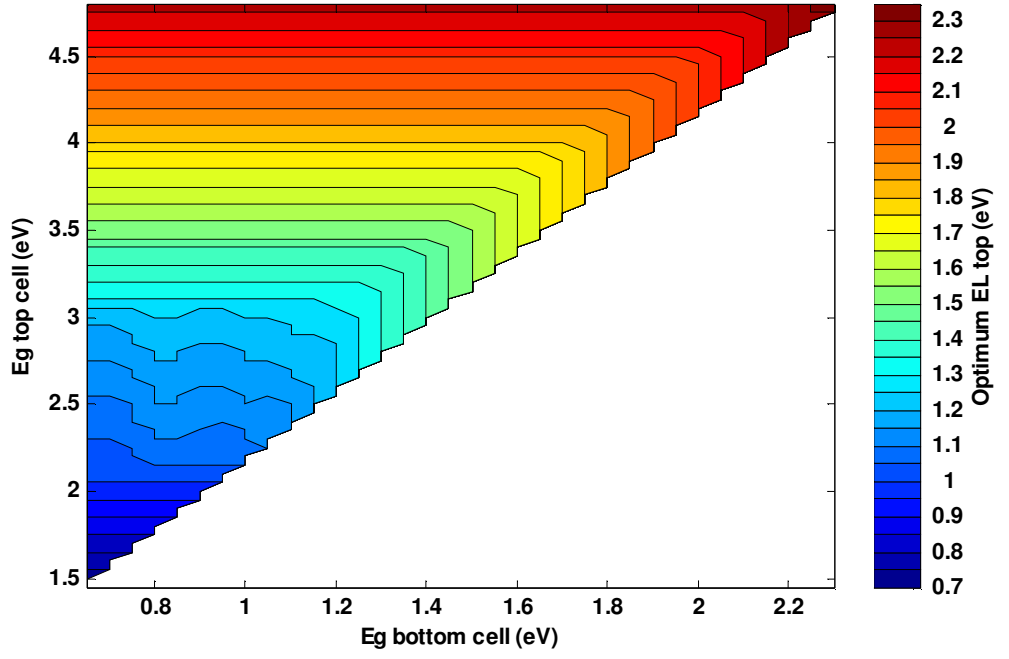

Figure 7.24: The optimum lowest sub-band gap energies for the top cell ($E_{L,Top}$). Concentration level is 100 suns.

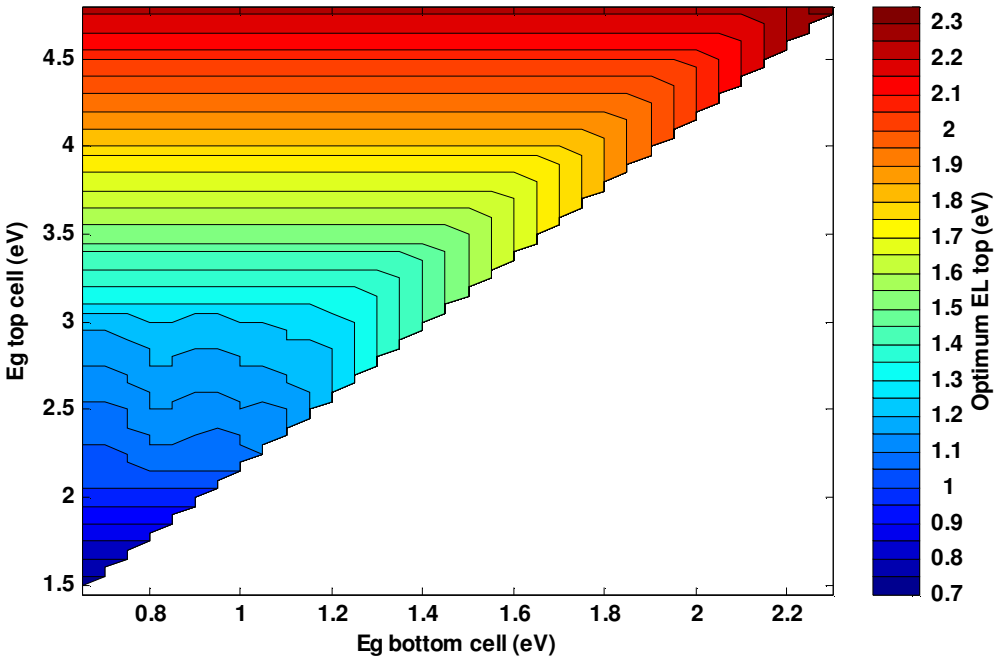

Figure 7.25: The optimum lowest sub-band gap energies for the top cell ($E_{L,Top}$). Concentration level is 1000 suns.

Similar to the plot in figure 7.23, the cells under concentrated radiation, see figures 7.24 and 7.25, have differences for $E_{L,Top}$ compared to the four tandem cell in figures 7.11 and 7.12. Significant variations are found for the lower main band gaps of the top cell, but only up to the energy of about 2.85 eV. Comparing figure 7.24 and 7.25 shows that an increase in concentration level does not seem to give a significant difference in the values of $E_{L,Top}$.

Discussion

Comparing the results for the two terminal cell with the four terminal cell, we find that the most significant difference is in the low main band gap ranges for the top cell. The two terminal cell has lower values for $E_{L,Top}$ at these ranges, and the difference is at most 0.30 eV. For higher values of $E_{G,Top}$ there is only a small increase in $E_{L,Top}$ for some main band gap combinations. The ratio between the optimum lowest sub-band gap and the main band gap are similar to the four terminal case for the top IBSC.

Sub-band gap energies, bottom cell

Figures 7.26, 7.27 and 7.28 show the optimum lowest sub-band gap energies of the bottom IBSC for 1, 100 and 1000 suns respectively.

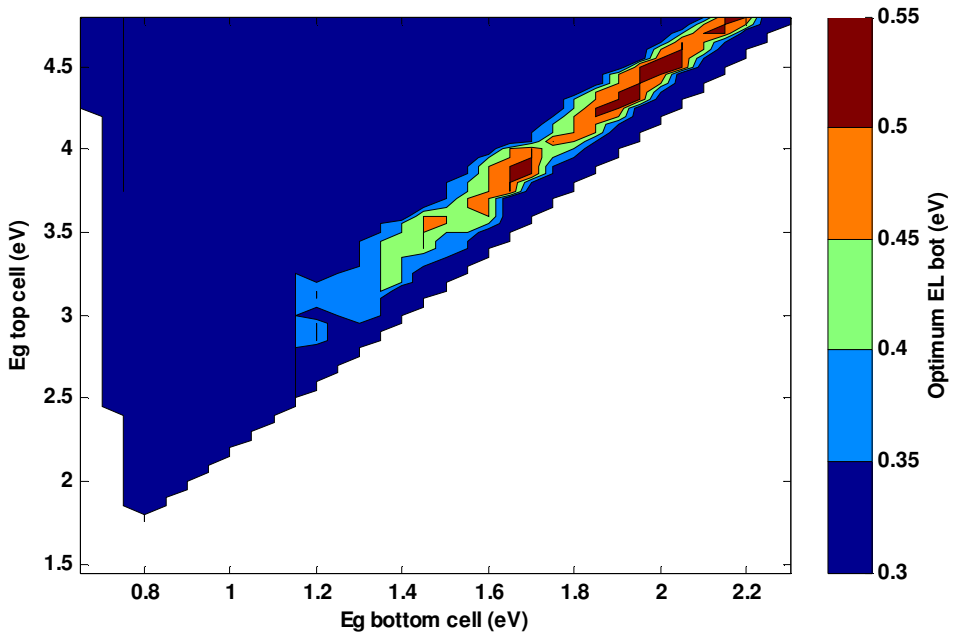

Figure 7.26: The optimum lowest sub-band gap energies for the bottom cell ($E_{L,Bot}$). Concentration level is at 1 sun.

0.30 eV, which is the smallest band gap used in the simulations, is the optimum lowest sub-band gap for most of the main band gap values as can be seen in figure 7.26. Higher values for $E_{L,Top}$ is found at high values for both $E_{G,Bot}$ and $E_{G,Top}$, reaching the value of 0.50 eV.

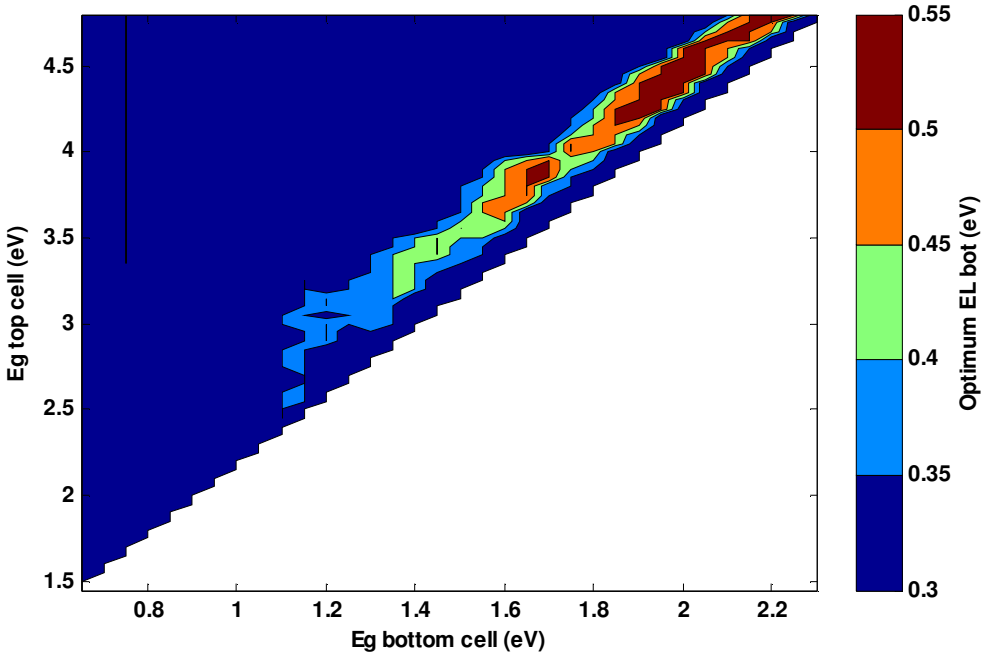

Figure 7.27: The optimum lowest sub-band gap energies for the bottom cell ($E_{L,Bot}$). Concentration level is at 100 suns.

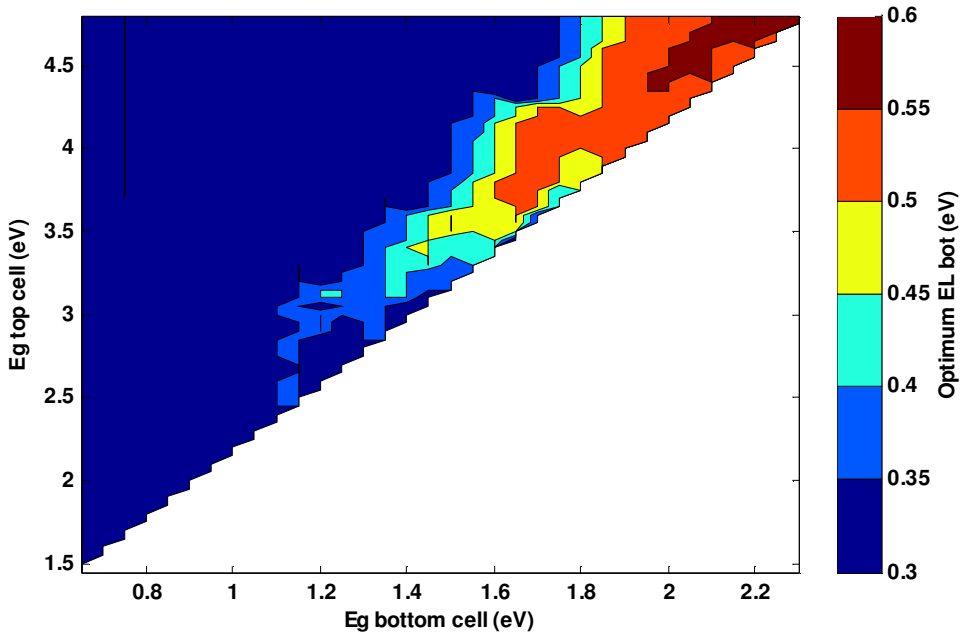

Figure 7.28: The optimum lowest sub-band gap energies for the bottom cell ($E_{L,Bot}$). Concentration level is at 1000 suns.

Increasing the concentration level also increases the values of $E_{L,Bot}$ for some of the main band gap energies, as can be seen from figure 7.27 and 7.28, but for most of the lower main band gap values for the bottom cell, $E_{L,Bot}$ is still at its lowest value of 0.30 eV. Similar to concentration level 1 the highest values for $E_{L,Bot}$ are at high values of both main band gaps.

Discussion

The values for $E_{L,Bot}$ in the two terminal IBSC are very different from the ones found in the four terminal tandem IBSC. For the two terminal tandem IBSC, the optimum values for $E_{L,Bot}$ do not increase with the $E_{G,Bot}$ for all values of $E_{L,Top}$. The high optimum band gap values for $E_{L,Bot}$ are only found where both main band gaps are large and the ratio between them low, i.e. along the diagonal of the plot. For the four terminal tandem IBSC, the values for $E_{L,Bot}$ are at 0.30 eV only for low main band gap energies for the bottom cell. It is clear that the ratio between the sub-band gap and the main band gap for the bottom IBSC in the two terminal tandem cell is generally much lower than for the four terminal cell.

As stated earlier in the discussion of the efficiencies for the two terminal cell, the top cell has a low current at high $E_{G,Top}$ values. A low current for the top cell is also a consequence when $E_{L,Top}$ increases close to its maximum value, just below half the value of $E_{G,Top}$. The values for $E_{L,Top}$ are pushed up by an increase in $E_{G,Bot}$ when $E_{G,Bot}$ reaches its highest values possible for a specific $E_{G,Top}$. The highest efficiency is then found when the bottom cell provides a high voltage at a low current, equal to the top cell current. This can be seen by plotting the I-V characteristics for the bottom IBSC with various $E_{L,Bot}$ and compare the curves with the highest current achievable in the top IBSC, see figure 7.29.

The figure shows the I-V characteristics of the bottom cell for two different $E_{L,Bot}$ values: 0.30 eV, the optimum for the two terminal cell, and 0.50 eV, the four terminal optimum value. The other band gaps are $E_{G,Top}$ = 4 eV, $E_{G,Bot}$ = 1.60 eV, and $E_{L,Top}$ = 1.75 eV. Concentration level for this cell is 1 sun. The green line represents the highest current for the top cell at these band gap values.

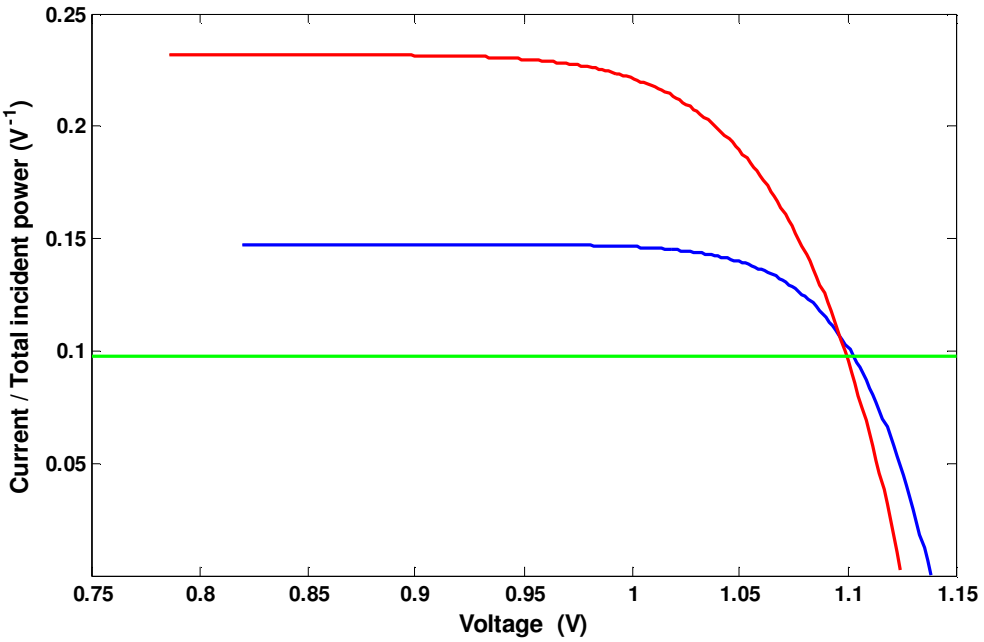

Figure 7.29: The I-V characteristics of the bottom cell for two different values of $E_{L,Bot}$: $E_{L,Bot}$ is 0.30 eV (blue) and $E_{L,Bot}$ is 0.50 eV (red). The green line represents the highest value (Current / Total incident power) for the top cell. The other band gaps are: $E_{G,Top}$ is 4 eV, $E_{G,Bot}$ is 1.60 eV, $E_{L,Top}$ is 1.75 eV.

It is clear from figure 7.29 that below the maximum current for the top cell the value of $E_{L,Bot}$ at 0.30 eV provides a higher voltage than $E_{L,Bot}$ at 0.50 eV. This explains why low values of $E_{L,Bot}$ provide the highest efficiency for the two terminal cell at certain main band gap combinations. An increase in the concentration level increases the photon flux and thus the current in the top cell, and higher values for $E_{L,Bot}$ can then give better efficiencies for higher levels of concentration.

7.2.3 Two and four terminal summary

The maximum efficiencies for the two terminal and four terminal tandem IBSCs and the corresponding band gaps, are listed in table 7.3.

Table 7.3: Band gap energies and maximum efficiencies for the tandem IBSC.

Concentration level	$E_{G,top}$ (eV)	$E_{G,bot}$ (eV)	$E_{L,top}$ (eV)	$E_{L,bot}$ (eV)	Maximum Efficiency (%)
4 terminal tandem IBSC					
1 sun	4.05	1.65	1.8	0.55	54.93
100 suns	3.75	1.5	1.65	0.5	62.74
1000 suns	4.3	1.5	1.95	0.5	67.23
2 terminal tandem IBSC					
1 sun	3.3	1.35	1.4	0.4	53.88
100 suns	3.2	1.25	1.35	0.35	61.01
1000 suns	2.95	0.95	1.2	0.3	65.34

From the table, we see that the maximum efficiencies for the two terminal tandem IBSC are, as expected, lower than for the four terminal cell. Differences in the efficiencies are 1.91%, 2.76% and 2.81% for the 1 sun, 100 suns and 1000 suns concentration respectively. The efficiency has a larger loss for the tandem IBSC than for the six junction tandem cell under the AM1.5 global radiation treated in [14]. In [14] the loss in efficiency is 0.67% when series connecting the six junction tandem cell for 1 sun, but the resolution of the band gap energies is much higher (up to 0.001 eV) than in this master's thesis (0.05 eV) and there can be differences in the AM1.5 spectrum. A higher resolution of the band gap energies would probably increase the efficiency of the two terminal cell more than for the four terminal cell. This is reinforced by the results in table 7.1, showing that the tandem IBSC under full concentrated black-body radiation (6000K) has a loss of 0.68% when series connected (in the results from [15]).

7.3 Single-junction and IB tandem cell under AM1.5 illumination

In this section the results of the tandem cell composed of one single-junction cell and one IB cell are presented and discussed. Simulations have been run with the IBSC as the top cell and the single-junction cell as bottom cell, and the IBSC as the bottom cell and the single-junction cell as the top cell. The single-junction cell has a different range of band gaps than the IBSC, see table 6.1. The black line in the efficiency plots, shows where the efficiency is 90% of maximum.

7.3.1 Four terminal IB top cell and single-junction bottom cell

Efficiencies for 1, 100 and 1000 suns

The efficiencies for a tandem cell with an IB top cell and a single-junction bottom cell are presented in figure 7.30 (1 sun), 7.31 (100 suns) and 7.32 (1000 suns).

The maximum efficiency for 1 sun is calculated to 53.18% at the band gap values $E_{G,Top}$ = 2.85 eV, $E_{G,Bot}$ = 0.70 eV and $E_{L,Top}$ = 1.15 eV. For concentration level of 100 and 1000 suns the maximum efficiencies are at 60.23% and 64.48% respectively. Both maximum efficiencies are set at band gap values $E_{G,Top}$ = 2.45 eV, $E_{G,Bot}$ = 0.50 eV and $E_{L,Top}$ = 0.95 eV.

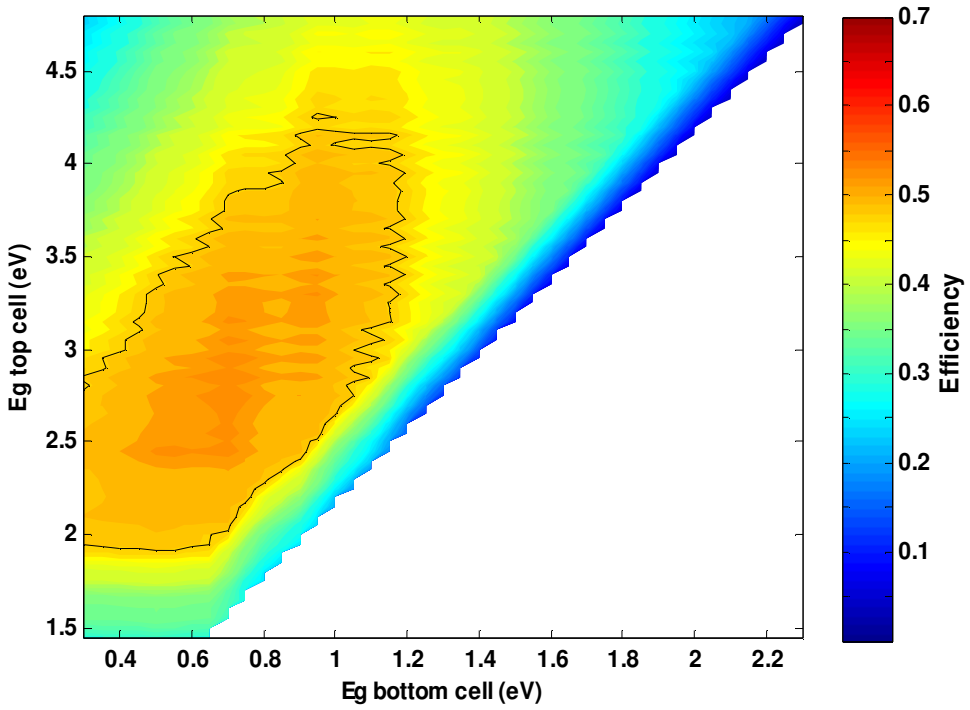

Figure 7.30: Efficiency of the tandem cell under 1 sun, area function of the main band gap energies of the IB top cell and single-junction bottom cell.

High efficiencies over 47.86% for 1 sun are achieved with band gap combinations in the $E_{G,Top}$ range from 1.95 eV to 4.25 eV and the $E_{G,Bot}$ range from 0.30 eV to 1.15 eV. For 100 suns the high efficiencies are over 54.21%, and the band gap range for $E_{G,Top}$ is from 1.85 eV to 3.95 eV and for $E_{G,Bot}$ from 0.30 eV to 1.05 eV. The high efficiencies for 1000 suns are over 58.03%, with band gap combinations within the $E_{G,Top}$ range from 1.85 eV to 3.85 eV and the $E_{G,Bot}$ range from 0.30 eV to 1 eV.

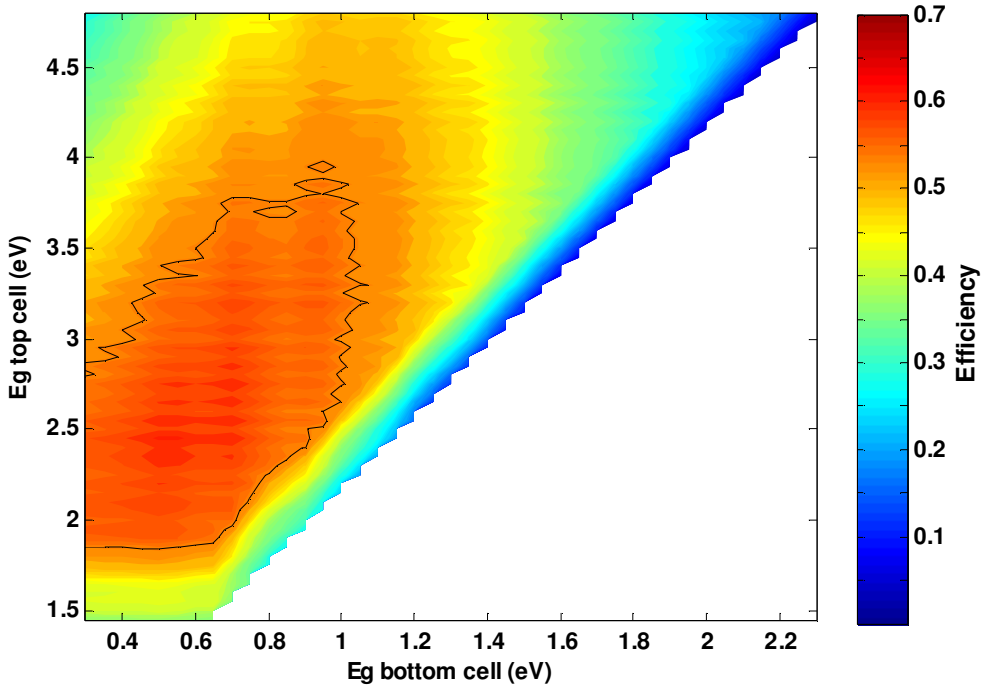

Figure 7.31: Efficiency of the tandem cell under 100 suns, area function of the main band gap energies of the IB top cell and single-junction bottom cell.

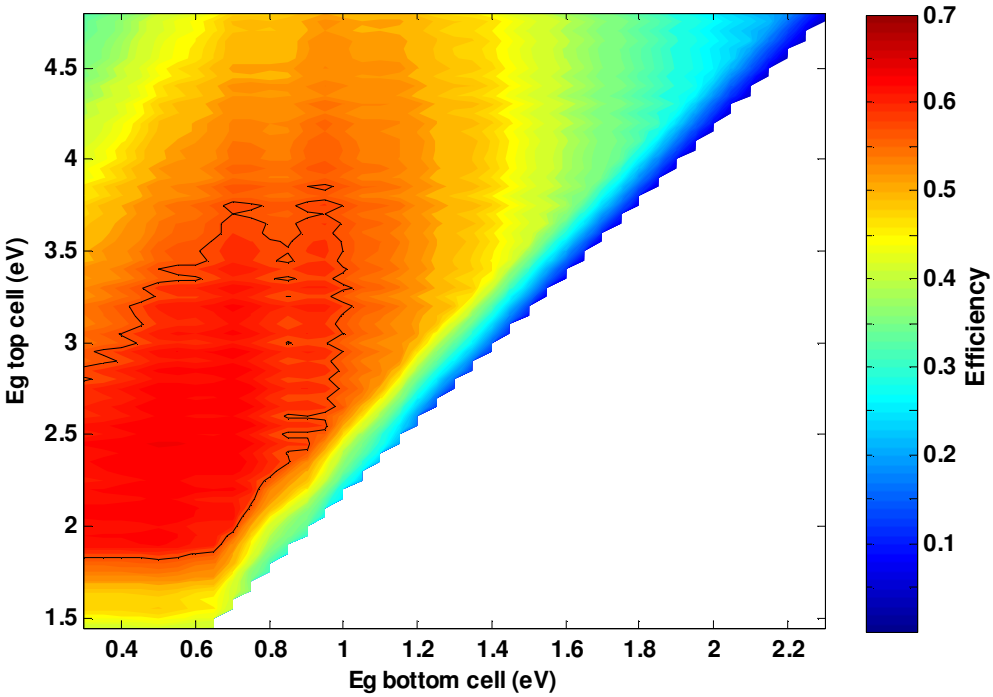

Figure 7.32: Efficiency of the tandem cell under 1000 suns, area function of the main band gap energies of the IB top cell and single-junction bottom cell.

Discussion

Comparing this cell with the single IBSC shows that the maximum efficiency is increased at most with 7.63%. The highest increase is for the tandem cell with a concentration level of 1 sun. The band gaps at the maximum efficiency are larger for the IB top cell compared to the single IBSC. The single IBSC has a high efficiency at the main band gap energies close to 2.85 eV (for 1 sun), as can be seen in figure 7.5. Thus semiconductor materials with band gaps providing high efficiency for the top IBSC in the tandem cell also have a high efficiency when used in a single IBSC.

The band gaps for the maximum efficiency are lower for the tandem cells under concentrated radiation, similar to the single IBSC. As discussed earlier in this chapter this is an effect of the difference in distribution of the radiation as well as the concentration of the radiation.

Sub-band gap energies for the top cell

The following three figures show the optimum lowest sub-band gap energies for the IBSC in the tandem cell at various concentration levels.

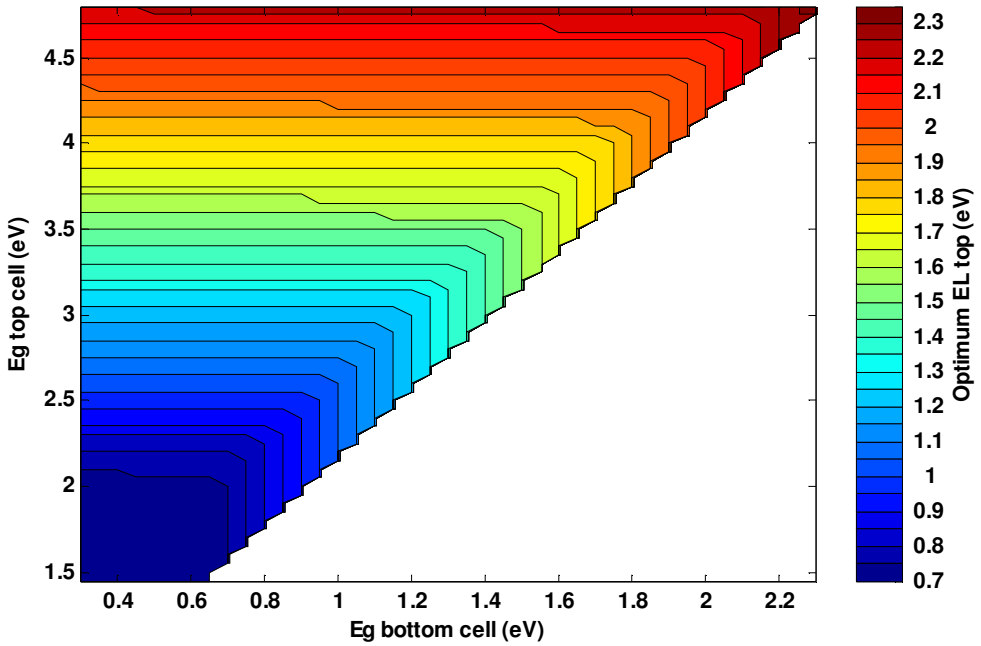

Figure 7.33: The optimum lowest sub-band gap energies for the top cell ($E_{L,Top}$). Concentration level is 1 sun.

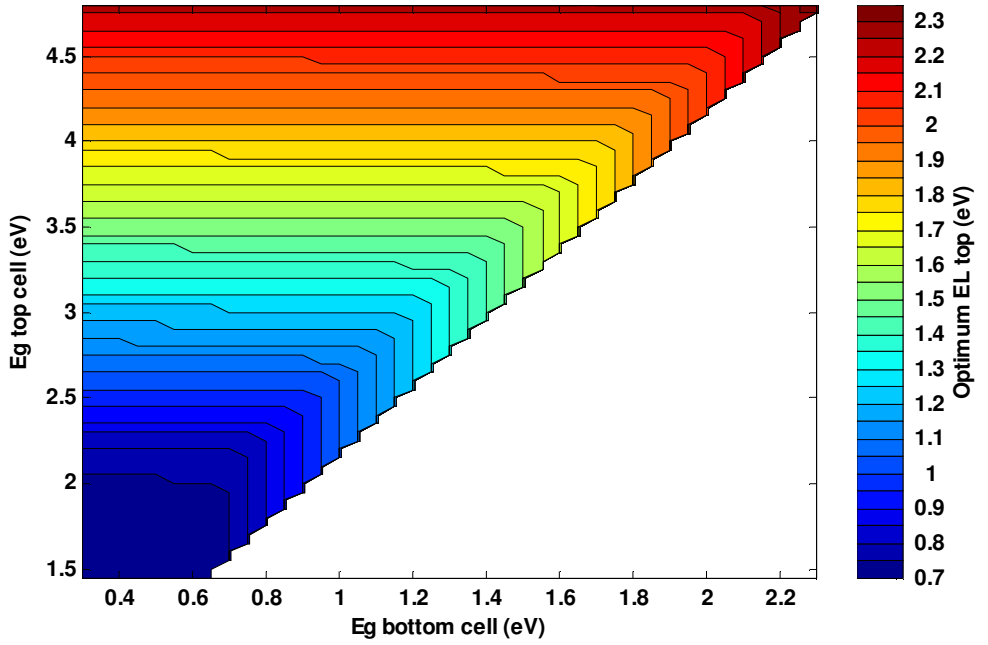

Figure 7.34: The optimum lowest sub-band gap energies for the top cell ($E_{L,Top}$). Concentration level is 100 suns.

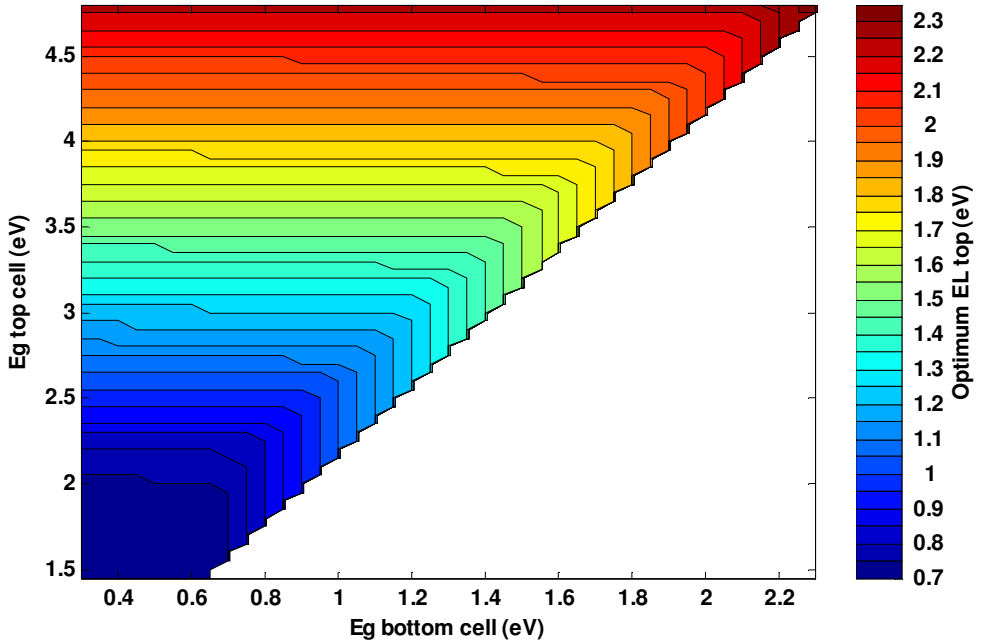

Figure 7.35: The optimum lowest sub-band gap energies for the top cell ($E_{L,Top}$). Concentration level is 1000 suns.

As seen from figures 7.33, 7.34 and 7.35, $E_{L,Top}$ increases with the values of the main band gap of the top cell. The plots are very similar to those of the $E_{L,Top}$ values for the tandem IBSC in section 7.2.1. When comparing these plots with the plots in section 7.2.1, notice the difference in the range of $E_{G,Bot}$, as this causes some difference in the appearance of the plots.

Discussion

The optimum values for $E_{L,Top}$ are very similar for the tandem IBSC and the tandem cell with an IB top cell and single-junction bottom cell, showing that the choices for $E_{L,Top}$ are not strongly affected by the bottom cell.

The lowest value used in the simulations for $E_{L,Top}$ is 0.70 eV. The cell would probably have higher efficiency for the lowest main band gap values if lower values for $E_{L,Top}$ had been used in the calculations. This is seen as the efficiencies in figure 7.30, 7.31 and 7.32 all decrease abruptly for $E_{G,Top}$ values lower than 1.85 eV. The maximum efficiencies are all found for higher $E_{G,Top}$ values, and the efficiencies are decreasing as $E_{G,Top}$ goes from 2 eV to 1.85 eV. It is therefore assumed that a higher maximum efficiency would not be found in the region where $E_{G,Top}$ is below 1.85 eV, but that the high efficiency band gap range for $E_{G,Top}$ will be larger than found in these results.

7.3.2 Four terminal single-junction top cell and IB bottom cell

In this section the results for the four terminal tandem cell with a single-junction top cell and an IB bottom cell are presented and discussed. The single-junction top cell has been calculated for a smaller range of main band gaps than the IBSC, but the results still includes the band gaps that provide the cell with high efficiencies.

Efficiencies for 1, 100 and 1000 suns

The following three plots show the efficiencies for the tandem cell at 1 sun, 100 suns and 1000 suns concentration.

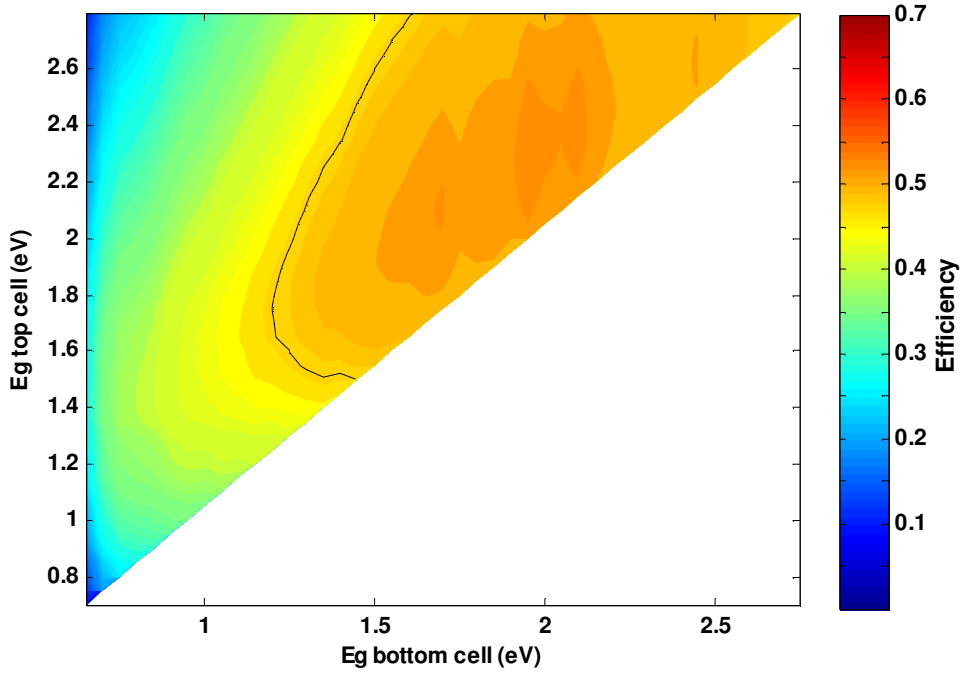

Figure 7.36: Efficiency of the tandem cell under 1 sun, area function of the main band gap energies of the single-junction top cell and IB bottom cell.

For the tandem cell with the concentration of 1 sun the maximum efficiency is 52.62%, and found at the band gap values $E_{G,Top}$ = 2.30 eV, $E_{G,Bot}$ = 1.95 eV and $E_{L,Bot}$ = 0.70 eV.

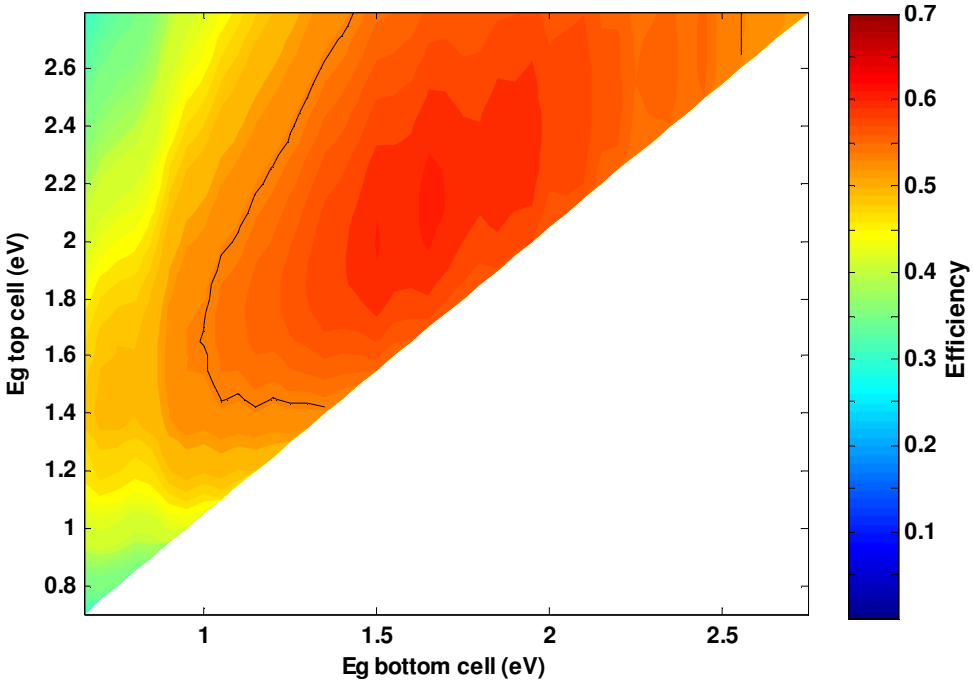

Figure 7.37: Efficiency of the tandem cell under 100 suns, area function of the main band gap energies of the single-junction top cell and IB bottom cell.

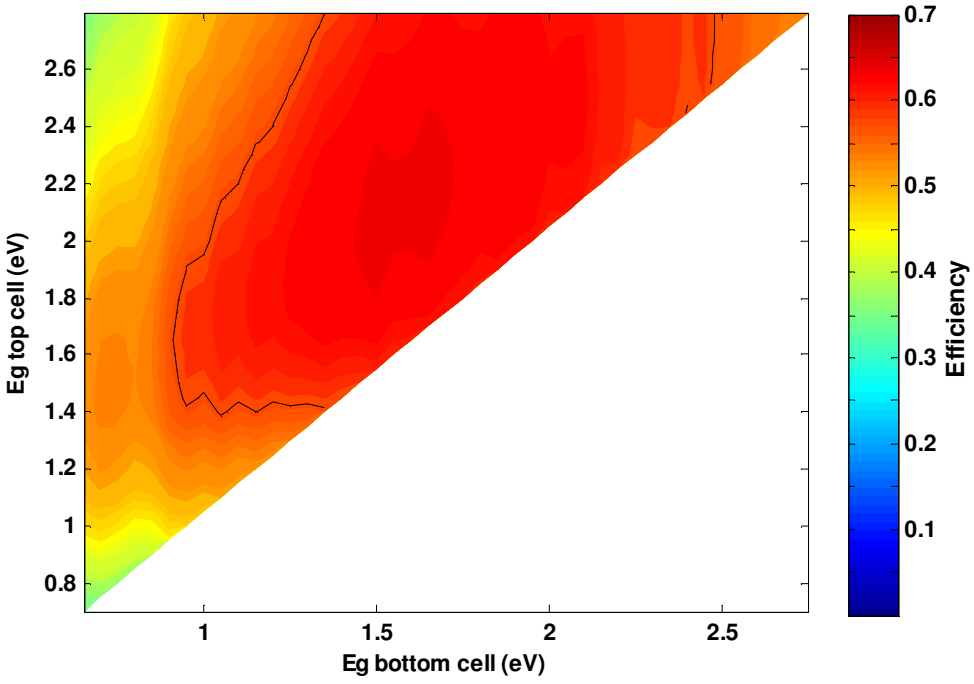

Figure 7.38: Efficiency of the tandem cell under 1000 suns, area function of the main band gap energies of the single-junction top cell and IB bottom cell.

The maximum efficiency calculated for 100 and 1000 suns are 60.31% and 64.81% respectively, at band gap values $E_{G,Top}$ = 2.10 eV, $E_{G,Bot}$ = 1.65 eV and $E_{L,Bot}$ = 0.55 eV for 100 suns and $E_{G,Top}$ = 2.05 eV, $E_{G,Bot}$ = 1.50 eV, and $E_{L,Bot}$ = 0.50 eV for 1000 suns.

For 1 sun the high efficiencies are calculated to be over 47.35% and found for band gap combinations in the $E_{G,Top}$ range from 1.50 eV to 2.80 eV and the $E_{G,Bot}$ range from 1.20 eV to 2.75 eV. The high efficiencies for 100 suns and 1000 suns are over 54.28% and 58.33% respectively, and the corresponding band gap ranges are $E_{G,Top}$ from 1.45 eV to 2.80 eV and $E_{G,Bot}$ from 1 eV to 2.55 eV for 100 suns and $E_{G,Top}$ from 1.40 eV to 2.80 eV and $E_{G,Bot}$ from 0.95 eV to 2.55 eV for 1000 suns. It is clear from figures 7.36, 7.37 and 7.38 that band gap combinations giving high efficiency are also found for $E_{G,Top}$ values above 2.80 eV, but higher values for $E_{G,Top}$ are not used in these calculations.

Discussion

The highest increase in maximum efficiency compared to the single IBSC is 6.5%, and is for the 1 sun concentration. Compared to the tandem cell with an IB top cell and single-junction bottom cell, the maximum efficiency is lower for 1 sun concentration, but higher for the concentration levels of 100 and 1000 suns. This can be an effect of the different distributions of the AM1.5D and AM1.5G spectra, the AM1.5G spectrum slightly favouring the IBSC as the top cell and AM1.5D slightly favouring the IBSC as the bottom cell. Because of the low band gap resolution and that the maximum efficiency values are in close vicinity of each other, it is only a guess.

Sub-band gap energies, bottom cell

Figures 7.39, 7.40 and 7.41 show the optimum lowest sub-band gap energies for the bottom IBSC, for 1, 100 and 1000 suns.

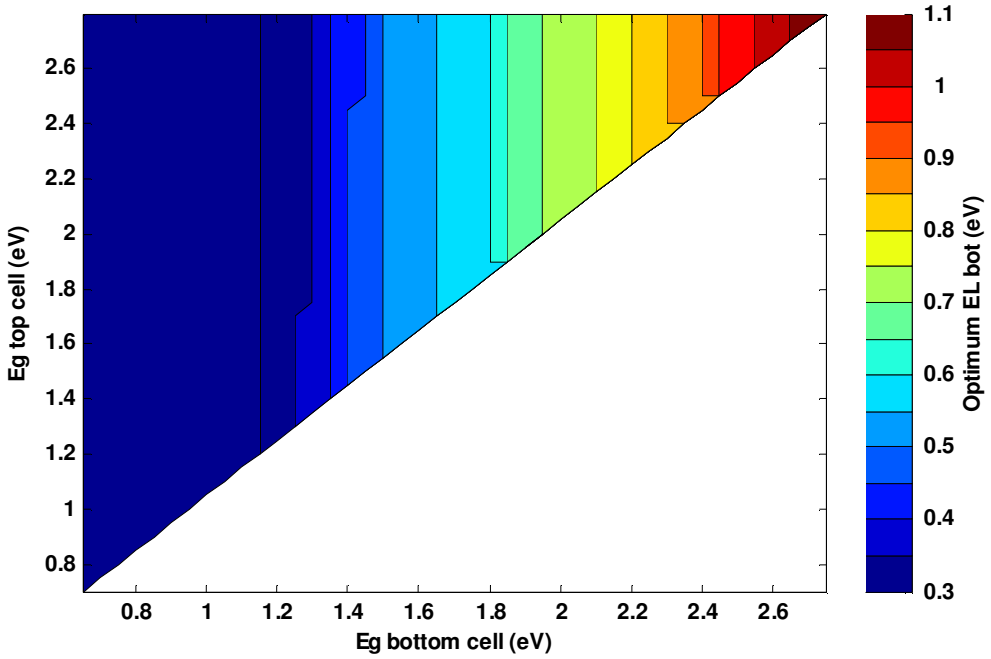

Figure 7.39: The optimum lowest sub-band gap energies for the bottom cell ($E_{L,Bot}$). Concentration level is 1 sun.

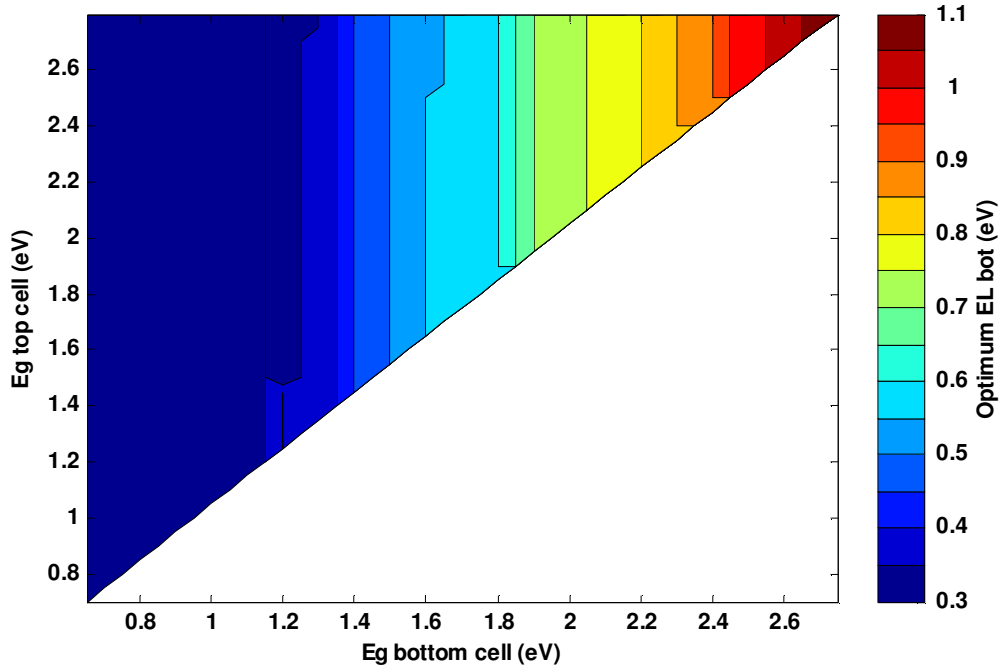

Figure 7.40: The optimum lowest sub-band gap energies for the bottom cell ($E_{L,Bot}$). Concentration level is 100 suns.

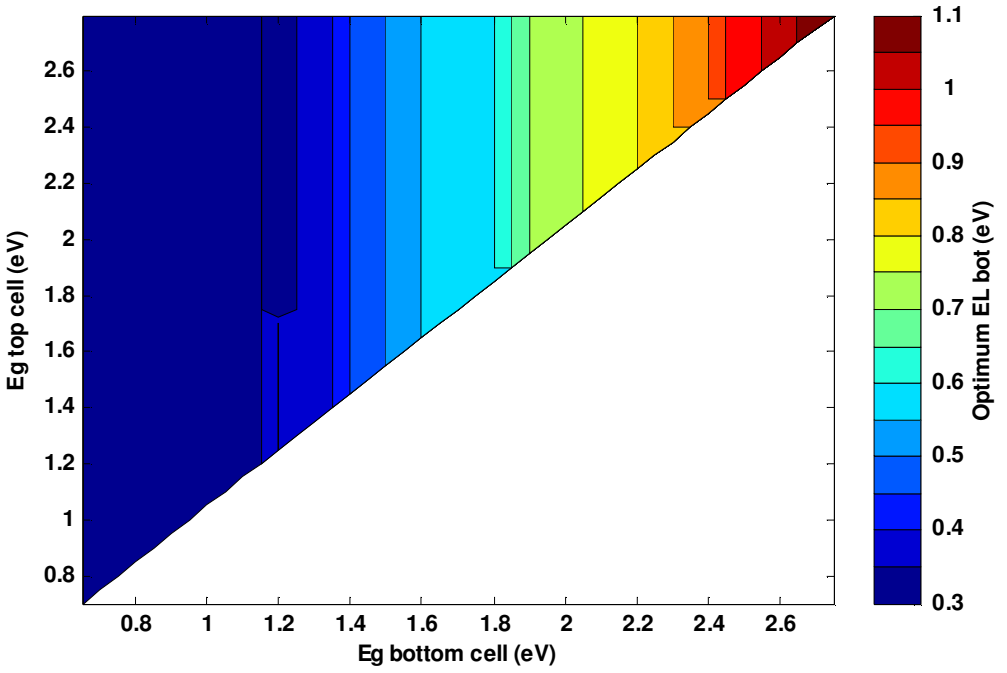

Figure 7.41: The optimum lowest sub-band gap energies for the bottom cell ($E_{L,Bot}$). Concentration level is 1000 suns.

The optimum values for $E_{L,Bot}$ of the bottom IBSC range from 0.3 eV, which is the lowest used in the simulation, to 1.1 eV. $E_{L,Bot}$ increases with the main band gap of the bottom IBSC, but have some deviations where $E_{L,Bot}$ is lower for high values of $E_{G,Top}$.

Discussion

In the tandem IBSC only photons with an energy lower than $E_{L,Top}$ reaches the bottom IBSC. For the tandem cell with a single-junction top cell however, this energy limit is $E_{G,Top}$, which is the main band gap of the single-junction top cell. This allows the main band gap of the bottom IBSC to have larger values, up to 2.75 eV, and the optimum values for $E_{L,Bot}$ will consequently increase to higher values. The optimum sub-band gaps for the bottom IBSC in figures 7.39, 7.40, and 7.41 are comparable with the values for the tandem IBSC found in figures 7.13, 7.14, and 7.15, for the same values of $E_{G,Bot}$. The decrease in the lowest sub-band gap, when the $E_{G,Top}$ value increases for a set value of $E_{L,Bot}$, has been discussed earlier in section 7.2.1.

7.3.3 Two terminal IB top cell and single-junction bottom cell

The results from simulating the two terminal tandem cell, with an IB top cell and single-junction bottom cell, are presented in this section.

Efficiencies for 1, 100 and 1000 suns

The maximum efficiencies for the series connected IB top cell and single-junction bottom cell are seen in figure 7.42 for 1 sun, figure 7.43 for 100 suns and figure 7.44 for 1000 suns.

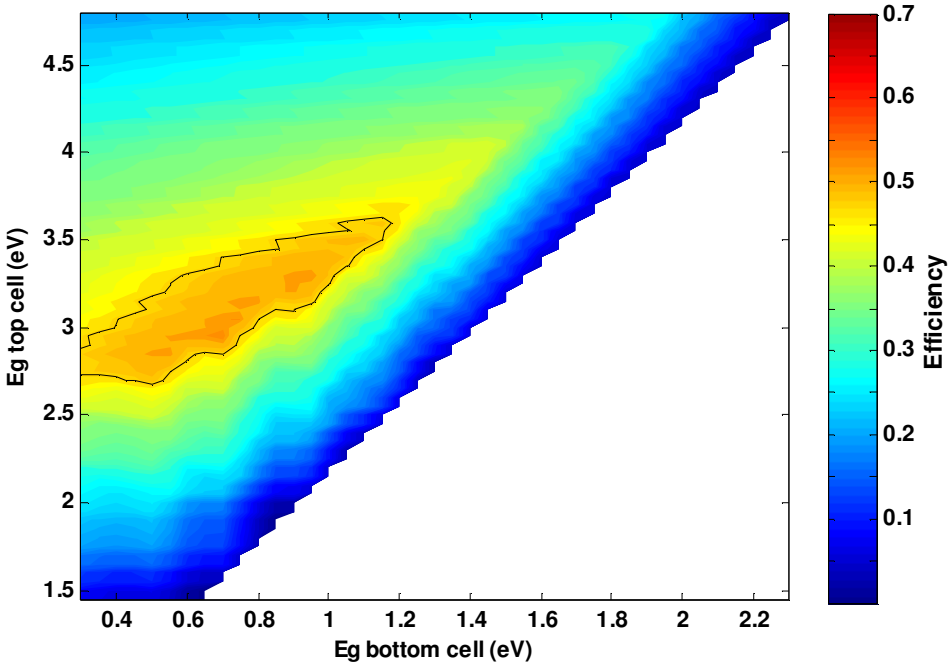

Figure 7.42: Efficiency of the tandem cell under 1 sun, area function of the main band gap energies of the IB top cell and single-junction bottom cell.

Maximum efficiency is 52.51% at the band gap values $E_{G,Top}$ = 2.95 eV, $E_{G,Bot}$ = 0.70 eV, and $E_{L,Top}$ = 1.20 eV for the 1 sun cell. The same band gaps also provide the tandem cell with the maximum efficiency of 59.19%, for 100 suns concentration.

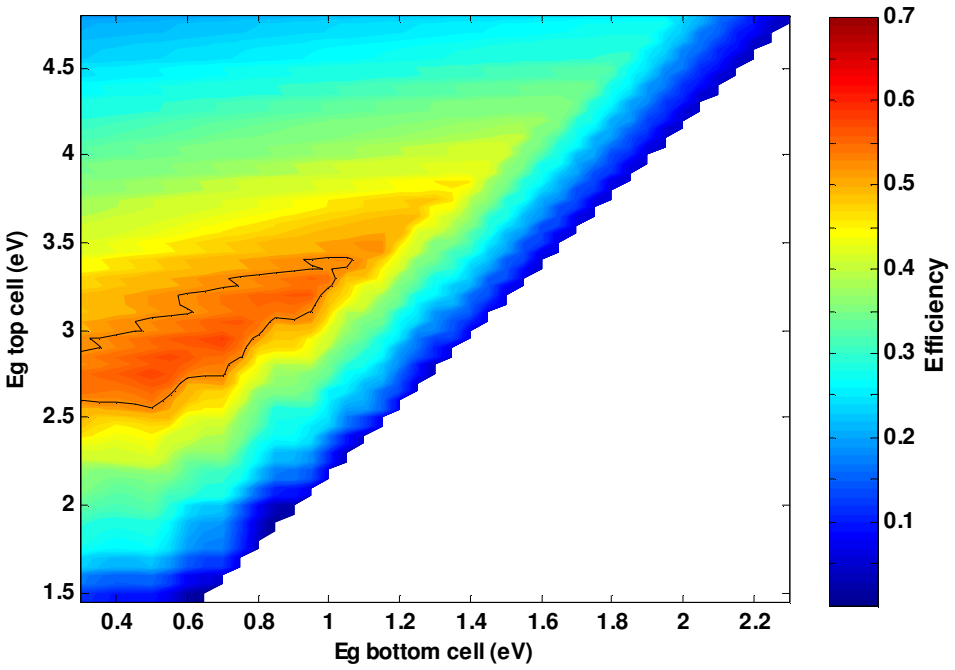

Figure 7.43: Efficiency of the tandem cell under 100 suns, area function of the main band gap energies of the IB top cell and single-junction bottom cell.

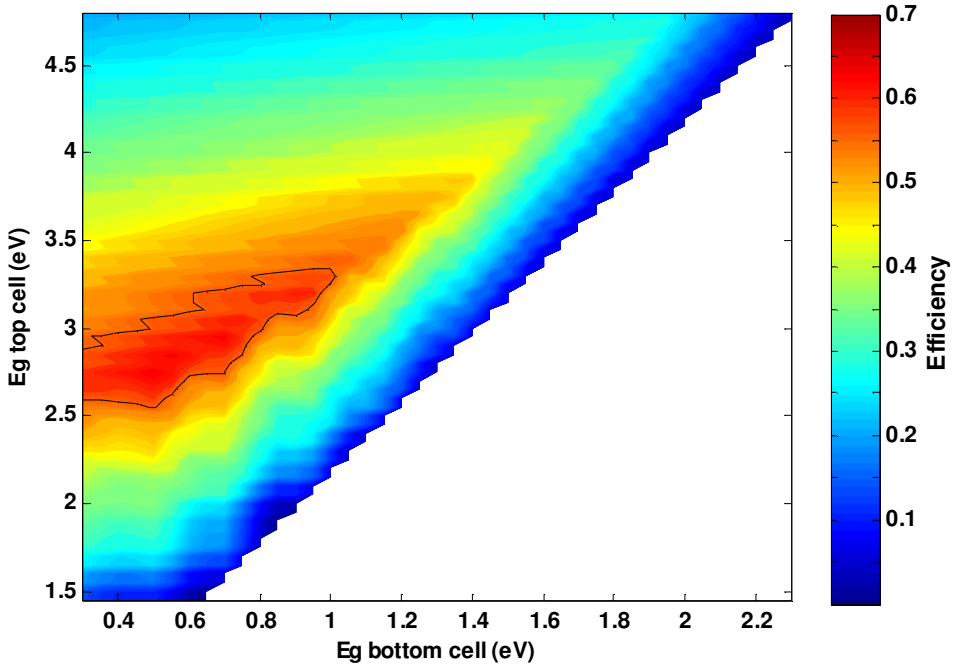

Figure 7.44: Efficiency of the tandem cell under 1000 suns, area function of the main band gap energies of the IB top cell and single-junction bottom cell.

For the tandem cell with concentration level of 1000 suns the maximum efficiency is 63.11% with the band gap values $E_{G,Top}$ = 2.75 eV, $E_{G,Bot}$ = 0.50 eV, and $E_{L,Top}$ = 1.10 eV.

Efficiencies over 47.26% for 1 sun are found in the band gap range from 2.70 eV to 3.60 eV for $E_{G,Top}$ and from 0.30 eV to 1.15 eV for $E_{G,Bot}$. For 100 suns, high efficiencies over 53.27% are given at band gap combinations in the $E_{G,Top}$ range from 2.60 eV to 3.40 eV and $E_{G,Bot}$ range from 0.30 eV to 1.05 eV. In the $E_{G,Top}$ range from 2.55 eV to 3.30 eV and $E_{G,Bot}$ range from 0.30 eV to 1 eV, efficiencies over 56.80% are achieved for 1000 suns.

Discussion

The band gaps for the maximum efficiency are lower for the concentration level of 1000 suns than the cell with 100 suns concentration. There is a local peak in efficiency (62.76%) for the cell with 1000 suns concentration, at the same band gap energies for the maximum efficiency of the cell with 100 suns concentration. This shows some kind of stability for the efficiency of the cell when the concentration increases.

Similar to the tandem IBSC, the series connected tandem cell has a slightly lower maximum efficiency compared to the four terminal cell, but a much narrower range of main band gaps with high efficiency.

Sub-band gap energies, top cell

The optimum values for $E_{L,Top}$, as for the other tandem cell configurations, providing the top IBSC with the maximum efficiency are presented in the three following figures.

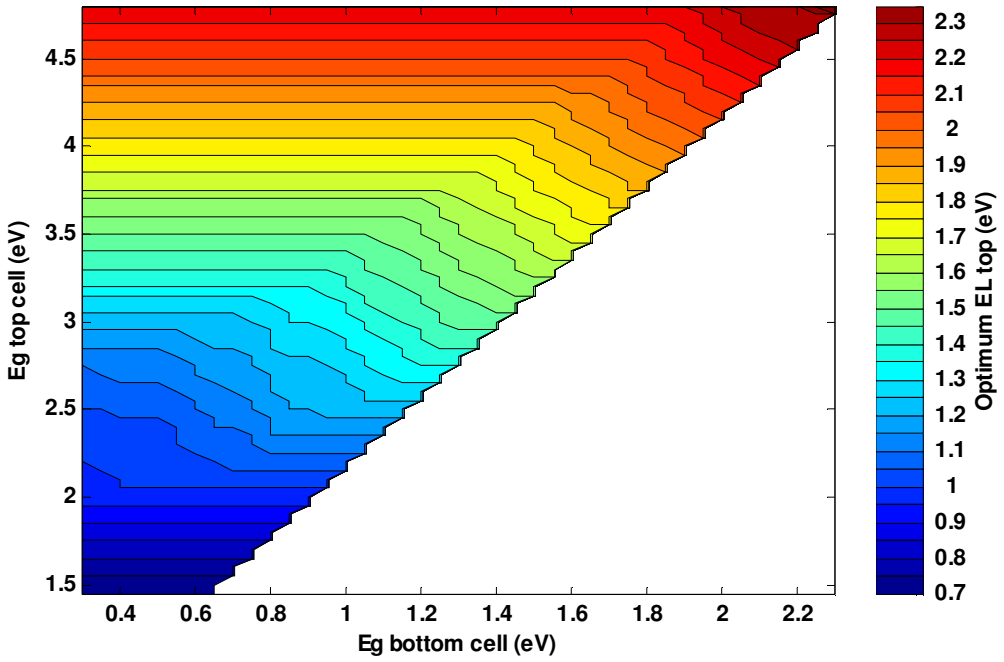

Figure 7.45: The optimum lowest sub-band gap energies for the top cell ($E_{L,Top}$). Concentration level is 1 sun.

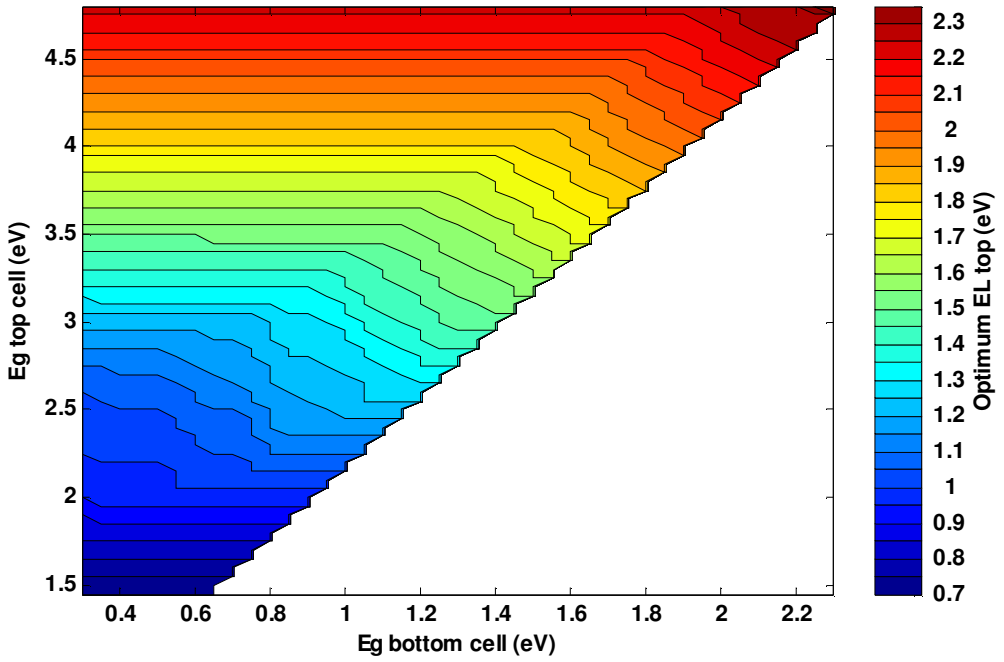

Figure 7.46: The optimum lowest sub-band gap energies for the top cell ($E_{L,Top}$). Concentration level is 100 and 1000 suns.

The values of $E_{L,Top}$ are very similar to the four terminal case. But for low band gap energies of the main band gap of the top cell, larger values for $E_{L,Top}$ are found to be optimum. For a specific $E_{G,Top}$ the values of $E_{L,Top}$ also starts to increase for lower values of $E_{G,Bot}$.

Discussion

The two terminal tandem cell has a generally higher value for $E_{L,Top}$, compared to the optimum values for $E_{L,Top}$ in the four terminal cell. As the $E_{L,Top}$ increases, so does the photon flux transmitted through the top cell, thus increasing the absorbed photon flux in the bottom single-junction cell. The top IBSC has a higher current than the single-junction bottom cell. By increasing the photon flux in the bottom cell, and thereby the current in the bottom cell, the current available in the series connected tandem cell is increased and so is the efficiency.

7.3.4 Two terminal single-junction top cell and IB bottom cell

The results for the two terminal tandem cell, with a single-junction top cell and an IB bottom cell, are treated in this section.

Efficiencies for 1, 100 and 1000 suns

The maximum efficiencies for the two terminal tandem cell with a single-junction top cell and an IB bottom are shown in figure 7.47 (1 sun), 7.48 (100 suns) and 7.49 (1000 suns).

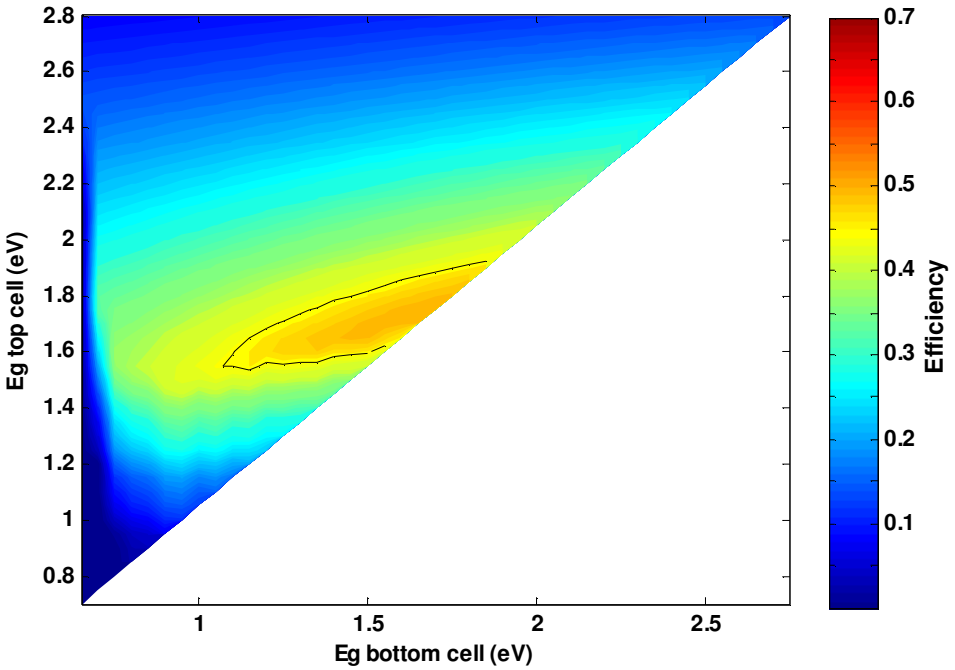

Figure 7.47: Efficiency of the tandem cell under 1 sun, area function of the main band gap energies of the single-junction top cell and IB bottom cell.

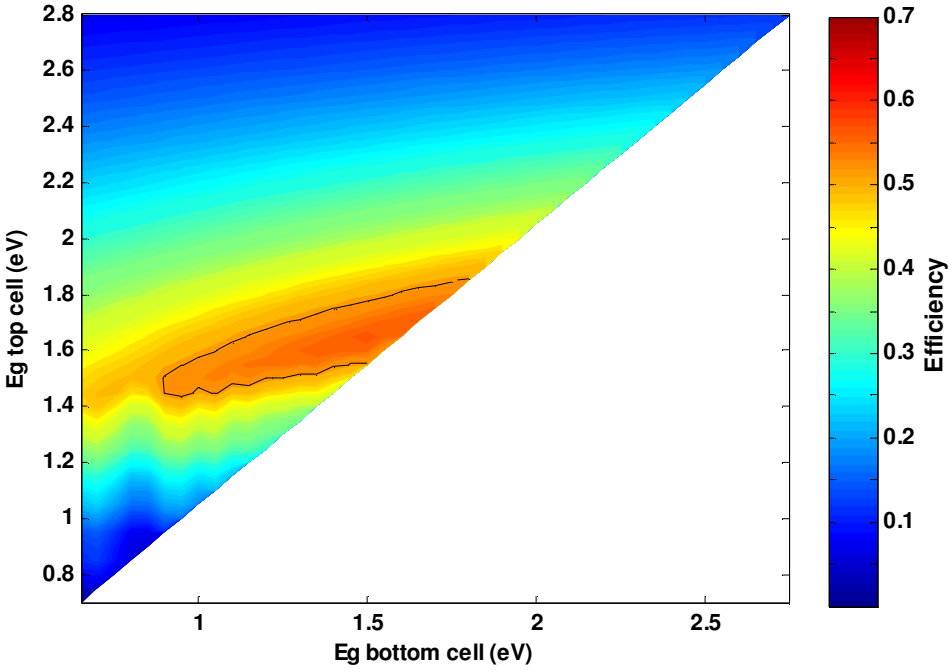

Figure 7.48: Efficiency of the tandem cell under 100 suns, area function of the main band gap energies of the single-junction top cell and IB bottom cell.

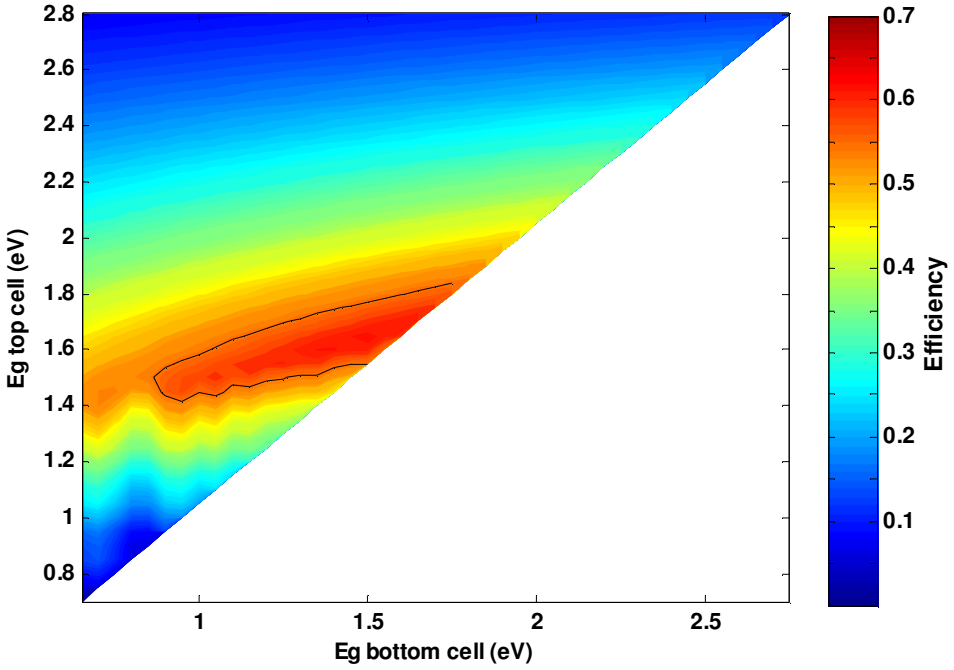

Figure 7.49: Efficiency of the tandem cell under 1000 suns, area function of the main band gap energies of the single-junction top cell and IB bottom cell.

The maximum efficiency for the tandem cell is 50.32%, 57.65% and 61.71% for concentration levels of 1 sun, 100 suns and 1000 suns respectively. Band gap combinations for the lowest concentration level are $E_{G,Top}$ = 1.75 eV, $E_{G,Bot}$ = 1.70 eV and $E_{L,Bot}$ = 0.55 eV. For the 100 and 1000 suns concentration the maximum efficiency is found when $E_{G,Top}$ is 1.65 eV, $E_{G,Bot}$ is 1.50 eV, and $E_{L,Bot}$ is 0.50 eV.

For 1 sun the high efficiencies (over 45.29%) are given at band gap combinations in the $E_{G,Top}$ range from 1.55 eV to 1.90 eV and $E_{G,Bot}$ range from 1.10 eV to 1.85 eV. The band gap ranges for the 100 suns giving efficiencies over 51.88% are from 1.45 eV to 1.85 eV for $E_{G,Top}$ and from 0.9 eV to 1.8 eV for $E_{G,Bot}$. Efficiencies over 55.54% are given for 1000 suns in the $E_{G,Top}$ range from 1.45 eV to 1.80 eV and $E_{G,Bot}$ range from 0.90 eV to 1.75 eV.

Discussion

The maximum efficiencies are increased with less than 2.23% when compared with the single IBSC. The main band gap of the bottom IBSC is set very close to the main band gap of the top single-junction cell, and the maximum efficiency is very close to that of the single IBSC. For the cell under 1 sun, the main band gap of the bottom cell is as close to the top cell main band gap the simulation allows, hence displaying a clear limitation of the model used in the simulations. At higher levels of concentration, the maximum efficiency is found with a larger difference between the main band gap energies of the two cells.

Sub-band gap energies, bottom cell

In figures 7.50, 7.51 and 7.52 the optimum lowest sub-band gap energies for the bottom IBSC are presented for 1, 100 and 1000 suns respectively.

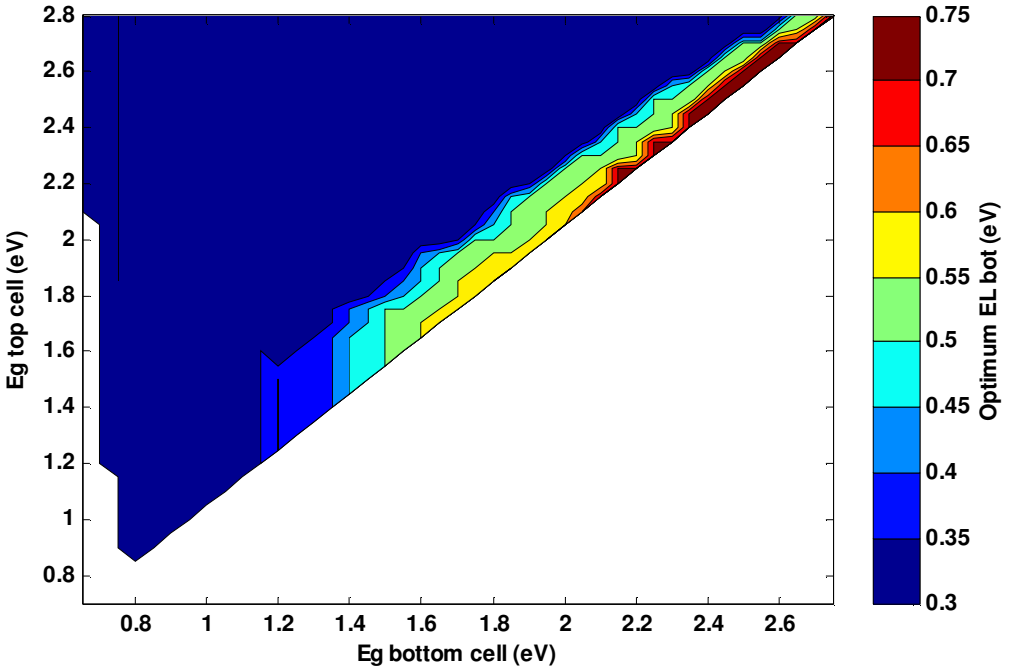

Figure 7.50: The optimum lowest sub-band gap energies for the bottom cell ($E_{L,Bot}$). Concentration level is 1 sun.

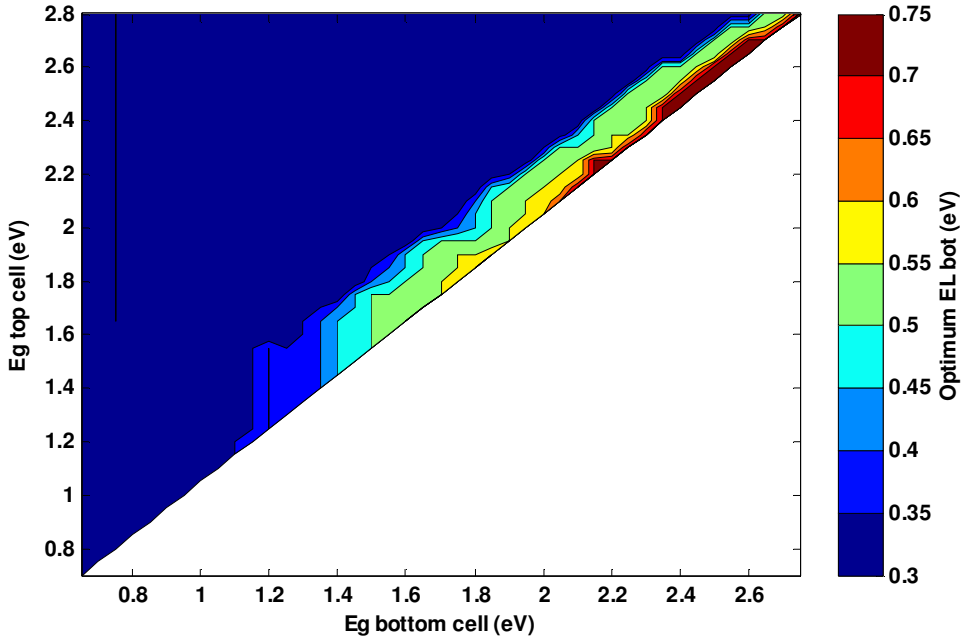

Figure 7.51: The optimum lowest sub-band gap energies for the bottom cell ($E_{L,Bot}$). Concentration level is 100 suns.

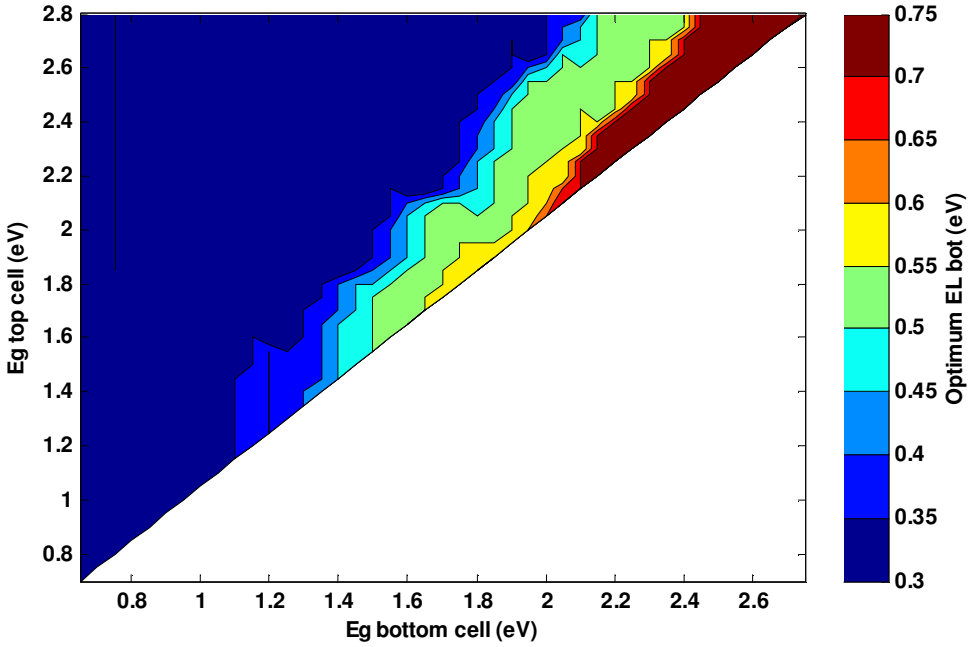

Figure 7.52: The optimum lowest sub-band gap energies for the bottom cell ($E_{L,Bot}$). Concentration level is 1000 suns.

For most of the main band gaps of both cells, the minimal value for $E_{L,Bot}$ (0.30 eV) is chosen for the optimum efficiency values. There is little difference between the $E_{L,Bot}$ values for concentration levels of 1 sun and 100 suns, but there is an increase in $E_{L,Bot}$ for some main band gap values for the 1000 suns concentration level.

Discussion

Similar to the tandem IBSC in section 7.2.2, the values for $E_{L,Bot}$ are very different from the four terminal case. For most main band gap values, the smallest values for the $E_{L,Bot}$ are chosen as optimum for high efficiency. The reason for the low values of $E_{L,Bot}$ is discussed in section 7.2.2.

For the tandem IBSC, the values for $E_{L,Bot}$ are also low for the highest values of $E_{G,Bot}$ at a certain top cell main band gap energy. As this is a result of the $E_{L,Top}$ values getting close to the other sub-band gap of the top cell, the tandem cell with a single-junction top cell does not have the same result. It is clearly seen by comparing figure 7.50 with figure 7.26, as the values for $E_{L,Bot}$ are high at these band gap combinations in figure 7.50 and low in figure 7.26.

7.3.5 Two and four terminal tandem cell

The efficiencies found for the two and four terminal tandem cells that combine an IBSC and a single-junction cell, are compared in this section with each other and the conventional four single-junction tandem cell in [14]. Table 7.4 shows the maximum efficiencies and corresponding band gap energies for the tandem IB and single-junction cell.

Table 7.4: Band gap energies and maximum efficiencies for the tandem IB and single-junction cell.

Concentration level	$E_{G,Top}$ (eV)	$E_{G,Bot}$ (eV)	$E_{L,Top}$ (eV)	$E_{L,Bot}$ (eV)	Maximum Efficiency (%)
4 terminal IB/single tandem cell					
1 sun	2.85	0.7	1.15		53.18
100 suns	2.45	0.5	0.95		60.23
1000 suns	2.45	0.5	0.95		64.48
4 terminal single/IB tandem cell					
1 sun	2.3	1.95		0.7	52.62
100 suns	2.1	1.65		0.55	60.31
1000 suns	2.05	1.5		0.5	64.81
2 terminal IB/single tandem cell					
1 sun	2.95	0.7	1.2		52.51
100 suns	2.95	0.7	1.2		59.19
1000 suns	2.75	0.5	1.1		63.11
2 terminal single/IB tandem cell					
1 sun	1.75	1.7		0.55	50.32
100 suns	1.65	1.5		0.5	57.65
1000 suns	1.65	1.5		0.5	61.71

In Brown's paper [14] the maximum efficiencies for the four junction tandem cells calculated with the 1 sun AM1.5G radiation are 55.6% for the unconstrained cell and 54.9% for the series connected tandem cell. This shows a decrease in maximum efficiency of 1.26%, which is larger than for the six junction cell, considered in section 7.2.3.

The two terminal tandem cell with the IB bottom cell has the largest decreases in efficiencies when compared to the four terminal cell. All of the maximum efficiencies are decreased by at least 4.37%. The maximum efficiency decreases from the four to the two terminal tandem cell with the IB top cell with 1.26%, 1.73%, and 2.12% for the concentration of 1 sun, 100 suns and 1000 suns respectively. In this thesis the tandem cell with an IB top cell and a single-junction bottom cell has the smallest decrease in maximum efficiency when series connected. The decrease in maximum efficiency for 1 sun concentration is equal to that of the four junction tandem cell in [14]. There is still an inaccuracy in these results because of the large steps between the band gap energies in the calculations. From the results in table 7.1 the tandem cell with an IB top cell is seen to have a lower decrease in maximum efficiency when

series connected than the tandem cell with an IB bottom cell. The decrease in maximum efficiency for the tandem cell with an IB top cell is 0.88% and for the tandem cell with an IB bottom cell the decrease is 5.83%, for a tandem cell under full concentrated black-body radiation (6000K). Series connecting the tandem cell with a single-junction top cell and an IB bottom cell is thus concluded to have the largest decrease in maximum efficiency from the four terminal case to the two terminal case.

7.4 Discussion of the energy resolution

The results in this thesis are calculated with an energy resolution of 0.05 eV, which reduces the resolution in the plots and the accuracy of the band gap combination for the maximum efficiency. This energy resolution is, as stated earlier, low because of the time the calculations need to run for each combination of band gaps. It is the calculations of the bottom cell that make a higher energy resolution impractical. In this section calculations for the IB top cell and single-junction bottom cell will be repeated with an energy step of 0.01 eV, to discuss how the energy resolution affects the results. The results presented in this section will only be discussed in this section and not be included later in the thesis.

The main band gap ranges used in these calculations are $E_{G,Top}$ between 2 eV and 4 eV and $E_{G,Bot}$ between 0.50 eV and 2 eV. The efficiencies for the two different energy steps are both plotted with these main band gap ranges, for an easier comparison of the difference in efficiencies.

Efficiencies for the IB top cell and single-junction bottom cell, 1 sun

The first plot (figure 7.53) shows the efficiency for the calculations with an energy step of 0.05 eV, and the second (figure 7.54) with an energy step of 0.01 eV. Table 7.5 shows the band gap combinations for the maximum efficiency in the two cases.

Table 7.5: Band gap combinations for the maximum efficiency.

Energy step (eV)	$E_{G,Top}$ (eV)	$E_{G,Bot}$ (eV)	$E_{L,Top}$ (eV)	$E_{L,Bot}$ (eV)	Maximum Efficiency (%)
0.05	2.85	0.7	1.15		53.18
0.01	2.81	0.7	1.13		53.25

The band gap difference is 0.04 eV for $E_{G,Top}$ and 0.02 eV for $E_{G,Bot}$ when comparing the band gap energies for the maximum efficiency. The maximum efficiency is increased by 0.13%.

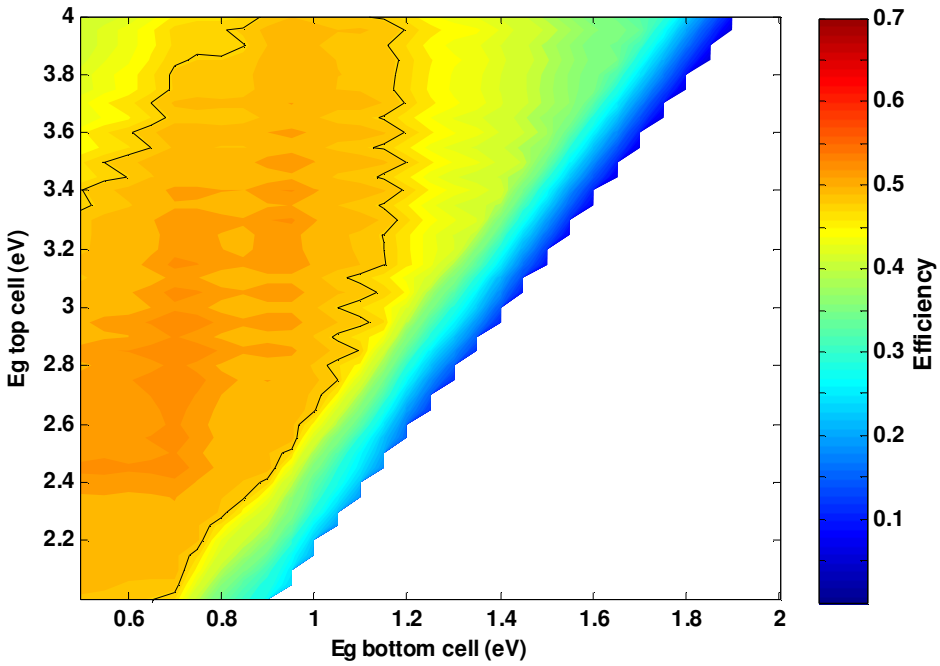

Figure 7.53: Efficiency of the tandem cell under 1 sun, axes show the main band gap energies of the IB top cell and single-junction bottom cell. Energy step set to 0.05 eV.

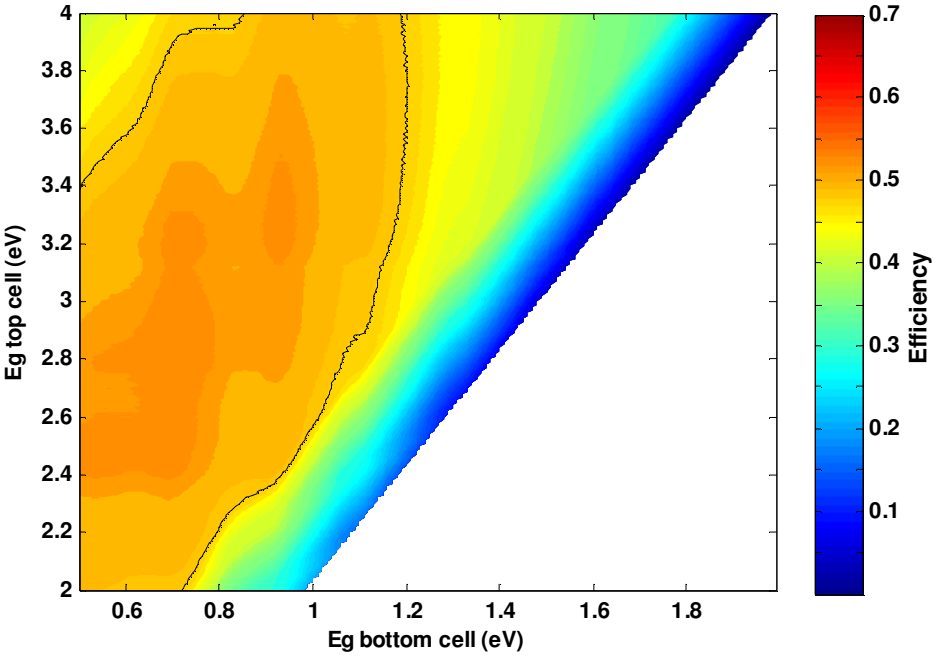

Figure 7.54: Efficiency of the tandem cell under 1 sun, axes show the main band gap energies of the IB top cell and single-junction bottom cell. Energy step set to 0.01 eV.

The resolution and smoothness of the plots are greatly increased with a decrease in the band gap energy step, seen from comparing figure 7.53 and 7.54. There is also an increase in efficiency overall seen in the plot with the highest resolution. The black line showing the band gap area with high efficiency is very similar for the two plots, considering the poor resolution in figure 7.53. For the calculations with a smaller energy step the area with high efficiency is a little larger overall, especially close to the band gap ranges from 3.40 eV to 3.90 eV for $E_{G,Top}$ and 0.50 eV to 0.80 eV for $E_{G,Bot}$.

Discussion

The increase in maximum efficiency when using a lower energy step is small in this case, but can be larger for the other tandem cells, especially the tandem IBSC, as this cell has more band gaps. When comparing figures 7.53 and 7.54, the band gap area with high efficiency is also similar for both cases, but the plot with smaller energy steps is smoother and a little larger. As the sub-band gap is also affected by having a smaller energy step, a higher maximum efficiency and change in the main band gap energy value is very likely. Note that the value for $E_{G,Top}$ (2.81 eV) for the maximum efficiency of the calculations with a higher energy resolution is closer to 2.80 eV than 2.85 eV. The band gap values with maximum efficiency are thus close to the ones found in the calculations with low resolution, but not necessarily closest to the band gap step where the maximum efficiency is given for the low resolution results.

The sub-band gaps for the top cell follow a similar pattern as for the results with an 0.05 eV energy step.

The plotted efficiencies in figure 7.54 have much smoother contours and show results expected from the simulations, thus resolution and irregularities in the plots are mostly a result of the low energy resolution.

7.5 Effects of variations in band gap energies

For some of the tandem cells, the increase in efficiency compared with the single IBSC is low. Thus it is interesting to discuss other benefits of using the IBSC in tandem cells. As stated earlier, the tandem cell increases the potential for use of other semi-conductor materials with other band gaps that are not useful for single IBSCs or single-junction cells. Tables 7.2, 7.3 and 7.4 show that the band gap combinations with maximum efficiencies for the IBSC used in a tandem cell and in a single cell device differ greatly. These specific band gap combinations can not always be achieved, as they are material dependent. In this section the band gap ranges providing the tandem cell with high efficiency will be closer examined and discussed. High efficiency is still assigned to efficiencies above 90% of the maximum efficiency for the cell under the same conditions. In section 7.5.1 the range of the main band gaps giving high efficiencies are calculated and discussed. The lowest sub-band gap ranges giving high efficiencies are treated in section 7.5.2.

Similar to the results presented earlier in this chapter, the band gap steps are set at 0.05 eV if not specifically stated otherwise. S+IB indicates a tandem cell with a single-junction top cell and an IB bottom cell, while IB+S indicates the opposite configuration. The tandem IBSC is signified by 2 x IBSC.

7.5.1 Variations in the main band gaps

For practical applications, it is interesting to see which range of main band gaps gives high efficiencies for the solar cell. If one of the main band gaps for the maximum efficiency is found in a material, it can be valuable information to know which range of main band gap energies is needed for the other cell, to provide the complete tandem cell with a high efficiency. In this section one of the main band gaps is varied, while the other main band gap is held at the value for maximum efficiency for the total cell. The sub-band gaps will also be varied to obtain the highest efficiency for each combination of main band gap values, but the optimum sub-band gaps are not indicated. The combinations of band gaps at 90% of the maximum efficiency are plotted in the efficiency plots previously in this chapter, marked with a black line.

Main band gap ranges resulting in high efficiencies

The following figures display some of the main band gap combinations for each cell that are within the high efficiencies of the cell. The main band gap range for the top cell, while keeping the bottom main band gap fixed, is shown in figure 7.55. In figure 7.56 the upper cell main band gap is fixed, while the lower is varied. The main band gap ranges for the single-junction cell and the single IBSC are also shown to compare with the tandem cells. The energy resolution for both of the single cells is 0.01 eV. Note that the main band gap ranges are restricted by the highest band gaps used in the simulations (4.80 eV) and that the main band gap of the top cell in the simulations have to be larger than the main band gaps of the bottom cell.

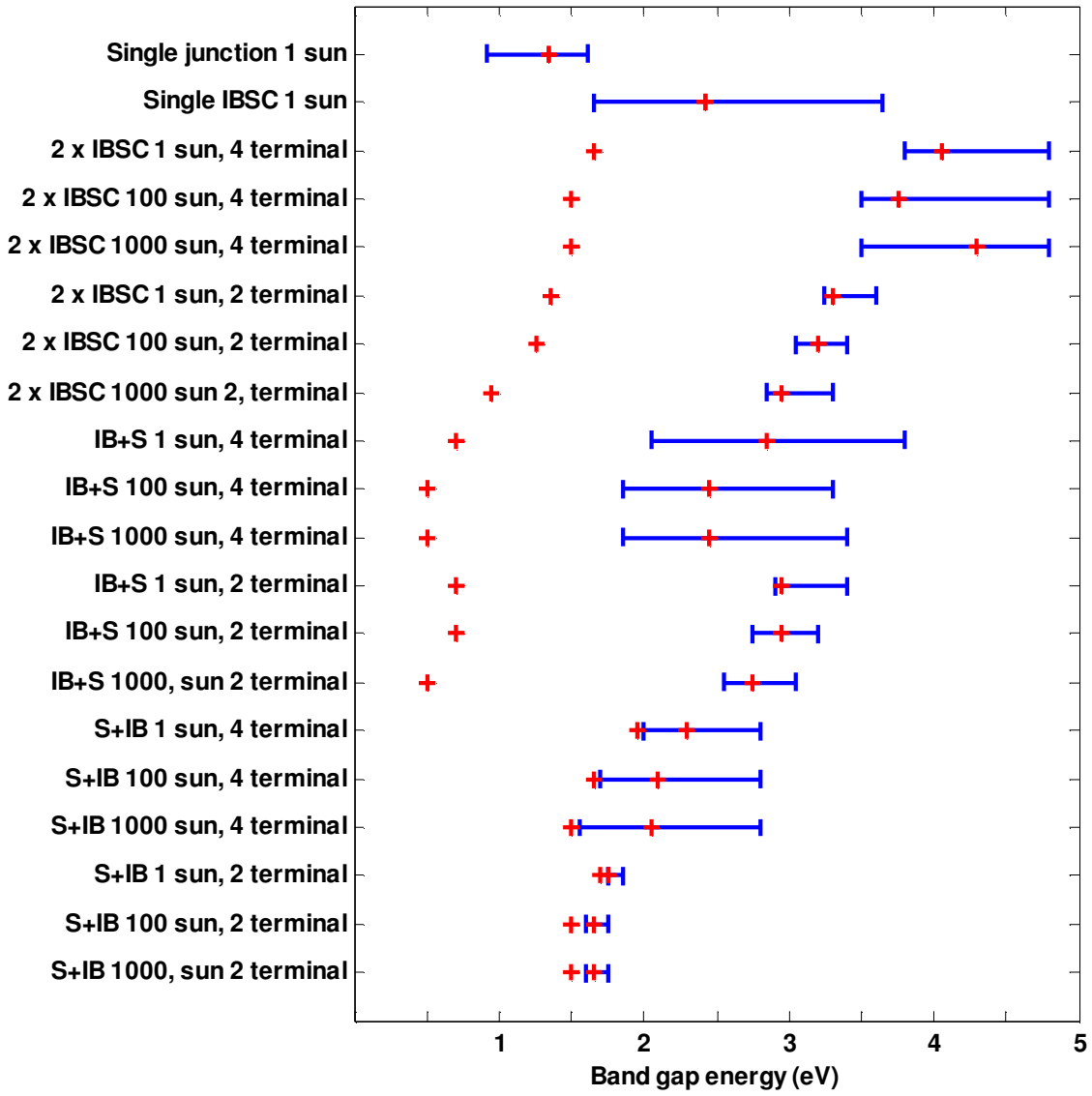

Figure 7.55: Main band gap ($E_{G,Top}$) range (blue lines) for the upper cells that provide the complete tandem cell with high efficiencies. The red crosses represent the main band gap energies providing the maximum efficiency.

As seen from figure 7.55, the single IBSC has a large range of main band gap values giving high efficiency, and the range is higher than for any of the top cells of the tandem solar cells. Even the single-junction cell has a wider range of main band gaps giving high efficiency, when compared to the series connected tandem cells.

The series connected tandem cells have, as expected, a much smaller range for the top main band gap energies than the four terminal tandem cells. The smallest range is only 0.1 eV (S+IB 1 sun, 2 terminal), and the highest range is 1.75 eV (IB+S 1 sun, 4 terminal).

Another noticeable trait with the tandem cell with a single-junction top cell and IB bottom cell configuration (S+IB), is that the main band gaps are much closer in energy than for the

other tandem cells at high efficiency. The range of $E_{G,Top}$ gets very close to the main band gap of the bottom cell, and the lowest value $E_{G,Top}$ can have in this model is 0.05 eV above $E_{G,Bot}$.

Figure 7.56 shows the main band gap ranges for the bottom cell, with fixed main band gap for the top cell.

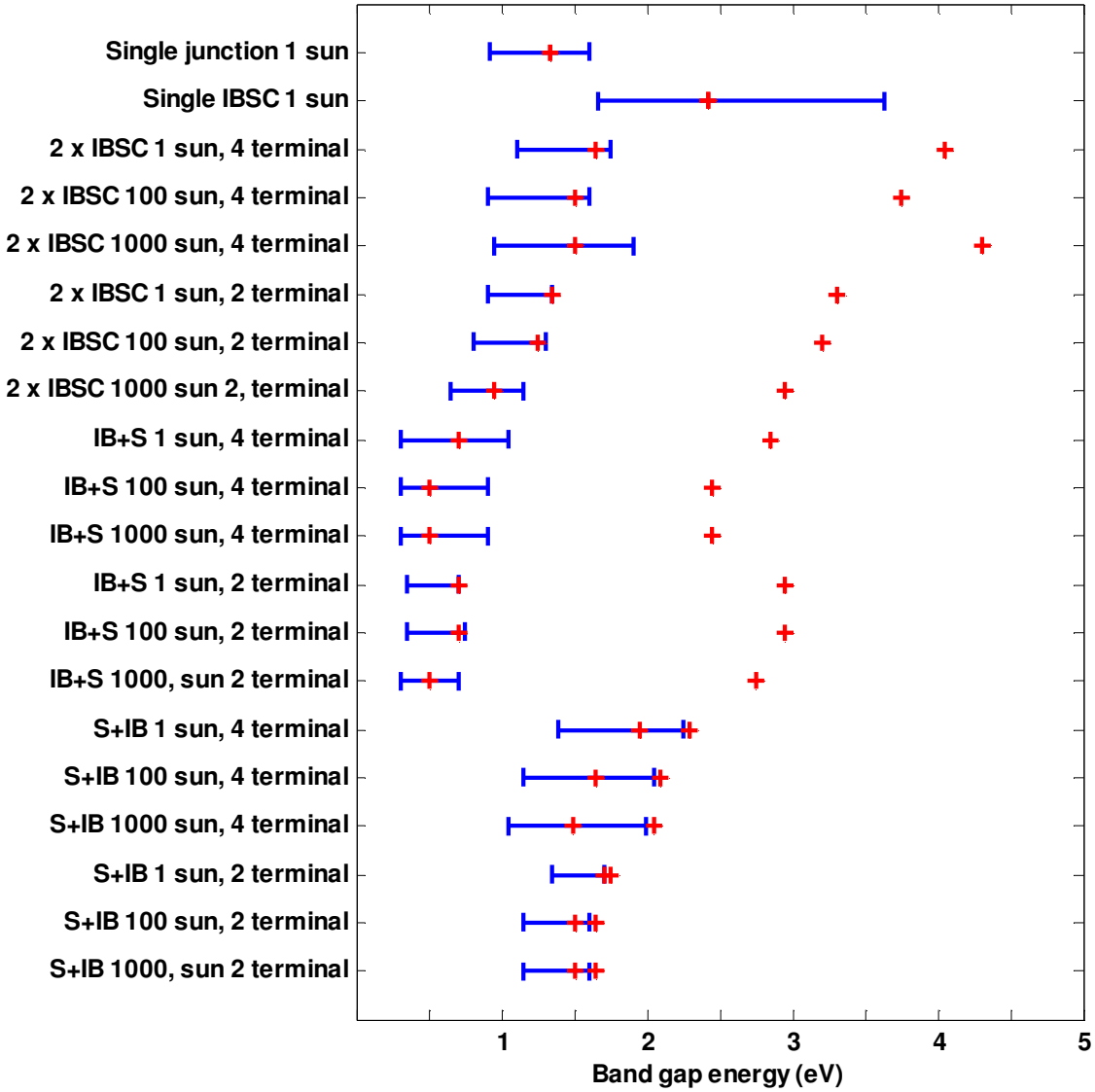

Figure 7.56: Main band gap ($E_{G,Bot}$) ranges (blue lines) for the lower cells, providing the complete tandem cell with high efficiencies. The red crosses represent the main band gap energies providing the maximum efficiency.

The largest range for the main band gaps of the bottom cell is 0.95 eV (IBSC and S+IB, 1000 suns and four terminal) and the lowest range is 0.35 eV (IB+S and S+IB , 1 sun and two terminal).

The difference in energy range between the two and four terminal tandem cells is not as significant for $E_{G,Bot}$ as for the $E_{G,Top}$ ranges.

The main band gap range for the bottom S+IB tandem cell goes (, as for the ranges of the top cell,) as close to the main band gap of the other cell in the configuration as possible in these simulations.

Discussion

The main band gap ranges for the top cell ($E_{G,Top}$) of the tandem IBSC go as high as 4.80 eV, which is the highest band gap used in these calculations. These band gap ranges are likely to reach higher band gap energies, and thus be larger than found in this thesis work.

Some of the ranges for the S+IB tandem cells are restricted by the other main band gap, and therefore could have a wider range if the other main band gap was allowed to have other values. If the main band gap values of the S+IB tandem cell get very close to each other, the top single-junction cell will contribute little to the efficiency of the tandem cell. The tandem cell will then achieve an efficiency similar to a single IBSC with the band gap values equal to that of the bottom IBSC in the S+IB tandem cell.

The ranges for the top cell clearly show the restriction of series connecting the cells, as the band gap ranges are reduced strongly for the two terminal tandem cells. This is also seen from the numerous efficiency plots for each of the tandem cells in the previous sections. Ranges for the band gaps of the bottom cell are not affected in the same degree by series connecting the cells. Thus the bottom cell is less affected by the constraint in having equal current.

The band gap energy range does not seem to be affected in any specific way by the concentration level. As the maximum efficiency is also increased with a higher concentration level, this is expected.

Efficiencies at the main band gap range edges

Fabrication of a solar cell with a specific main band gap energy can be difficult in practice, hence the effect on the efficiency by small variations in the main band gap is interesting. Tables 7.6 and 7.7 show the efficiency at the edges of the main band gap ranges (found in figures 7.55 and 7.56), where the main band gap for the other cell is varied with 0.10 eV. The efficiencies for some of these band gap combinations are not available because of restrictions in the model used in this thesis and these cells in the tables are left blank.

Discussion

For some of the tandem cells, varying the main band gap to either a larger or smaller value will increase the efficiency, and altering it oppositely will decrease the efficiency. The increase in efficiency is merely a consequence of the new band gap combinations giving a higher efficiency, and is obvious when looking at the figures showing the maximum efficiencies for the various tandem cells found in sections 7.2 and 7.3. Variations in $E_{G,Bot}$ at the edges of $E_{G,Top}$ have the largest decrease in efficiency, close to 40%. Variations in $E_{G,Top}$ only cause a decrease of maximum 14%. Both of the largest decreases are for the two terminal tandem IBSC with 1 sun concentration.

Table 7.6: Efficiency for $E_{G,Top}$ range edges when varying $E_{G,Bot}$.

Concentration level	$E_{G,Top}$ (eV)	$E_{G,Bot}$ (eV)	Efficiency (%) values of $E_{G,Bot}$ (eV)		
			-0.10 eV	0	+0.10 eV
4 terminal tandem IBSC (2xIBSC)					
1 sun	3.8	1.65	53.83	51.23	38.29
1 sun	4.8	1.65	51.79	52.76	52.39
100 suns	3.5	1.5	61.00	58.14	43.41
100 suns	4.8	1.5	57.89	59.42	59.40
1000 suns	3.5	1.5	65.02	62.03	46.66
1000 suns	4.8	1.5	62.89	64.28	63.97
2 terminal tandem IBSC (2xIBSC)					
1 sun	3.25	1.35	52.73	50.52	30.52
1 sun	3.6	1.35	47.75	48.83	49.84
100 suns	3.05	1.25	59.13	55.89	37.10
100 suns	3.4	1.25	55.31	56.53	57.58
1000 suns	2.85	0.95	55.19	60.19	59.44
1000 suns	3.3	0.95	57.57	59.07	60.41
4 terminal IB/single tandem cell (IB+S)					
1 sun	2.05	0.7	48.83	48.71	36.97
1 sun	3.8	0.7	45.52	48.20	48.38
100 suns	1.85	0.5	54.29	54.77	53.48
100 suns	3.3	0.5	52.52	55.43	56.40
1000 suns	1.85	0.5	58.91	59.39	57.83
1000 suns	3.4	0.5	54.93	58.04	58.94
4 terminal single/IB tandem cell (S+IB)					
1 sun	2	1.95	51.48	51.65	
1 sun	2.8	1.95	49.59	50.83	50.83
100 suns	1.7	1.65	57.77	57.61	
100 suns	2.8	1.65	55.98	57.27	57.11
1000 suns	1.55	1.5	60.41	60.48	
1000 suns	2.8	1.5	59.04	61.03	61.34
2 terminal IB/single tandem cell (IB+S)					
1 sun	2.9	0.7	49.24	50.59	42.25
1 sun	3.4	0.7	45.90	47.29	48.51
100 suns	2.75	0.7	54.55	53.88	43.83
100 suns	3.2	0.7	53.63	55.15	56.30
1000 suns	2.55	0.5	55.21	57.03	50.04
1000 suns	3.05	0.5	55.74	57.40	58.86
2 terminal single/IB tandem cell (S+IB)					
1 sun	1.75	1.7	49.47	50.32	
1 sun	1.85	1.7	45.52	46.94	48.18
100 suns	1.6	1.5	56.90	56.35	
100 suns	1.75	1.5	51.81	53.38	54.95
1000 suns	1.6	1.5	61.18	60.48	
1000 suns	1.75	1.5	55.19	56.83	58.43

Table 7.7: Efficiency for $E_{G,Bot}$ range edges when varying $E_{G,Top}$.

Concentration level	$E_{G,Top}$ (eV)	$E_{G,Bot}$ (eV)	Efficiency (%) values of $E_{G,Top}$ (eV)		
			-0.10 eV	0	+0.10 eV
4 terminal tandem IBSC (2xIBSC)					
1 sun	4.05	1.1	50.01	49.55	48.83
1 sun	4.05	1.75	48.32	53.75	53.75
100 suns	3.75	0.9	57.49	57.40	56.54
100 suns	3.75	1.6	55.39	61.57	61.66
1000 suns	4.3	0.95	61.11	60.53	59.66
1000 suns	4.3	1.9	58.33	64.01	64.09
2 terminal tandem IBSC (2xIBSC)					
1 sun	3.3	0.9	49.39	48.81	47.28
1 sun	3.3	1.35	46.33	53.88	52.75
100 suns	3.2	0.8	54.75	55.38	53.37
100 suns	3.2	1.3	53.09	60.78	59.77
1000 suns	2.95	0.65	62.04	61.65	59.33
1000 suns	2.95	1.15	52.29	59.65	63.32
4 terminal IB/single tandem cell (IB+S)					
1 sun	2.85	0.3	48.30	48.03	47.00
1 sun	2.85	1.05	47.86	48.60	49.02
100 suns	2.45	0.3	57.50	57.94	57.02
100 suns	2.45	0.9	50.68	55.81	56.25
1000 suns	2.45	0.3	61.91	62.26	61.28
1000 suns	2.45	0.9	53.82	59.17	59.57
4 terminal single/IB tandem cell (S+IB)					
1 sun	2.3	1.4	48.41	47.72	46.89
1 sun	2.3	2.25		50.38	50.67
100 suns	2.1	1.15	55.56	54.86	54.00
100 suns	2.1	2.05		57.65	58.23
1000 suns	2.05	1.05	59.83	59.09	58.23
1000 suns	2.05	2		60.58	61.39
2 terminal IB/single tandem cell (IB+S)					
1 sun	2.95	0.35	48.72	47.79	46.36
1 sun	2.95	0.7	47.16	52.51	51.92
100 suns	2.95	0.35	55.24	53.66	51.67
100 suns	2.95	0.75	53.58	56.19	57.65
1000 suns	2.75	0.3	59.91	59.70	58.22
1000 suns	2.75	0.7	51.12	57.31	59.31
2 terminal single/IB tandem cell (S+IB)					
1 sun	1.75	1.35	48.50	45.65	41.86
1 sun	1.75	1.7		50.32	46.94
100 suns	1.65	1.15	55.35	52.10	47.67
100 suns	1.65	1.6		55.89	54.95
1000 suns	1.65	1.15	59.89	55.90	50.90
1000 suns	1.65	1.6		59.76	58.43

7.5.2 Variation in the sub-band gaps

Variations in the sub-band gap are treated in this section. As it is easier to find a semiconductor material with the appropriate main band gap than to implement a specific position for the intermediate band in the material, the variations in the sub-band gaps that still provide the cell with a high efficiency are important to study.

Sub-band gap ranges with high efficiencies

The results for the lowest sub-band gap ranges are presented in figures 7.57 and 7.58, starting with the ranges for the top cell. All other band gaps are kept at the value they have at the maximum efficiency for the cell, including the intermediate band for the other cell. Confer with tables 7.3 and 7.4 for these values. The energy steps for the single IBSC is more accurate, with an energy resolution of 0.01 eV.

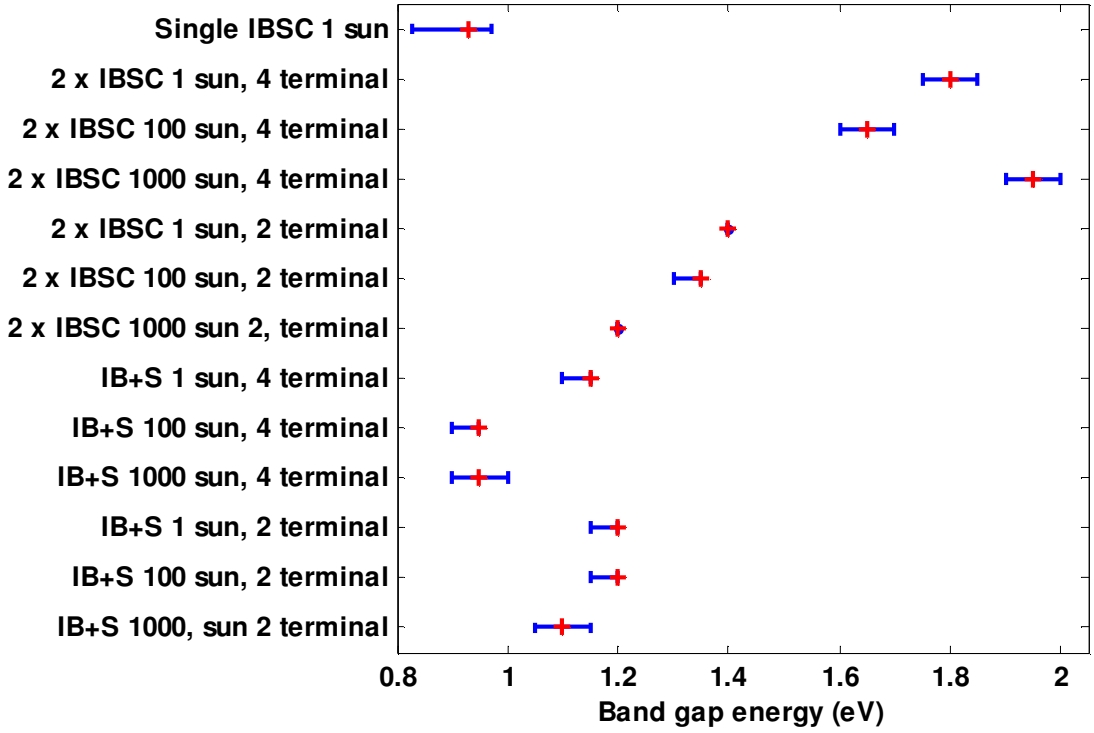

Figure 7.57: Lowest sub-band gap ($E_{L,Top}$) range (blue lines) for the upper cells that provide the complete tandem cell with high efficiencies. The red crosses represent the sub-band gap energies providing the maximum efficiency.

The $E_{L,Top}$ ranges are at most 0.10 eV for the upper cells. Compared with the single IBSC with a range of 0.14 eV, the range is not much smaller considering that the single IBSC has been calculated with a smaller energy step. It is expected that for these small energy ranges, the length of the band gap step has a strong effect on the results. For the connected tandem cells, the smallest range of zero is found, thus only the specific intermediate energy band will give the cell a high efficiency. The two terminal IB+S has a generally larger range than the two terminal tandem IBSC.

The following plot shows the $E_{L,Bot}$ ranges of the bottom cell in various tandem cell configurations.

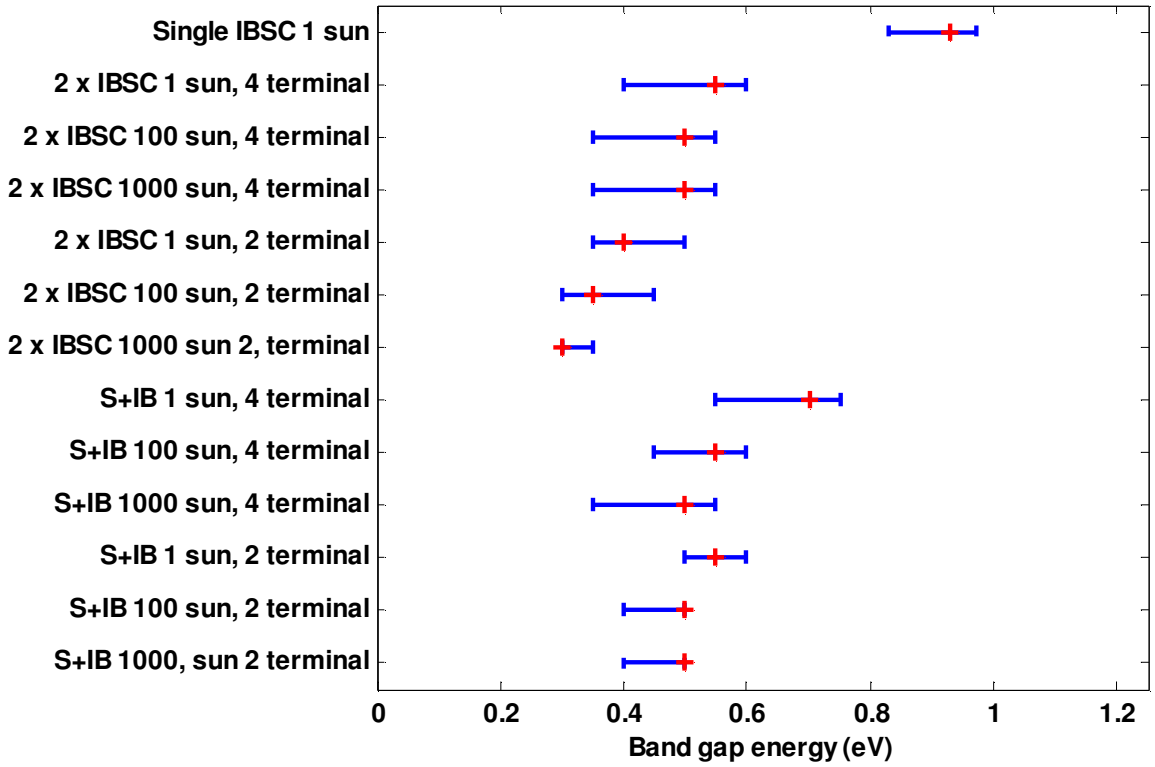

Figure 7.58: Lowest sub-band gap ($E_{L,Bot}$) range (blue lines) for the lower cells that provide the complete tandem cell with high efficiencies. The red crosses represent the sub-band gap energies providing the maximum efficiency.

Compared to the top cell, the lowest sub-band gap ranges of the bottom cell are much larger, with a 0.20 eV at most. Most of the ranges are between 0.10 eV and 0.20 eV, with the exception of the connected tandem IBSC under 1000 suns concentration with a range of 0.5 eV.

Discussion

The ranges for the sub-band gaps of the top cell are very restricted compared to the sub-bands in the bottom cell. Changes in $E_{L,Top}$ will both change the photon flux absorbed within the top cell and the bottom cell, as the photons with a smaller energy than $E_{L,Top}$ will be transmitted through the top cell and absorbed in the bottom cell. $E_{L,Top}$ also restricts the radiative recombination in the bottom cell, because of filters between the cell reflecting the emitted flux from the bottom cell. The smaller range in the values of $E_{L,Top}$ is a consequence of all the physical processes affected by $E_{L,Top}$.

The tandem cell is thus very dependent on the value of $E_{L,Top}$, and the intermediate band energy will need high precision during fabrication, which can complicate the production of tandem IBSC.

8 Conclusion

In this thesis Matlab has been used to simulate the detailed balance principle on various types of tandem cells. The tandem cells consist of either two IBSCs, or one IBSC and one single-junction cell. The standard AM1.5 spectra have been used and the cells have been simulated for concentration levels of 1 sun, 100 suns and 1000 suns. Because of a long runtime for the Matlab code, results for only a limited amount of band gap combinations spread over a larger range, are calculated.

The largest efficiencies found are for the four terminal tandem IBSC with maximum efficiencies of 54.91% for 1 sun, 62.74% for 100 suns concentration, and 67.23% for 1000 suns. This is an increase of about 11% from the maximum efficiency of a single IBSC, for all concentration levels.

The two terminal tandem cells show a decrease in efficiency compared to the four terminal tandem cell, as for conventional multi-junction tandem cells. For the tandem IBSC, the decrease in maximum efficiency is larger than for the conventional six-junction tandem cell, but for the tandem cell with IB top cell and single-junction bottom cell the decrease in maximum efficiency is very close to that of the conventional four-junction tandem cell. Series connecting the tandem cell with a single-junction top cell and IB bottom cell shows the largest decrease in maximum efficiency compared to the four terminal tandem cell. This configuration of the IBSC and the single-junction cell is thus less viable for a two terminal tandem cell.

The tandem IBSC has, similar to the case for a single IBSC, large ranges of band gaps with a reasonably high efficiency, especially for the four terminal tandem cells. For the two terminal tandem cells, the ranges of band gaps with high efficiencies for the two separate cells are found to be smaller than for the single IBSC. The maximum efficiencies for the tandem IBSCs are mostly at band gap energies far from the band gaps with the maximum efficiency of the IBSC. A larger group of semiconductor materials can then be effectively used in solar cell devices.

The optimum lowest sub-band gap is found at a width above 35% to 40% of the main band gap for the top IBSC in both a two terminal and a four terminal tandem cell, and the ratio increases with the main band gap values. For the bottom IBSC in two terminal tandem cell, the ratio between the optimum sub-band gap and the main band gap of the bottom cell is very low for many of the band gap configurations. In the four terminal tandem cell the optimum lowest sub-band gap has a larger value compared to the main band gap for the bottom IBSC, and ranges from about 23.5% to 35% of the bottom cell main band gap. The ratio for both the top and bottom IBSC seems to be close to that of the single IBSC for the main band gaps compared in this thesis (from 1.5 eV to 2.5 eV).

The efficiency of the tandem IBSC is very sensitive to variations in the positioning of the intermediate band in the top IBSC, especially for the two terminal tandem IBSC. The efficiency is less affected by variation in the sub-band gaps in the bottom IBSC.

9 Further work

In section 7.4 the low resolution in band gaps used in the simulations is discussed. Using a smaller step between each band gap value in the simulations will increase the maximum efficiency for the tandem cells. A faster script and more computer power can be used to run simulations for more band gap energies and produce more accurate results.

In this thesis the standard reference spectra for the AM1.5 has been used as the incident radiation. The tandem IBSC uses a larger part of the spectra, and will probably be more sensitive to changes in the spectra. Running simulations with various radiation distributions from measurements at different locations would perhaps show another interesting feature of the tandem IBSC.

As the detailed balance principle has been used to model the tandem IBSC in this thesis, a real cell would have lower efficiencies. A drift/diffusion model for the tandem IBSC could be made to get more realistic results, and used to further study the tandem IBSC device.

Bibliography

1. *Global Market Outlook for Photovoltaics until 2015. European Photovoltaic Industry Association (EPIA)*. [downloaded 2010 5-10] Available from: http://www.epia.org/fileadmin/EPIA_docs/public/Global_Market_Outlook_for_Photovoltaics_until_2014.pdf.
2. A. Luque and S. Hegedus, *Handbook of Photovoltaic Science and Engineering*. (John Wiley & Sons, 2003).
3. M.A. Green. *Third Generation Photovoltaics: Advanced Solar Energy Conversion*. (Springer-Verlag Berlin Heidelberg, 2006).
4. T. Markvart, *Solar electricity*. (John Wiley and Sons, 2000).
5. M.A. Green, *Solar cells: operating principles, technology and system applications*. (University of New South Wales, 1992).
6. *National Renewable Resource Data Center*. National Renewable Energy Laboratory. [downloaded 2010 10-27] Available from: http://rredc.nrel.gov/solar/spectra/am1.5/.
7. J. Nelson, *The Physics of Solar Cells*. (Imperial collage Press, 2003).
8. A. Martí and G.L. Araújo, *Limiting efficiencies for photovoltaic energy conversion in multigap systems.* Solar Energy Materials and Solar Cells, **43** (1996) p. 203-222.
9. M.A. Green, et al., *Solar cell efficiency tables (version 37).* Progress in Photovoltaics: Research and Applications, **19** (2011) p. 84-92.
10. A. Luque and A. Martí, *The Intermediate Band Solar Cell: Progress Toward the Realization of an Attractive Concept.* Advanced Materials, **22** (2010) p. 160-174.
11. A. Luque and A. Martí, *Increasing the Efficiency of Ideal Solar Cells by Photon Induced Transitions at Intermediate Levels. Phys. Rev. Lett.* **78** (1997) p. 5014-5017.
12. P.C. Hemmer, *Kvantemekanikk*. (Tapir Akademisk Forlag, 2005).
13. T. Soga, *Intermediate Band Solar Cells (IBSC) Using Nanotechnology, chapter 17 in Nanostructured materials for solar energy conversion*. (Elsevier, 2006).
14. Brown, A.S. and M.A. Green, *Detailed balance limit for the series constrained two terminal tandem solar cell.* Physica E: Low-dimensional Systems and Nanostructures, **14** (2002) p. 96-100.
15. E.A. Fernández, *Development of experimental techniques for the demonstration of the operation principles of the intermediate band solar cell*. (Universidad Politécnica de Madrid, 2009).
16. M.Y. Levy, and C.B. Honsberg, *Rapid and precise calculations of energy and particle flux for detailed-balance photovoltaic applications.* Solid-State Electronics, **50** (2006) p. 1400-1405.
17. S.P. Bremner, M.Y. Levy, and C.B. Honsberg. *Limiting efficiency of an intermediate band solar cell under terrestrial spectrum.* Applied Physics Letters **92** (2008).

Appendix A

In this appendix the code for some of the scripts from Matlab are shown.

The first function is used to import the data for the AM1.5 spectra, do some adjustments them so that they are easier used later, and saved in matrixes.

The colorbars in the efficiency plots have been made by the function cbarf, downloaded 09.03.2011 from the mathworks web page:
http://www.mathworks.com/matlabcentral/fileexchange/14290.

```
function ret=EnergyfromSuncalc()
%This function uses the spectrum datapoints from NREL found at
%(http://rredc.nrel.gov/solar/spectra/am1.5/).The datapoints are placed in
%different matrixes, some interpolation is done to add some datapoints at
%the lower photon energies, and the energyscale is set to eV for some of
%the values. Photon flux is also calculated and placed in matrixes for
%later use.

%loading the datapoints
EnergyfromSun=xlsread('D:\Skole\Mastermappen\DIV\ASTMG173numbers.xls');
%colomns : energy scale in nm , ETR(extraterrestrial) W/m^2/nm ,
%Global tilt W/m^2/nm,Direct + circumsolar W/m^2/nm.
%The last colomn will be ignored further on.

%Interpolating a 1nm scale
length=(EnergyfromSun(end,1)-EnergyfromSun(1,1)+1);
EnergyfromSun1nmscale=zeros(length,4);
EnergyfromSun1nmscale(:,1)=EnergyfromSun(1,1):1:EnergyfromSun(end,1);
EnergyfromSun1nmscale(:,2)=interp1(EnergyfromSun(:,1),...
    EnergyfromSun(:,2),EnergyfromSun1nmscale(:,1),'spline');
EnergyfromSun1nmscale(:,3)=interp1(EnergyfromSun(:,1),...
    EnergyfromSun(:,3),EnergyfromSun1nmscale(:,1),'spline');
EnergyfromSun1nmscale(:,4)=interp1(EnergyfromSun(:,1),...
    EnergyfromSun(:,4),EnergyfromSun1nmscale(:,1),'spline');

%removing the negative values in EnergyfromSun1nmscale
for x=(1:1:length)
   if(EnergyfromSun1nmscale(x,2)<0)
       EnergyfromSun1nmscale(x,2)=0;
   end
   if(EnergyfromSun1nmscale(x,3)<0)
       EnergyfromSun1nmscale(x,3)=0;
   end
   if(EnergyfromSun1nmscale(x,4)<0)
       EnergyfromSun1nmscale(x,4)=0;
   end
end


% Need to manipulate to get the photonflux at a eV scale so I do this here
% to make it easier later on.

%Variables
h = 4.13566733*10^-15;      % eV s
c = 299792458;              % m s^-1
jtoeV = 6.24150974*10^18;   % 1 joule equals 6.24150974*10^18 eV
fromnmtom = 10^-9;          % as 1m equals 10^9nm

hcnm=h*c/fromnmtom;

%pflux_1nmscale_AM0 : wavelength, photonenergy, photonflux*s^-1*m^-2*nm^-1
```

```
pflux_1nmscale_AM0=zeros(length,3);
pflux_1nmscale_AM0(:,1)=EnergyfromSun1nmscale(:,1);
pflux_1nmscale_AM0(:,2)=hcnm./EnergyfromSun1nmscale(:,1);
pflux_1nmscale_AM0(:,3)=...
    jtoeV*(EnergyfromSun1nmscale(:,2)./pflux_1nmscale_AM0(:,2));

%pflux_1nmscale_AM15 global:wavelength,photonenergy,photonflux*s^-1*m^-2*nm^-1
pflux_1nmscale_AM15=pflux_1nmscale_AM0;
pflux_1nmscale_AM15(:,3)=...
    jtoeV*(EnergyfromSun1nmscale(:,3)./pflux_1nmscale_AM15(:,2));

%pflux_1nmscale_AM15 global:wavelength,photonenergy,photonflux*s^-1*m^-2*nm^-1
pflux_1nmscale_AM15D=pflux_1nmscale_AM0;
pflux_1nmscale_AM15D(:,3)=...
    jtoeV*(EnergyfromSun1nmscale(:,4)./pflux_1nmscale_AM15(:,2));

%Powerfromsun_1nmscale : wavelength, photonenergy, eV*s^-1*m^-2*nm^-1
Powerfromsun_1nmscale_AM0=pflux_1nmscale_AM0;
Powerfromsun_1nmscale_AM0(:,3)=jtoeV*EnergyfromSun1nmscale(:,2);

Powerfromsun_1nmscale_AM15=pflux_1nmscale_AM0;
Powerfromsun_1nmscale_AM15(:,3)=jtoeV*EnergyfromSun1nmscale(:,3);

Powerfromsun_1nmscale_AM15D=pflux_1nmscale_AM0;
Powerfromsun_1nmscale_AM15D(:,3)=jtoeV*EnergyfromSun1nmscale(:,4);

%removing unwanted variables and saving the rest
clear x h c jtoeV fromnmtom length hcnm;

save 'EnergyfromSun.mat'
ret = 1;
```

The next functions calculate the power from the sun, and the photon flux from the sun and from the cells when called upon.

```
function ret=powerAM15(concentration)
%This function returns the total power from the sun, with a certain
%concentration level.

%Import the sun energy data
load('EnergyfromSun.mat')

%pflux_1nmscale_AM15 : wavelength, photonenergy, photonflux*m^-2*nm^-1
A=Powerfromsun_1nmscale_AM15;

ret=concentration*sum(A(:,3));
```

```
function ret=photonflux(Emin,Emax,T,u,X)
%This function calculates the photon flux of a blackbody with temperature
%T,chemical potential u and a concentration level X. The energy interval %in eV
is from Emin to Emax.

%Variables
h = 4.13566733*10^-15;      % eV s^-1
c = 299792458;              % m s^-1
k = 8.617343*10^-5;     % eV K^-1

%running the calculation
f=@(E) (E.^2)./(exp((E-u)./(k*T))-1);
integral=quadgk(f,Emin,Emax);
ret=(2*pi*X*integral)/(46050*h.^3*c.^2);
function ret=photonfluxAM15(Emin,Emax,X,FluxData)
%This function finds the photonflux from the Am15 datapoints, with a
```

```
%concentration level set at X, between the energyinterval (in eV) Emin and
%Emax. The datapoints are from the input data FluxData.

%Concentration level
concentration=X;

%If the top value of the energy that the photons can have is less than the
%lowest value for the data from the spectrum the photonflux is returned as
%zero. As there is no more datapoints below this energylevel.
if(Emax<FluxData(end,2))
    ret=0;
    return
end

%Finding the Minindex of FluxData, where the photonenergy is just below %Emax, if
possible.The photonenergy is strictly decreasing, so this check %counts down.
Minindex = 0;
for x=size(FluxData,1):-1:1
    if(FluxData(x,2)>Emax)
        break;
    end
    Minindex=x;
end

%Finding the Maxindex of FluxData, where the photonenergy is barely higher %than
the Emin value. This needs to count up as the photonenergy is %strictly
increasing
Maxindex = 0;
for x=1:1:size(FluxData,1)
    if(FluxData(x,2)<Emin)
        break;
    end
    Maxindex=x;
end

%Calculating the photonflux with the bounderies Emin and Emax, with
%concentration.
ret=concentration*sum(FluxData(Minindex:Maxindex,3));
```

The following functions calculate the efficiency for one cell. IBSC and single-junction have different scripts.

```
function ret=SCsingleAM15_more(Eg,Emax,Tc,X,vector,FluxData,Psun)
%This function finds the efficiency/voltage for numerous voltage values for
%a single junction cell.
%
%Input values are :
%   (The lowest Band gap El, the main band gap Eg, the highest photon energy
%   that reaches this cell Emax, temperature of the cell Tc,
%   Concentration (number of suns) X, the photon flux data Fluxdata and
%   total power from the sun) Psun.
%
%The function returns the following matrix:
%
%   MAT(i,1)=V(i);                  voltage
%   MAT(i,2)=TotElflow(i)/Psun;     efficiency/voltage

%The cell radiates out in all directions from its surface.(max
%concentration)
Fc=46050;

%Absorbtion of photons from the sun
absEcv = photonfluxAM15(Eg,Emax,X,FluxData);

%Finding a good starting position for the lowest voltage
El = 0;
error = 10^-6;                          %acceptable errorrange
vectorlength=vector/10;
```

```
Vt =  El:((Eg-El)/vectorlength):(Eg-((Eg-El)/vectorlength));
Startvolt=0;

Tempcurrent = -1;
Volttemp = El;
for vt = Vt
    %Total flow of electrons from the valence band to the conduction band, with
    %the use of detailed balance.
    Elflowcvt= absEcv - photonflux(Eg,Emax,Tc,vt,Fc);

    %To initialize the Tempcurrent factor the first run
    if (Tempcurrent == -1)
        Tempcurrent = Elflowcvt;
    end

    %Here the total flow of electrons is summerized and checked if it
    %changed from the first run.
    TotElflow = Elflowcvt;

    Err = abs((Tempcurrent-TotElflow)/(TotElflow+Tempcurrent));

    if (Err > error)
        Startvolt = Volttemp;
        break;
    end

    Volttemp=vt;
end

% Found a better starting voltage and now for electroncurrentdensity for
% different voltages

returnMat=zeros(vector,2);
V =  Startvolt:((Eg-Startvolt)/(vector)):(Eg-((Eg-Startvolt)/(vector)));

%creating the return matrix
index=1;
for v = V
    %the current divided by Power from the sun at a given voltage.
    returnMat(index,2) = (absEcv - photonflux(Eg,Emax,Tc,v,Fc))/Psun;
    returnMat(index,1) = v;
    index=index+1;
end

ret=returnMat;


function ret=IBSC_AM15_more(El,Eg,Emax,Tc,X,FluxData,Psun)
%This function runs calculations to find the efficiency/voltage, for
%different voltages of a IBSC cell.
%
%The function returns the following matrix:
%
%   MAT(i,1)=V(i);                  voltage
%   MAT(i,2)=TotElflow(i)/Psun;     efficiency/voltage
%   MAT(i,3)=Error(i);              an errorvector, explained later
%
%Input values are :
%   (The lowest Band gap El,the main band gap Eg,the highest photon energy
%   that reaches this cell Emax, temperature of the cell Tc,
%   Concentration (number of suns) X, the photon flux data Fluxdata and
%   total power from the sun) Psun.
%There is added a failsafe to stop the iterations as the lowest ulow
%gets close to the lowest energyband. If these gets equal the integral
%will get a singularity.

%input
vectorlength = 500;
ret=zeros(vectorlength,3);

%some band gap calculations
Ehigh = Eg-El;
```

```
Elow = El;

%The cell radiates out in all directions from its surface.(max %concentration)
Fc=46050;

%photonflux absorbed from the sun for each band
absEhigh = photonfluxAM15(Ehigh,Eg,X,FluxData);
absElow  = photonfluxAM15(Elow,Ehigh,X,FluxData);
absEcv = photonfluxAM15(Eg,Emax,X,FluxData);

%calculating for each voltage where qV = ucv = uci + uiv using that no
%current is extracted from the intermediate band then the photonflux from
%the v-band to the i-band equals the flux from the i-band to the c-band.

%Finding a better starting point
errorvolt = 10^-5;
vectorl = vectorlength/10;
Lowvolt = IBSC_AM15_voltfinder...
    (El,Eg,Emax,Tc,vectorl,errorvolt,absEhigh,absElow,absEcv);

%setting up the matrixes before I start
Effect    = zeros(vectorlength,1);
Error     = zeros(vectorlength,1);
TotElflow = zeros(vectorlength,1);
Elflowcv  = zeros(vectorlength,1);
V         = Lowvolt:((Eg-Lowvolt)/vectorlength):(Eg-((Eg-Lowvolt)/vectorlength));

%starting the calculations for the currents
indexcounter = 0;
for v = Lowvolt:((Eg-Lowvolt)/vectorlength):(Eg-((Eg-Lowvolt)/vectorlength))
    indexcounter = indexcounter + 1;

    %Total flow of electrons from the valence band to the conduction band,
    %with the use of detailed balance.
    Elflowcv(indexcounter)= absEcv - photonflux(Eg,Emax,Tc,v,Fc);

    %Finding the uvi and uci (uhigh/ulow) by use of the equations in IBSC
    %section in the thesis,using Ehigh and Elow
    utop = min(v,Ehigh);
    ubottom = v-Elow;
    uhigh = (utop+ubottom)/2;
    ulow = v-uhigh;

    Ehighphotonflux = absEhigh -  photonflux(Ehigh,Eg,Tc,uhigh,Fc);
    Elowphotonflux = absElow - photonflux(Elow,Ehigh,Tc,ulow,Fc);
    temperror = ...
  abs(Ehighphotonflux-Elowphotonflux)/abs(Ehighphotonflux+Elowphotonflux);


    temper=1;
    temp=0;

    %here I vary utop and ubottom to reduce the value of temperror and find
    %the solution to the equation equallizing the current through the IB.
    while (temperror > 10^-5 && temper > 0)
        temp = temperror;
        if (Ehighphotonflux < Elowphotonflux)
           utop = uhigh;
        else
            ubottom = uhigh;
        end

        uhigh = (utop+ubottom)/2;
        ulow = v-uhigh;

        Ehighphotonflux = absEhigh -  photonflux(Ehigh,Eg,Tc,uhigh,Fc);
        Elowphotonflux = absElow - photonflux(Elow,Ehigh,Tc,ulow,Fc);
        temperror = abs(Ehighphotonflux-Elowphotonflux)/...
            abs(Ehighphotonflux+Elowphotonflux);
        if(abs(temp - temperror)<10^-6)
            temper=-1;
        end
```

```
        if(abs(ulow-Elow)<10^-6)
            temper=-1;
        end
    end

    %Saving the error
    Error(indexcounter)= temperror;

    %Here the total flow of electrons is summerized
    TotElflow(indexcounter) = ...
        min(Ehighphotonflux , Elowphotonflux) + Elflowcv(indexcounter);

    %The effect for each value of the voltage in eV
    Effect(indexcounter) = v * TotElflow(indexcounter);
end

%Efficiency for each voltage
ret(:,1)=V(:);
ret(:,2)=TotElflow(:)/Psun;
ret(:,3)=Error(:);



function ret=IBSC_AM15_voltfinder(El,Eg,Emax,Tc,vectorl,error,absEhigh
,absElow,absEcv)

%                           Comments
%This function uses the same methods as IBSC but is used to find a
%suitable starting point, in the border of where the current starts to
%change depended on the voltage. The only difference is that this function
%uses 10 times lesser voltagepoints than the IBSC_AM15_more function.
%
%I have left a error analysis in if there is need for it would be easy
%to return as part of the function.
%
%For better comments see IBSC_AM15_more


%Some constants and initiations
vectorlength = vectorl;
Tester=-1;

%The cell radiates out in all directions from its surface.(max %concentration)
Fc=46050;

% some calculations
Ehigh = Eg-El;
Elow = El;
Startvolt=El;

%calculating the current from the different voltages and breaking when the
%current starts to change.

Tempcurrent = -1;
Volttemp = Startvolt;

for v=Startvolt:((Eg-Startvolt)/(vectorlength)):...
        (Eg-((Eg-Startvolt)/(vectorlength)))

    %Total flow of electrons from the valence band to the conduction band,
    %with the use of detailed balance.
    Elflowcv = absEcv - photonflux(Eg,Emax,Tc,v,Fc);

    %Finding the uvi and uci (uhigh/ulow)
    utop = min(v,Ehigh);
    ubottom = v-Elow;
    uhigh = (utop+ubottom)/2;
    ulow = v-uhigh;

    Ehighphotonflux = absEhigh -  photonflux(Ehigh,Eg,Tc,uhigh,Fc);
    Elowphotonflux = absElow - photonflux(Elow,Ehigh,Tc,ulow,Fc);
    temperror = abs(Ehighphotonflux-Elowphotonflux)/...
```

```
        abs(Ehighphotonflux+Elowphotonflux);


    temper=1;
    temp=0;
    while (temperror > 10^-5 && temper > 0)
        temp = temperror;
        if (Ehighphotonflux < Elowphotonflux)
           utop = uhigh;
        else
            ubottom = uhigh;
        end

        uhigh = (utop+ubottom)/2;
        ulow = v-uhigh;

        Ehighphotonflux = absEhigh -  photonflux(Ehigh,Eg,Tc,uhigh,Fc);
        Elowphotonflux = absElow - photonflux(Elow,Ehigh,Tc,ulow,Fc);
        temperror = abs(Ehighphotonflux-Elowphotonflux)/...
            abs(Ehighphotonflux+Elowphotonflux);
        if(temp == temperror)
            temper=-1;
        end
    end

    %To initialize the Tempcurrent factor the first run
    if (Tempcurrent == -1)
        Tempcurrent = Ehighphotonflux + Elflowcv;
    end


    %Here the total flow of electrons is summerized and checked if it
    %changed from the first run.
    TotElflow = Ehighphotonflux + Elflowcv;

    Err = abs(Tempcurrent-TotElflow)/(TotElflow+Tempcurrent);

    if (Err > error)
        Tester=Volttemp;
        break;
    end

    Volttemp=v;

end

%returning the new Startvoltage for IBSC_AM15_more, or the first one if
%there has been some sort of error
if(Tester==-1)
    ret=Startvolt;
else
    ret=Tester;
end
```

The following scripts calculate the efficiency for a cell in tandem configuration for various main band gap energy values. The top cell and bottom cell have different scripts, as well as different scripts for the single-junction cell and the IBSCs. All data is saved in a matrix.

```
%This script calculates numerous IBSCs, and is used for the bottom cell of
%the tandem cell. All values are saved in one matrix, where each cell is
%identified by the Main band gap (Eg) and the intermediate band (El) on %the
first row and the maximum photon energy (E) on the second row.
%The other rows have the voltage and the efficiency/voltage, in two %columns for
each cell.

%Setting up some of the starting values
Tc=300;                         %Cell temperature
X=1;                            %Concentration level
vector=500;                     %Number of voltage points
steplength=0.05;                %Difference between each band gap energy
Elmin = 0.1;                    %Minimum intermediate band energy
Egmin = 0.3;                    %Minimum main band gap energy
Emax  = 2.8;                    %Maximum photon energy absorbed
Emin  = 0.5;                    %Minimum photon energy absorbed


%Name for the savefile
savefile='test.mat';

%Import the sun energy data
load('EnergyfromSun.mat')
A=Powerfromsun_1nmscale_AM15;
Psun=X*sum(A(:,3));
FluxData=pflux_1nmscale_AM15;

%counting how many times this will run
count=0;
for E=Emin:steplength:Emax
    Egmax=E-steplength/10;
    for j=Egmin:steplength:Egmax
        Elmax=j/2-steplength/10;
        for x=Elmin:steplength:Elmax
            count=count+1;
        end
    end
end

%creating the matrix, each cell has two columns with the following
%configuration:  first row           Eg      , El
%                second row          0       , Emax
%                rest of the rows    voltage , efficiency/voltage
RangeMat=zeros(vector+2,count*2);

clear j x count
%Calculating for all the maximum energy photon energies
counter=0;
for E=Emin:steplength:Emax
    %finding the highest main band gap value
    Egmax=E-steplength/10;
    %Calculating for all Eg
    for Eg=Egmin:steplength:Egmax
        %finding the highest intermediate band value
        Elmax=(Eg/2)-steplength/10;
        %Calculating for all El
        for El=Elmin:steplength:Elmax
            %Finding the data for one cell
            a=IBSC_AM15_more(El,Eg,E,Tc,X,FluxData,Psun);
            %Saving data in the return matrix
            RangeMat(1,(2*counter)+1)=Eg;
            RangeMat(1,(2*counter)+2)=El;
            RangeMat(2,(2*counter)+2)=E;
            RangeMat(3:end,(2*counter)+1)=a(:,1);
            RangeMat(3:end,(2*counter)+2)=a(:,2);
```

```
            counter=counter+1;
        end
    end
end
%saving the retun matrix
save(savefile,'RangeMat');



%This script calculates numerous IBSCs, and is used for the top cell of
%the tandem cell. All values are saved in one matrix, where each cell is
%identified by the Main band gap (Eg) and the intermediate band (El) on %the
first row. The other rows have the voltage and the %efficiency/voltage, in two
columns for each cell.

%Setting up some of the starting values
Emax=Inf;                       %Highest photon energy
Tc=300;                         %Cell temperature
X=1;                            %Concentration level
vector=500;                     %Number of voltage points
steplength=0.05;                %Difference between each band gap energy
Elmin=0.7;                      %Minimum intermediate band energy
Egmin=2.64;                     %Minimum main band gap energy
Egmax=3;                        %Maximum main band gap energy

%Name for the savefile
savefile='IBSCtopeg2.64-with0.01int.mat';

%Import the sun energy data and setting the used data to specific variable
%names
load('EnergyfromSun.mat')
A=Powerfromsun_1nmscale_AM15;
Psun=X*sum(A(:,3));
FluxData=pflux_1nmscale_AM15;

%counting how many times this will run
count=0;
for j=Egmin:steplength:Egmax
    Elmax=j/2-steplength/10;
    for x=Elmin:steplength:Elmax
        count=count+1;
    end
end

%creating the matrix, each cell has two coloums with the following
%configuration:  first row           Eg      , El
%                rest of the rows    voltage , efficiency/voltage
RangeMat=zeros(vector+1,count*2);

clear j x count
%Calculating for all Eg
counter=0;
for Eg=Egmin:steplength:Egmax
    %Finding the maximum value of the intermediate band
    Elmax=Eg/2-steplength/10;
    %Calculating for all values of the intermediate band (El)
    for El=Elmin:steplength:Elmax
        %Finding the data for one cell
        a=IBSC_AM15_more(El,Eg,Emax,Tc,X,FluxData,Psun);
        %Saving data in the return matrix
        RangeMat(1,(2*counter)+1)=Eg;
        RangeMat(1,(2*counter)+2)=El;
        RangeMat(2:end,(2*counter)+1)=a(:,1);
        RangeMat(2:end,(2*counter)+2)=a(:,2);
        counter=counter+1;
    end
end
%saving the retun matrix
save(savefile,'RangeMat');


%This script calculates numerous single junction cells, and is used for the
```

```
%bottom cell of the tandem cell. All values are saved in one matrix, where
%each cell is identified by the Main band gap (Eg) and the maximum photon
%energy (E) in the first row. The other rows have the voltage and the
%efficiency/voltage, in two columns for each cell.


%Setting up some of the starting values
Emax=2;                         %Maximum photon energy absorbed
Emin=0.7;                       %Minimum photon energy absorbed
Tc=300;                         %Cell temperature
X=1;                            %Concentration level
vector=500;                     %Number of voltage points
steplength=0.05;                %Difference between each band gap energy (eV)
Egmin=0.5;                      %Minimum main band gap

%Name of the file the matrix is saved as
savefile='single_AM15_0.01step_conc1.mat';

%Adding the data for the irradiance hitting the cell

%Import the sun energy data and setting the used data to specific variable
%names
load('EnergyfromSun.mat')
A=Powerfromsun_1nmscale_AM15;
Psun=X*sum(A(:,3));
FluxData=pflux_1nmscale_AM15;

%counting how many times this will run
count=0;
for j=Emin:steplength:Emax
    Egmax=j-steplength/10;
    for x=Egmin:steplength:Egmax
        count=count+1;
    end
end

%Lagrer på første rad: Eg, Emax
%Neste radene lagres :  v, strøm/power_in
RangeMat=zeros(vector+1,count*2);

clear j x count
%Calculating for all Eg
counter=0;
%Calculating for all the photon energies absorbed
for E=Emin:steplength:Emax
    %Setting the highest main band gap energy for the cell
    Egmax=E-steplength/10;
    %Calculating for each value of Eg
    for Eg=Egmin:steplength:Egmax
        %Finding the data for one cell
        a=SCsingleAM15_more(Eg,E,Tc,X,vector,FluxData,Psun);
        %Saving data in the return matrix
        RangeMat(1,(2*counter)+1)=Eg;
        RangeMat(1,(2*counter)+2)=E;
        RangeMat(2:end,(2*counter)+1)=a(:,1);
        RangeMat(2:end,(2*counter)+2)=a(:,2);
        counter=counter+1;
    end
end
%saving the return matrix
save(savefile,'RangeMat');
%This script calculates numerous single junction cells, and is used for %the top
cell of the tandem cell. All values are saved in one matrix, %where each cell is
identified by the Main band gap (Eg) in the first row. %The other rows have the
voltage and the efficiency/voltage, in two %columns for each cell.


%The starting values
Emax=Inf;                       %Highest photon energy
Tc=300;                         %Cell temperature
X=1;                            %Concentration level
vector=500;                     %Number of voltage points
```

```
steplength=0.05;                %Difference between each band gap energy (eV)
Egmin=0.5;                      %Minimum main band gap
Egmax=4.5;                      %Maximum main band gap

%Name of the file the matrix is saved as
savefile='newstep005_singletop_AM15_Emax0.5,4.5_conc1.mat';

%Import the sun energy data and setting the used data to specific variable
%names
load('EnergyfromSun.mat')
A=Powerfromsun_1nmscale_AM15;
Psun=X*sum(A(:,3));
FluxData=pflux_1nmscale_AM15;

%counting how many times it will run
count=0;
for x=Egmin:steplength:Egmax
    count=count+1;
end

%creating the matrix, each cell has two coloums with the following
%configuration:  first row           Eg      , 0
%                rest of the rows    voltage , efficiency/voltage
RangeMat=zeros(vector+1,count*2);

clear j x count

%Calculating for all Eg
counter=0;
for Eg=Egmin:steplength:Egmax
    %Finding the data for one cell
    a=SCsingleAM15_more(Eg,Emax,Tc,X,vector,FluxData,Psun);
    %Saving data in the return matrix
    RangeMat(1,(2*counter)+1)=Eg;
    RangeMat(1,(2*counter)+2)=0;
    RangeMat(2:end,(2*counter)+1)=a(:,1);
    RangeMat(2:end,(2*counter)+2)=a(:,2);
    counter=counter+1;
end
%saving the retun matrix
save(savefile,'RangeMat');
```

The following scripts process the data from the previous scripts, finding the configurations with the highest efficiency. Two and four terminal tandem cells have different scripts.

```
%This script prosesses some of the calculated data for the unconnected
%tandem cells. The maximum efficiency is found for the each of the two cells,
%top and bottom, seperately.

%Filename that this script saves to
filename='MaxeffIBSCunconnectedAM15conc1';

%Loading the data for the top cell
load 'newstep005_IBSCtop_AM15_inf_conc1_Eg1.1to4.8.mat'
IBSCtopMat=RangeMat;

%Loading the data for the bottom cell
load 'newstep005_IBSCbot_AM15_Emax0.5,2.8_conc1.mat'
IBSCbotMat=RangeMat;

%Top cell highest efficiency for all band gap values
%Want rows: Eg : Elow : efficiency
IBSCtopeff=zeros(size(IBSCtopMat,2)/2,3);
for i=1:1:(size(IBSCtopMat,2)/2)
    IBSCtopeff(i,1)=IBSCtopMat(1,2*i-1);
    IBSCtopeff(i,2)=IBSCtopMat(1,2*i);
    IBSCtopeff(i,3)=max(IBSCtopMat(2:end,2*i-1).*IBSCtopMat(2:end,2*i));
```

```
end

%Bottom cell highest efficiency for all band gap values and highest photon
%energy absorbed.
%Want rows: Eg : Elow : Emax :efficiency
IBSCboteff=zeros(size(IBSCbotMat,2)/2,4);
for i=1:1:(size(IBSCbotMat,2)/2)
    IBSCboteff(i,1)=IBSCbotMat(1,2*i-1);
    IBSCboteff(i,2)=IBSCbotMat(1,2*i);
    IBSCboteff(i,3)=IBSCbotMat(2,2*i);
    IBSCboteff(i,4)=max(IBSCbotMat(3:end,2*i-1).*IBSCbotMat(3:end,2*i));
end


%%Finding the highest efficiency for all the different values of the
%%intermediate band in the top cell.

%Finding the energy step for the band gap energies.
for i=2:1:size(IBSCtopeff,1)
    if (abs(IBSCtopeff(i,1)-IBSCtopeff(1,1))>10^-5)
        step=IBSCtopeff(i,1)-IBSCtopeff(1,1);
        break;
    end
end

%Setting some values used later
Elowmin=IBSCtopeff(1,2);
Elowmax=IBSCtopeff(end,2);
Counter=0;
Tempeff=0;
TempEg=0;

%Finding the highest efficiency for the IBSC top cell
%           Elow : Egtop : efficiency
IBSCtopElow=zeros(round((Elowmax-Elowmin)/step),3);

%Running for each Elow
for Elow=Elowmin:step:Elowmax
    Tempeff=0;
    TempEg=0;
    Counter=Counter + 1;
    IBSCtopElow(Counter,1)=Elow;

    %Checking through each Elow to find the highest efficiency
    for i=1:1:(size(IBSCtopeff,1))
        if((abs(IBSCtopeff(i,2)-Elow)<(step/10)) && IBSCtopeff(i,3)>Tempeff)
            Tempeff=IBSCtopeff(i,3);
            TempEg=IBSCtopeff(i,1);
        end
    end
    IBSCtopElow(Counter,2)=TempEg;
    IBSCtopElow(Counter,3)=Tempeff;
end


%%Finding the highest efficiency for all the different values of the
%%highest photon energy absorbed in the bottom cell. This energy is the
%%same as the lowest intermediate band in the top cell, and connects the
%%two separate cells together.

%Finding the highest efficiency for the IBSCbot
%           Emax : Egbot : Elow : efficiency
IBSCbotElow=zeros(round((Elowmax-Elowmin)/step),4);

Counter=0;
%Running for each Emax
for Emax=Elowmin:step:Elowmax
    Tempeff=0;
    TempEg=0;
    TempElow=0;
    Counter=Counter + 1;
    IBSCbotElow(Counter,1)=Emax;
```

```
    %Checking through each Emax to find the highest efficiency
    for i=1:1:(size(IBSCboteff,1))
        if((abs((IBSCboteff(i,3)-Emax))<(step/10)) ...
             && IBSCboteff(i,4)>Tempeff)
            Tempeff=IBSCboteff(i,4);
            TempEg=IBSCboteff(i,1);
            TempElow=IBSCboteff(i,2);
        end
    end
    IBSCbotElow(Counter,2)=TempEg;
    IBSCbotElow(Counter,3)=TempElow;
    IBSCbotElow(Counter,4)=Tempeff;
end


%Setting up a return matrix that will have the following row setup:
%           Elowtop/Emax : Egtop : Egbot : Elow bot: efficiency
RetMat=zeros(round((Elowmax-Elowmin)/step),5);

Counter=0;
for Elow=Elowmin:step:Elowmax
    Counter=Counter + 1;
    RetMat(Counter,1)=Elow;
    RetMat(Counter,2)=IBSCtopElow(Counter,2);
    RetMat(Counter,3)=IBSCbotElow(Counter,2);
    RetMat(Counter,4)=IBSCbotElow(Counter,3);
    RetMat(Counter,5)=IBSCbotElow(Counter,4)+IBSCtopElow(Counter,3);
end

%saving the data
save(filename,'IBSCtopElow','IBSCtopeff','IBSCboteff','IBSCbotElow',...
'RetMat');


%This script creates a surface of the maximum efficiencies for different
%main band gap energies of the two IBSCs connected in a four terminal tandem
%cell. The intermediate bands at those efficiencies are also stored in a
%matrix. These surface matrixes are later used for plotting.


%importing the data matrix
load 'MaxeffIBSCunconnectedAM15conc1000.mat'
%Name of the savefile
savename='IBSCUnconnectedconc1000.mat';

%IBSCtandem
%top : Egtop : elow : eff
%bot : Egtop : elow : emax : eff

%Finding the lowest Emax for Bottomcell to give the startingpoint for the
%Topcell

Emaxmin=IBSCboteff(1,3);
DatatopMat=IBSCtopeff(IBSCtopeff(:,2)>(Emaxmin-0.0001),:);
DatabotMat=IBSCboteff;
clear x i Emaxmin

%Finding the energy step interval
step=DatatopMat(end,2)-DatatopMat(end-1,2);

%Creating main band gap vectors
Egtop=(DatatopMat(1,1):step:DatatopMat(end,1)+step/10)';
Egbot=(DatabotMat(1,1):step:DatabotMat(end,1)+step/10)';

%Creating the blank surfaces
Surface=zeros(size(Egtop,1),size(Egbot,1));
Surfacebot=Surface;
Surfacetop=Surface;
Elowtop=Surface;
Elowbot=Surface;
```

```
%Manipulation of the DatabotMat, only saving the highest values for each %Eg and
Emax.
indexcounter=1;
tempeg=DatabotMat(1,1);
tempeffmax=-10;
topeff=1;
for i=1:1:size(DatabotMat,1)
    if(tempeg~=DatabotMat(i,1) || i==size(DatabotMat,1) || (i==1 &&
abs(DatabotMat(1,1)-DatabotMat(2,1))<0.00001))
        tempeg=DatabotMat(i,1);
        Index(indexcounter)=topeff;
        indexcounter=indexcounter+1;
        tempeffmax=-10;
    end
    if(tempeffmax<DatabotMat(i,4))
        topeff=i;
        tempeffmax=DatabotMat(i,4);
    end
end

DatabotMat=DatabotMat(Index,:);

%Now I want the surface to show the efficiency at the appropriate places.
for top=1:1:size(DatatopMat,1)
    for bot=1:1:size(DatabotMat,1)
        if(abs(DatatopMat(top,2)-DatabotMat(bot,3))<10^-4)
            x=round((DatatopMat(top,1)-DatatopMat(1,1))/step)+1;
            y=round((DatabotMat(bot,1)-DatabotMat(1,1))/step)+1;
            if(Surface(x,y)==0)
                Surface(x,y)=DatatopMat(top,3)+DatabotMat(bot,4);
                Surfacetop(x,y)=DatatopMat(top,3);
                Surfacebot(x,y)=DatabotMat(bot,4);
                Elowtop(x,y)=DatatopMat(top,2);
                Elowbot(x,y)=DatabotMat(bot,2);
            elseif(Surface(x,y)<DatatopMat(top,3)+DatabotMat(bot,4))
                Surface(x,y)=DatatopMat(top,3)+DatabotMat(bot,4);
                Surfacetop(x,y)=DatatopMat(top,3);
                Surfacebot(x,y)=DatabotMat(bot,4);
                Elowtop(x,y)=DatatopMat(top,2);
                Elowbot(x,y)=DatabotMat(bot,2);
            end
        end
    end
end

%just changing the vector row/coloums
Egbot=Egbot';
Egtop=Egtop';

%saving the data
save(savename,'Surface','Surfacetop','Surfacebot','Elowtop','Elowbot',...
'Egtop','Egbot');




%This script creates a surface of the maximum efficiencies for different
%main band gap energies of the two IBSCs series connected in a two %terminal
tandem cell. The intermediate bands at those efficiencies are %also stored in a
matrix. These surface matrixes are later used for %plotting.

%Name of the savefile
filename='IBSCConnected1000.mat';

%importing the datapoints for the top cell
load 'newstep005_IBSCtop_AM15_inf_conc1000_Eg1.1to4.8.mat'
IBSCMat=RangeMat;

%importing the datapoints for the bottom cell
load 'newstep005_IBSCbot_AM15_Emax0.5,2.8_conc1000.mat'
IBSCbotMat=RangeMat;
clear RangeMat
```

```
%will set it up following: for each Eg of the topcell it will run through
%each of the Eg of the botcell that are available for each of the Elow %from the
top cell. The maximum will remain and be set at the surface.

%This is for the IBSC top and single bot
%
%IBSC: 1.row: Eg , Elow
%      2.row: voltage, current
%
%IBSCbot: 1.row: Eg , Elow
%        2.row: 0  , Emax
%        3.row: voltage, current

%Finding the energy step for the band gap energies
step=IBSCMat(1,end)-IBSCMat(1,end-2);
%Containing the main band gap energies of the two IBSCs
Egtop=IBSCMat(1,1):step:IBSCMat(1,end-1)+step/10;
Egbot=IBSCbotMat(1,1):step:IBSCbotMat(1,end-1)+step/10;
%Setting up the blank surfaces
Surface=zeros(size(Egtop,2),size(Egbot,2));
errorsurface=Surface;
Elowtop=Surface;
Elowbot=Surface;

%Going through each of the "datapoints" in the top
for i=1:2:size(IBSCMat,2)
    %Going through each of the bottom "datapoints" that have a Emax that
    %corresponds (equals) the Elow possible for this "datapoint" in the
    %top
    for j=1:2:size(IBSCbotMat,2)
        if(abs(IBSCMat(1,i+1)-IBSCbotMat(2,j+1))<(step/100))
            x=round((IBSCMat(1,i)-IBSCMat(1,1))/step)+1;
            y=round((IBSCbotMat(1,j)-IBSCbotMat(1,1))/step)+1;
            %Here I will find the highest efficiency and add it to the
            %surface and so on.
            if((IBSCMat(2,i+1))<IBSCbotMat(3,j+1))
                a=IBSCbotMat(3:end,j:j+1);
                b=IBSCMat(2:end,i:i+1);
            else
                b=IBSCbotMat(3:end,j:j+1);
                a=IBSCMat(2:end,i:i+1);
            end

            %If the current is negative it is no point in using the data
            if(b(1,2)>0)
                %the a matrix has the highest current and b the lowest
                %Finding the voltages of a at currents equal to b as b
                %can't have higher current than its maximum value.
                 %(currents are decreasing down the matrix).

                %Need to remove duplicates in a and b currents for
                %inpolation operations
                indexb=zeros(size(b,1),1);
                counterb=1;
                temp=1;
                for r=1:1:size(b,1)-1
                    temp=1;
                    for r2=r+1:1:size(b,1)
                        if(b(r,2)==b(r2,2))
                            temp=0;
                            break;
                        end
                    end
                    if(temp==1)
                        indexb(counterb)=r;
                        counterb=counterb+1;
                    end
                end
                indexb(counterb)=r+1;
                indexb=indexb(indexb>0);
                if(size(indexb,1)<size(b,1))
```

```
                    b=b(indexb,:);
                end

                indexa=zeros(size(a,1),1);
                countera=1;
                for r=1:1:size(a,1)-1
                    temp=1;
                    for r2=r+1:1:size(a,1)
                        if(a(r,2)==a(r2,2))
                            temp=0;
                            break;
                        end
                    end
                    if(temp==1)
                        indexa(countera)=r;
                        countera=countera+1;
                    end
                end
                indexa(countera)=r+1;
                indexa=indexa(indexa>0);
                if(size(indexa,1)<size(a,1))
                    a=a(indexa,:);
                end

                %Now I have removed dublicates, and continue to find the
                %maximum efficiency.
                a_voltage_at_b_current =...
interp1(a(:,2),a(:,1),b(:,2),'linear');
                Eff=max(abs(a_voltage_at_b_current(:)+b(:,1)).*b(:,2));
                %This checks if the efficiency at the specific main band
                %gap energies allready has a higher efficiency found. If
                %not it replaces this spot with the new efficiency,
                 %and the corresponding intermediate band energies.
                if Eff>Surface(x,y)
                    Surface(x,y)=Eff;
                    Elowtop(x,y)=IBSCMat(1,i+1);
                    Elowbot(x,y)=IBSCbotMat(1,j+1);
                end
            end
        end
    end
end

%saving the data
save(filename,'Surface','Elowtop','Elowbot','Egtop','Egbot')
```